Unified Performance Analysis for Third-Generation CDMA Systems

A Thesis
Presented to
The Academic Faculty

by

Loran A. Jatunov

In Partial Fulfillment
of the Requirements for the Degree
Doctor of Philosophy

School of Electrical and Computer Engineering
Georgia Institute of Technology
April 2004

Unified Performance Analysis for Third-Generation CDMA Systems

Approved by:

Dr. Vijay Madisetti, Adviser	Dr. John R. Barry
Dr. Steven W. McLaughlin	Dr. Leonid Bunimovich (School of Mathematics)
Dr. Ye (Geofferey) Li	

Date Approved: _____

To Mama and Papa.

To my great High School professors Ricardo Gallardo, Gerardo Molina, Boris Chow, Larissa de Osorio, Elizabeth de Cabrera, and my other Math professors.

To my sixth-level teacher, Alina Borrero de Ramírez.

ACKNOWLEDGEMENTS

I would like to express my gratitude to my advisor, Professor Vijay Madisetti, for his guidance during this work.

I would also like to thank the School of Electrical and Computer Engineering for the Teaching Assistanships.

TABLE OF CONTENTS

LIST OF TABLES

LIST OF FIGURES

LIST OF ABBREVIATIONS

3G	Third Generation.
4G	Fourth Generation.
AMRC	Apropriate MRC.
AWGN	Additive White Gaussian Noise.
BER	Bit Error Rate.
BPSK	Binary Phase Shift Keying.
BS	Base Station.
BTN	A "Better than" Nyquist.
CDMA	Code-Division Multiple Access.
CF	Characteristic Function.
CIR	Carrier-to-Interference Ratio.
DS	Direct Sequence.
FT	Fourier Transform.
ICI	Interchip Interference.
IGA	Improved Gaussian Approximation.
ISI	Intersymbol Interference.
MAI	Multiple Access Interference, Multiuser Interference.
MC	Multi Carrier.
MRC	Maximum Ratio Combining.
MS	Mobile Station.
OPT	Optimum.
OQPSK	Offset QPSK.
PN	Pseudorandom Noise.
QOS	Quasi Orthogonal.
QPSK	Quadrature Phase Shift Keying.
RC	Raised Cosine.
RRC	Root Raised Cosine.

SGA Standard Gaussian Approximation.

SIGA Simplified Improved Gaussian Approximation.

SMRC Simplified MRC.

SNR Signal-to-Noise Ratio.

SSMA Spread Spectrum Multiple Access.

WCDMA Wideband CDMA.

WH Walsh-Hadamard.

SUMMARY

Analytic models for the performance of the forward link of 3G CDMA systems using different maximum ratio combining (MRC) RAKE finger weight assignments are presented. The spreading modulations under investigation are the balanced QPSK and the complex-spreading QPSK. The models are computationally efficient, accurate, and applicable to Root Raised Cosine (RRC) pulse shaping with any roll-off factor, variable processing gain, chip rate, and data rate for orthogonal codes, random codes, quasi-orthogonal codes, Gaussian noise, and realistic channel models. The expressions derived are then used to obtain the so-called orthogonality factor, which is commonly used in system-level simulations.

Next, closed-form mathematical expressions for the variance due to infinite chips interfering in systems using arbitrary Nyquist pulses are derived. These expressions are applicable to both the forward link and the reverse link. For the latter, the existing knowledge on the accurate and efficient estimation of the performance of CDMA systems is extended by presenting closed mathematical expressions for bandlimited systems using arbitrary Nyquist pulses for both BPSK and Offset-QPSK (OQPSK) modulation. The impact of adjacent channel interference in bandlimited systems is subsequently considered. Finally, mathematical expressions for the accurate and efficient estimation of a CDMA system using RRC pulse-shaping and a RAKE receiver in the presence of multipath interference are presented.

CHAPTER I

INTRODUCTION

Until now, spread spectrum analysis has usually been conducted by making several simplifying assumptions such as a square pulse-shaping function at the transmitter and a chip-spaced multipath channel model, which result in the number of chips causing interchip interference (ICI) being proportional to the number of channel paths and therefore relatively simple expressions. Analysis taking into account Root Raise Cosine (RRC) pulse shaping, commonly used in communication systems, results in an infinite number of chips that cause ICI. The complexity of the analysis is thus greatly increased.

Real channel models can have several paths arriving within a chip, and as the processing gain decreases (for high data rate 3G CDMA systems), the delay spread can be comparable to the bit period. It is going to be shown in this work that multipath[1]of the signal of the reference user can contribute to both the desired signal and the self-interference.

Several wideband CDMA systems are set to be deployed as alternatives for 3G wireless communication systems. These systems use different values for various parameters, such as chip rates, roll-off factors, and processing gain (see Table 1); moreover, to calculate the performance of these systems, there are different channel models. Previous versions of the proposals for these systems have also had different values for the parameters, and as they further transition into 4G systems, they will continue changing. Therefore, it would be convenient to obtain an analysis that could be easily adjusted to these changing parameters. At the same time, some of the services offered by 3G systems require a bit error rate (BER) on the order of 10^{-6}, which implies link-level simulations with 10^8 points; consequently, it also becomes necessary to have a computationally efficient method to estimate the performance.

The forward link (downlink) in wideband CDMA channels has increased its importance

[1]Multipath in this work is used as both an adjective and as a noun. In the latter case, it implies the ensemble of paths or replicas of the originally transmitted signal.

Table 1: Specifications for WCDMA and CDMA 2000, from [48].

	WCDMA	CDMA2000
Channel bandwidth	1.25, 5, 10, 20 MHz	1.25, 5, 10, 15, 20 MHz
Downlink RF channel structure	Direct spread	Direct spread or multicarrier
Chip rate	1.024, 4.096, 8.192, 16.384 Mcps	(1,3,6,12 x) 1.2288Mc/s for DS and MC
Roll-off factor for chip shaping	0.22	Similar to IS-95
Data Rate	2.3 Mbps Maximum	144, 307, 384, 2400,4800 Kbps
Spreading modulation	Balanced QPSK (downlink)	Balanced QPSK (downlink)
Data modulation	QPSK (downlink)	QPSK (downlink)
Multirate	Variable spreading and multicode	Variable spreading and multicode
Spreading factors	4-256	4-256
Spreading (downlink)	Variable-length WH and Gold-Sequence	Variable-length WH and M-Sequence

due to the appearance of high data-rate multimedia applications. In the downlink, a set of orthogonal codes is assigned to the users belonging to each cell; as a result, in the presence of a single path of transmission between the base station (BS) and the mobile user (MS), the interference caused by the rest of the in-cell users is zero, but in the presence of multipath, this orthogonality is destroyed; the degree of loss depends on the particular channel, the RAKE scheme used, the chip-rate, and the pulse-shaping function used. Determining this loss of orthogonality also becomes important in novel systems that are proposed in present-day research. The total interference perceived by a mobile user depends on its relative location in the cell: When close to the BS, the in-cell interference is predominant, when located at the border of a cell, the in-cell interference could be much less than 1/2 of the total. In other words, the advantage of using orthogonal codes depends on the channel, the system used, and the location of the mobile user. Consequently, it is again necessary to have good means to calculate the loss of the orthogonality.

In this work, an analysis is proposed that applies to different wideband channel models, various chip rates, RRC roll-off factors, different data rates, different processing gain, and choice of variable spreading or multicode. The analysis is to work for random, orthogonal

codes, quasi-orthogonal codes, or Gaussian noise. The spreading modulation under study is QPSK. Also, the analysis is to use a realistic model of MRC. The results are to be accurate and computationally efficient to obtain.

Furthermore, in the estimation of the system-level performance of novel architectures and schemes, usually some assumptions are made about the link level. Sometimes the effect of using orthogonal codes is not considered. Other times, the effect of using orthogonal codes, a particular waveform, chip rate, processing gain, RAKE receiver scheme, and modulation for a particular channel is lumped together into a single parameter called the orthogonality factor; sometimes, its value is rather arbitrarily chosen, although some work has been done to derive this figure of merit in [16] and [41].

We also propose a model for the loss of orthogonality of balanced and complex-spreading QPSK, using RRC pulse shaping with different roll-off factors, a simple model and another improved one for the finger weights of an MRC RAKE receiver (weights set to the composite of paths perceived at each finger) that allows sub-chip finger assignment analysis, and different chip rates for any given power delay profile.

Moreover, a simple-to-use closed-form expression for the inter-chip interference caused by a delayed RRC function is proposed; this implies QPSK SNR expressions (conditioned on the fading) that are also in closed form.

Next, closed forms of infinite sums are presented that would make the previous expressions for the forward link applicable not only to RRC pulses, but arbitrary Nyquist pulses. These closed forms are subsequently applied to an existing method for obtaining accurate reverse-link low-BER estimates, but for the performance of the BPSK and Offset-QPSK modulation with arbitrary Nyquist pulses. The method is then extended to ACI on one hand and a system that uses a RAKE receiver in a channel with two paths on the other hand.

1.1 Qualities Expected

The forward-link theoretical expressions derived are to be applicable to the following:

- Balanced QPSK and complex-spreading QPSK systems. IS-95 and 3G systems do not

use BPSK.

- Orthogonal codes, quasi-orthogonal random codes, and Gaussian noise.
- RRC waveshaping with variable roll-off factors.
- Variable spreading factors and multicode schemes; the first scheme is used for 3G systems to increase the data rate for a fixed chip rate; the second scheme was proposed.
- Any channel models. The maximum delay can be greater than the symbol period, especially when using a low processing gain. Also, the channel model does not need to be a set of paths equally spaced by multiples of a chip period.
- Variable processing gain, data rate, and chip rate.

Also the following is expected from the forward-link expressions

- To be fast to compute.
  –Only theoretical insight is gained from expressions that are as slow to compute as simulations.
- To be applicable to BER estimations up to 1E-6.
- To match simulation results. The theoretical Signal-to-Noise ratio (SNR) predicted must match that obtained from simulations.
- To match known simple-case expressions available in the literature.

The following is expected from the reverse-link expressions:

- To be applicable to arbitrary Nyquist pulses
- To be in closed form and to have a computational complexity of O(1).
- To match the Gaussian approximation at high BER.
- To be applicable to BER estimations with values less than 1E-3.

1.2 Background

1.2.1 Performance for Balanced Quaternary Transmitter

The transmitter and the receiver for the forward link of a CDMA system can be seen in Figs. 1 and 2, respectively. The received signal can be expressed as follows:

$$r(t) = \sum_{i=1}^{K} \sum_{l=1}^{L} \bar{\alpha}_l \sqrt{P^{(i)}} \left(\tilde{s}_I^{(i)}(t-\tau_l) - j\tilde{s}_Q^{(i)}(t-\tau_l) \right) + \mathcal{I}(t), \tag{1}$$

$$\tilde{s}_I^{(i)}(t) = \sum_{n=-\infty}^{\infty} d_{\lfloor \frac{n}{N} \rfloor}^{(i)} c_{I,n}^{(i)} g_1(t-nT_c), \quad \tilde{s}_Q^{(i)}(t) = \sum_{n=-\infty}^{\infty} d_{\lfloor \frac{n}{N} \rfloor}^{(i)} c_{Q,n}^{(i)} g_1(t-nT_c), \tag{2}$$

where these parameters and others to be used later are defined as

K, L, F	total number of users, paths, and RAKE fingers, respectively;
$\bar{\alpha}_l, \alpha_l, \theta_l, \tau_l$	the complex attenuation, fading coefficient, received carrier phase, and delay of path l, respectively; $\bar{\alpha}_l = \alpha_l e^{j\theta_l}$, $\lvert\bar{\alpha}_l\rvert = \alpha_l$; the attenuation coefficients are normalized such that $\sum_{l=1}^{L} \alpha_l^2 = 1$;
$P^{(i)}$, P_m	power received from user i and mean power received from each user, respectively;
$c_I^{(i)}, c_Q^{(i)}$	in-phase and quadrature code chip sequence for user i;
$g_1(t)$	RRC waveshaping filter with roll-off factor β;
T, T_c, N	bit and chip duration, and processing gain, respectively; $N = T/T_c$;
$d_m^{(i)} = d_{\lfloor \frac{n}{N} \rfloor}^{(i)}$	m-th bit value corresponding to the n-th chip, $m = \lfloor \frac{n}{N} \rfloor$;
$\mathcal{I}(t)$	the sum of out-of-cell interference, adjacent channel interference, and AWGN noise; in the bandpass, it has a double-sided power spectrum density of $I_o/2$ (I_o in baseband);
Z	output of the RAKE receiver; $Z = Z_{\text{Des}} + Z_{\substack{\text{Self} \\ \text{Interf}}} + Z_{\text{MAI}}$, the sum of the desired, self-interference (interchip and intersymbol interference), and the multi-access interference (MAI); it excludes the effect of $I(t)$
R_f	output of finger f of the RAKE receiver; $Z = \sum_{f=1}^{F} R_f$;
$\bar{G}_f$	weight (complex number) used for finger f; $\bar{G}_f = G_f e^{j\theta_f}$, $\lvert\bar{G}_f\rvert = G_f$.

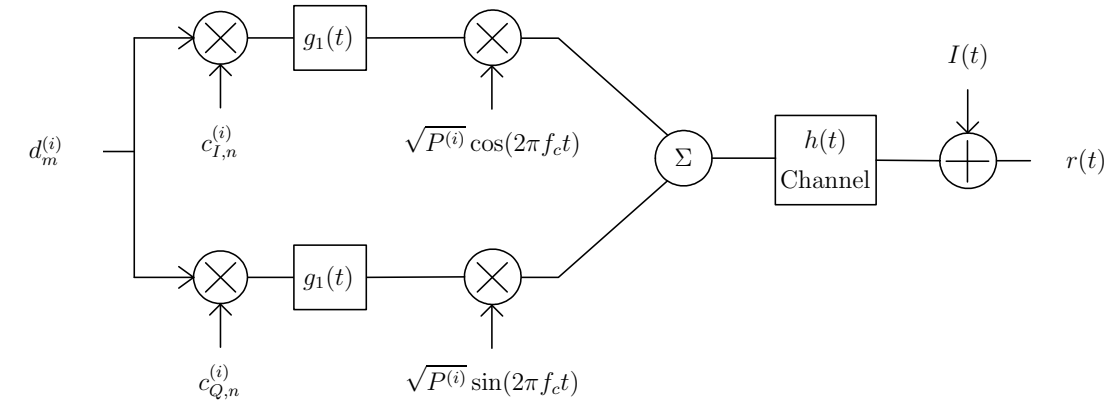

Figure 1: Balanced QPSK transmitter (just for user i) followed by the channel.

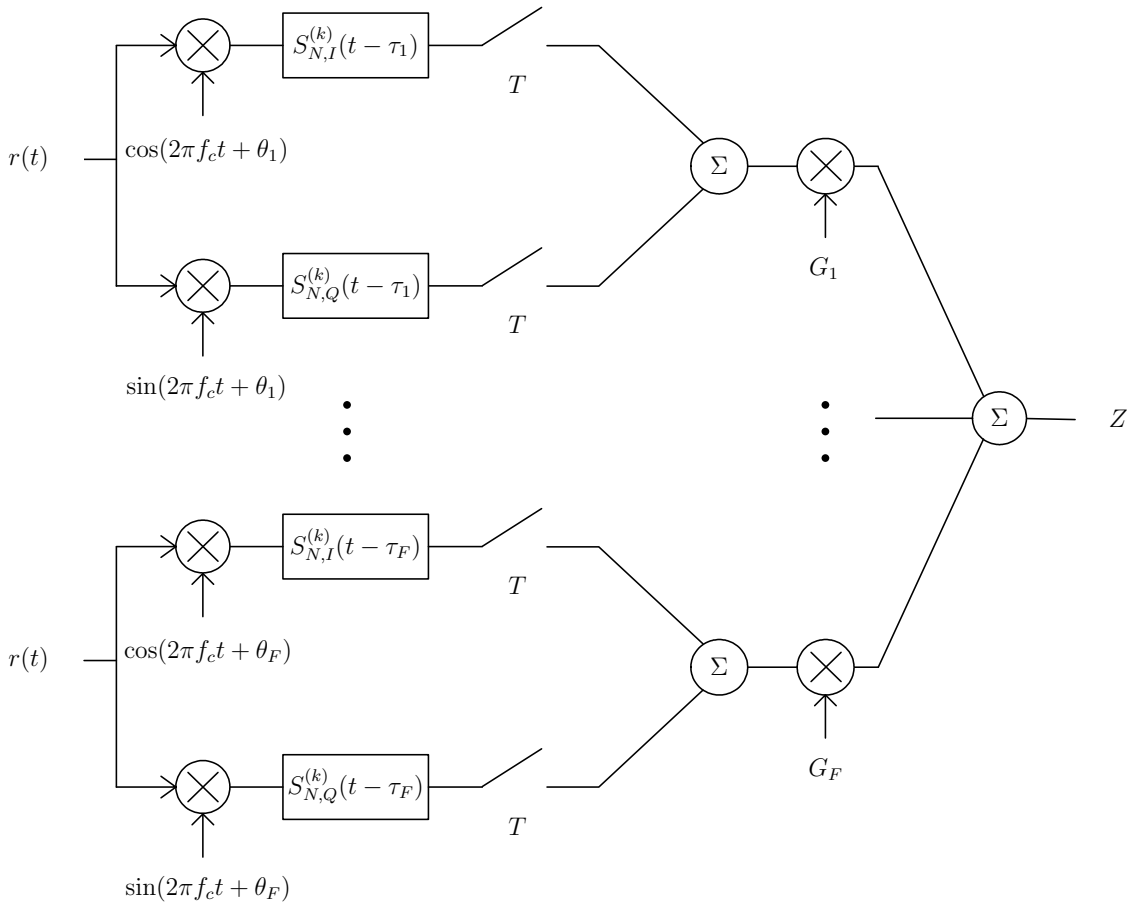

Figure 2: Balanced QPSK RAKE receiver for user k.

The variables $\tilde{s}_I^{(i)}$ and $\tilde{s}_Q^{(i)}$ represent, respectively, the spreading waveforms for the in-phase and quadrature of user i (the tilde entails that spreading waveforms are multiplied by the respective data bits).

It is implied that the channel response and the received signal are, respectively,

$$h(t) = \sum_{l=1}^{L} \bar{\alpha}_l \delta(t - \tau_l), \qquad r(t) = \left(\sum_{i=1}^{K} \sqrt{P^{(i)}} (\tilde{s}_I^{(i)}(t) - j\tilde{s}_Q^{(i)}(t)) \right) * h(t) + \mathcal{I}(t), \tag{3}$$

where $*$ stands for convolution.

At the receiver, in the bandpass domain, each RAKE finger multiplies $r(t)$ by coherent in-phase (I) and quadrature (Q) local oscillator references, namely, $\cos(\omega_c t + \theta_f)$ and $\sin(\omega_c t + \theta_f)$; the first and the second products are respectively correlated with a copy of $s_{I,N}^{(k)}(t - \tau_f)$ and $s_{Q,N}^{(k)}(t - \tau_f)$ (notice that the correlation includes the low-pass filtering); these two correlations are added together and the sum is then multiplied with G_f for MRC. The output of the fingers are added up to form the output of the QPSK RAKE receiver; this output, in the baseband domain, is equivalent to

$$Z = \frac{1}{2}\mathrm{Re}\left[\int_{-\infty}^{\infty} r(t) \cdot \mathrm{conj} \left\{ \sum_{f=1}^{F} \bar{G}_f \cdot (s_{N,I}^{(k)}(t - \tau_f) - j s_{N,Q}^{(k)}(t - \tau_f)) \right\} \right] \mathrm{d}t,$$

$$s_{N,I}^{(k)}(t) = \sum_{n=0}^{N-1} c_{I,n}^{(k)} g_1(t - nT_c), \quad s_{N,Q}^{(k)}(t) = \sum_{n=0}^{N-1} c_{Q,n}^{(k)} g_1(t - nT_c). \tag{4}$$

There has been a plethora of papers studying the performance of a CDMA system, starting with [54] and including papers such as [21] and [32].

In order to ease the analysis of CDMA systems, several simplifications have appeared throughout the literature; the following are some of them:

A) The assumption of short spreading codes, that is, codes that repeat every bit.

B) The autocorrelation of the spreading code is nonzero only when there is no offset.

C) The delay spread is smaller than T.

D) Rectangular pulse-shaping (waveform) instead of RRC.

E) Channel model where paths are spaced out by multiples of T_c instead of the more appropriate physical model where the paths can have any separation. In [63], these two models are respectively called the T-model (it will be called T_c-model because of the notation in this work) and the τ-model.

F) Maximum Ratio Combining (MRC) is accomplished by assuming that $\bar{G}_f = \bar{\alpha}_l$ when $\tau_f = \tau_l$ obtained from matching to $h(t)$; this type of simplified assignment is going to be referred as Simple MRC (SMRC). In reality, after despreading, a RAKE receiver perceives the composite $g(t) * h(t) * g(-t) = g_2(t) * h(t)$ where h(t) is a τ-model; therefore, the appropriate MRC should be obtained by matching to this composite; this assignment is going to be referred as Appropriate MRC (AMRC). In [63], it is mentioned that a T_c-model can be obtained from the composite by sampling at multiples of T_c, but these samples are correlated, yet in practice, this derived T_c-model (and a corresponding SMRC model matched to this T_c model) assumes that the samples are independent. The SMRC assumption is good when using rectangular pulse-shaping and a T_c-model, but not for RRC pulse shaping with subchip-spaced path delays.

Another key issue is that the delays corresponding to the local power maximums of this $g_2(t) * h(t)$ composite do not exactly correspond to the local maximums of $h(t)$; in other words, these new delays are a little different from the set of τ_l, $l = 1 \ldots L$.

Moreover, the optimum MRC takes into account the variance of the interference perceived by each finger as well as the correlation between each finger, but this fact is not considered in the 3G standards.

G) It is assumed that orthogonal codes have the same cross-correlation properties as two random codes when offset with respect to one another. This assumption results in a pessimistic estimation of the multipath interference for a system using orthogonal codes. In fact, it can be concluded from the work to be presented that the variance of the actual cross-correlation is always smaller or equal to the variance of the cross-correlation between random codes.

H) The spreading assumed is real (BPSK spreading); actually, CDMA systems use complex spreading.

A combination of C and D usually results in only two bits having to be considered.

The D and E assumptions result in the outputs of the fingers of the RAKE receiver to be mutually independent, which is not normally the case in practical situations.

The work by Pursley [54] presents a K-user BPSK system utilizing rectangular pulse shaping; the system is asynchronous in both the transmission time and the carrier phase for each user. The worst-case performance and the average signal-to-noise ratio are studied. This work contains the methodology, concepts, and notation that are used in studying CDMA systems up to the present (the notation presented above is more in terms of our work). Concepts such as the discrete aperiodic cross-correlation function (11) and the continuous-time partial croscorrelation functions (6) are utilized in his work.

Assuming that $0 < \tau_k \leq T$, the MAI interference of the k-th user to the i-th user is given as

$$I_{k,i} = T^{-1}[d_{-1}^{(i)} R_{k,i}(\tau_k) + d_0^{(i)} \hat{R}_{k,i}(\tau_k)] \cos \phi_n, \tag{5}$$

where

$$\begin{aligned} R_{k,i}(\tau) &= \int_0^{\tau} s^{(k)}(t+\tau_k)^* s^{(i)}(t) \mathrm{d}t, \\ \hat{R}_{k,i}(\tau) &= \int_{\tau}^{T} s^{(k)}(t-\tau_k)^* s^{(i)}(t) \mathrm{d}t; \end{aligned} \tag{6}$$

ϕ_n and τ_k represent the phase angle and delay of the waveform of the k-th user with respect to that of the i-th user.

Gilhousen et al. in [21] study the performance of both single-cell and multiple-cell CDMA systems from a system-level point of view, namely, from the point of view of power distributions and number and location of active users but not link-level considerations such as modulation, waveshaping, and spreading sequences.

With regards to the impact of waveshaping (including RRC) on CDMA performance, Anjaria and Wyrwas in [6] treat it for the first time, but their work is limited to waveshaping of one chip duration: $g(t) = \sqrt{\frac{2}{3}}(1-\cos(\frac{2\pi t}{T}))$ for $0 \leq t \leq T$, zero otherwise. The modulation is BPSK with differential data encoding; a T_c-model is utilized.

---

*Time-limited waveform (with duration T_c).

†Expression left in expectation form, i.e., $E[Z^2]$, etc.

‡Paths separated by T_c or more, but not necessarily multiples of T_c.

§Requires integration.

¶Infinite Sum.

Table 2: Assumptions made in representative studies. N. A. stands for not applicable.

Reference	Assumption								
	A	B	C	D	E	F	G	H	Closed
Sousa [16]			√		√	√	√	√	Yes
Pursley [54]	√	N.A.	√	√	N.A.	N.A.	N.A.	√	Yes
Kchao and Stuber [32]	√	√		√	√	N.A.	N.A.	√	Yes
Asano et al. [7]	N.A.			√*		N.A.	N.A.	√	Yes
Win et al. [67]	N.A.	√		√*	√	√	N.A.	√	Not Closed§
Cheun [13]				√	√‡	√	N.A.		Yes
Hwang [27]				√	√	√	N.A.	√	Not Closed§
Boujemaa and Siala [11]							N.A.		Yes
Ki, Kwon, et al. [33]							N.A.	√	Not Closed¶
Adachi [5]			√	√	√	√	√	√	Not Closed†
Fong et al. [17]			√	√	√	√	√	√	Not Closed†
Bottomley et al. [10]									Not Closed¶
Kuo [36]								√	Not Closed¶
Sun and Cox[64]									Not Closed†
Choi [15]				√	√	√	√		Yes
Geraniotis [20]				√	√	√	N.A.	√	Not Closed§
Proakis [52]		√		√	√	√	N.A.		Yes
Sebeni [58]			√	√	√	√	√	√	Yes

Assuming a BPSK system in the reverse link with large processing gain and random spreading sequences, Asano et al. [7] utilize RRC waveshaping for $g_1(t)$:

$$g_1(t) = 4\beta \frac{\cos[(1+\beta)\pi t/T_c] + \sin[(1-\beta)\pi t/T_c]/(4\beta t/T_c)}{\pi\sqrt{T_c}[(4\beta t/T_c)^2 - 1]}, \tag{7}$$

$$g_2(t) = g_1(t) * g_1(t) = \frac{\sin(\pi t/T_c)}{\pi t/T_c} \cdot \frac{\cos\beta\pi t/T_c}{1-(2\beta t/T_c)^2}. \tag{8}$$

The probability distribution of the MAI interference is assumed to be Gaussian; in the calculation of the variance, averaging is done over phases and path arrival time; the quantity $m_\phi = \frac{1}{T_c}\int_0^{T_c} g_2^2(t)\mathrm{d}t$ evaluates to $1 - \frac{\beta}{4}$. Therefore, for an asynchronous reverse-link system with one path and equal power received from each user, neglecting noise and self-interference, the probability of bit error becomes $P_e = Q\left(1/\sqrt{\frac{K-1}{2N}(1-\frac{\beta}{4})}\right)$ instead of $P_e = Q\left(\sqrt{\frac{3N}{K-1}}\right)$ for rectangular chips ($m_\phi = 1/3$), where

$$Q(x) = \int_x^\infty \frac{1}{\sqrt{2\pi}} e^{-(y^2/2)}\mathrm{d}y. \tag{9}$$

More recently, there have been some papers, such as [47] and [46], regarding the reverse link that could have some resemblance to the work presented here. These works study, respectively, the effect of processing gain (called chip rate) for CDMA and chip rate (properly called) for WCDMA, but both of these include only differential phase shift keying, RAKE receiver with equal-gain square law combining, and square pulse shaping.

The work by Kim et al. in [35] presents a simple comparison (ignores RAKE and multipath) of the reverse-link performance of a system using rectangular pulses and RRC with a roll-off factor of 0.35.

Using mathematical techniques, the work of Win et al. [67] results in simple expressions for the performance of the RAKE receiver as a function of bandwidth and number of fingers, but the receiver it considers uses BPSK, RRC waveform of chip duration, a T_c-model, and no MAI, just noise.

Cheun in [13] studies the performance of a single user of a long PN code (period of the code much larger than N) in the presence of only Gaussian noise. The system considers rectangle pulse-shaping and both BPSK and QPSK; for the RAKE receiver, selection combining, equal-gain combining, and simple MRC are considered. The finger selections are made based on the best paths instantaneously in one case and the best paths on average in another case. Given a certain time delay profile, path phases, and fading coefficients, a closed form is obtained after some simplifications. Nevertheless, since the analysis does not include MAI, just Gaussian noise and self-interference modelled as additional Gaussian noise, it does not correspond to a practical situation where multiple users share a cell. Moreover, the channel model utilized to arrive at the expressions is such that the paths are separated by at least T_c.

Using a BPSK system and rectangle pulse shaping, Hwang and Lee characterize the self-interference as a sum binomial variables in [27] and show that the Gaussian approximation is not accurate for processing gains that are less than 8; this fact has also been shown by Boujemaa and Siala in [11] for a QPSK system using RRC waveform with $\beta = 0.22$.

Ki et al. in [33] study the effect of finger spacing in the RAKE receiver, and it is a good work that includes RRC pulse shaping and AMRC, but only considers BPSK and leaves

many expressions in either convolution or matrix form.

Finally, [34] presents RRC, QPSK, and different chip rates, but no RAKE receiver.

Above all, the previous articles consider the reverse link, the link from the MS to the BS, has a set of implications that make it somewhat different from the forward link (BS to MS), to be considered here first. In the reverse link, the interference comes from many MSs; while in the forward link, it effectively comes from a few BSs. Same-cell users in the forward link are synchronized and their interference to the reference user travels through the same channel, which leads to an advantage in using orthogonal codes, even in multipath channels. In the reverse link, same-cell users are asynchronous (a synchronization procedure would be technically difficult) and the interference they cause travels through different channels. Since the BS is fixed and there is a multitude of MSs, on average, the power of the out-of-cell interference does not change much; on the other hand, the out-of-cell interference that MSs experience changes considerably as they move around. Moreover, same-cell-interference is a bigger problem in the reverse link than in the forward link. The overall effect of the same-cell and other-cell interference is that in the forward link you need a power control scheme that has less dynamic range, but is a function of both same-cell and other-cell interference. Moreover, a pilot signal is used in the forward link to demodulate the signals coherently, and QPSK is used in the forward link as opposed to OQPSK in the reverse link. More differences can be found in [38, p. 367].

The studies that most closely approach the one presented here are [5], [16], [17], and [10].

Adachi et al. [5] study the effect of using orthogonal codes multiplied by (concatenated with) random codes in the forward link. The type of spreading modulation is BPSK; the channel model is composed of paths separated by multiples of T_c; rectangle pulse-shaping is assumed.

DaSilva et al. [16] present a BPSK model where each user had a different phase; the pulse-shaping is RRC with a roll-off of zero (sinc function). The channel model is allowed to have any separation as long as the total delay spread is much smaller than T, the bit period. The processing gain is assumed to be high, and assumptions E and F are made. In obtaining

the performance, the power of the desired signal, the MAI, and the self-interference are averaged not only over the codes, but also over the phases of the paths; also, the weights of the fingers are set equal to the fading coefficients ($G_f = \alpha_f$ when $\tau_f = \tau_l$). Additionally, it is assumed that for each finger, the desired signal only comes from the path it is synchronized to, and assumption G is made. The performance is presented in terms of the cumulative distribution of the SNR due to orthogonal and random codes. Although this work presents the mentioned shortcomings, the approach is different from the line of papers dating back to [54]. In taking the expectation of the variances of the MAI and self-interference with respect to the codes, terms such as $\mathrm{E}[c_{n_1}^{(k)} c_{a_1}^{(i)} c_{n_2}^{(k)} c_{a_2}^{(i)} g_2((n_1 - a_1)T_c - \tau_{lf}) g_2((n_2 - a_2)T_c - \tau_{lf})]$ are obtained for both $i = k$ and $i \neq k$; taking into account whether the codes were random or orthogonal, this expectation is obtained for different possible cases such $n_1 = a_1$ when $n_2 = a_2$. A great deal of simplification is achieved in the expression for the SNR by using the following identity for sinc functions, which is obtained from the sampling theorem:

$$\sum_{n=-\infty}^{\infty} g^2(nT_c - \tau_{lf}) = \frac{1}{T_c} \int_{-\infty}^{\infty} g^2(t) \mathrm{d}t. \tag{10}$$

Fong et al. in [17] compare the performance of concatenating orthogonal with random codes on one hand and PN codes on the other hand. The discrete partial correlation functions are used, but the spreading modulation is BPSK, and the D, E, F assumptions are made. The $I_{k,i}$ expression in (5) is used to calculate the MAI. A Gaussian approximation is assumed. In calculating the variance of the interference, it is averaged not only over the codes, but also over the phases of the paths. The assumption that the MAI is Gaussian without being conditioned on the codes or phases of the paths appears to be good when D and E are also assumed.

Bottomley et al. [10] present the analysis of the performance of the RAKE receiver using MRC and maximum likelihood weights for the forward link, RRC waveshaping, orthogonal codes, and QPSK. To perform the analysis, the discrete aperiodic cross-correlation function,

defined in [54], is used. For a delay of τ and $0 \leq lT_c \leq \tau \leq (l+1)T_c \leq T$,

$$C_{k,i}(l) = \begin{cases} \sum_{n=0}^{N-1-l} c_n^{(k)} c_{n+l}^{(i)}, & : \quad 0 \leq l \leq N-1 \\ \sum_{n=0}^{N-1+l} c_{n-l}^{(k)} c_n^{(i)}, & : \quad 1-N \leq l \leq 0 \\ 0, & : \quad |l| \geq N. \end{cases} \tag{11}$$

The output of each finger in the RAKE receiver is obtained without the weights; this output is divided into desired signal y_d, interference due to ISI y_{ISI}, interference due to MAI y_{MAI}, and noise y_n. It is important to mention that their criteria for choosing what represents ISI and what is desired signal is that ISI includes only the signals belonging to the preceding and following bits ($m \neq 0$). The terms are assumed to be independent of one another; therefore, the correlation between different fingers (or the correlation of a finger) is assumed to be the sum of the correlation (or autocorrelation) due to ISI, MAI, and noise. Given fingers f_1 and f_2 synchronized to times τ_{f_1} and τ_{f_2}, these correlations and desired signal are given as

$$R_{ISI}(\tau_{f_1}, \tau_{f_2}) = \frac{1}{N^2} \sum_{l_1=0}^{L-1} \sum_{l_2=0}^{L-1} \bar{\alpha}_l \bar{\alpha}_f^* \cdot$$

$$\sum_{\substack{m=-\infty \\ m \neq 0}}^{\infty} \sum_{n=1-N}^{N-1} (N-|n|) g_2(\tau_{f_1} + nT_c - mT - \tau_{l_1}) g_2^*(\tau_{f_2} + nT_c - mT - \tau_{l_2}), \tag{12}$$

$$R_{MAI}(\tau_{f_1}, \tau_{f_2}) = \frac{1}{N^2} \sum_{l_1=0}^{L-1} \sum_{l_2=0}^{L-1} \bar{\alpha}_{l_1} \bar{\alpha}_{l_2}^* \cdot$$

$$\sum_{m=-\infty}^{\infty} \sum_{n=1-N}^{N-1} (N-|n|) g_2(\tau_{f_1} + nT_c - mT - \tau_{l_1}) g_2^*(\tau_{f_2} + nT_c - mT - \tau_{l_2})(1 - \delta(n)\delta(m)), \tag{13}$$

$$\bar{R}_{n'}(\tau_{f_1}, \tau_{f_2}) = g_2(\tau_{f_1}, \tau_{f_2}), \tag{14}$$

$$\bar{y}_d(\tau_{f_1}) = \sum_{l=0}^{L-1} \bar{\alpha}_l g_2(\tau_{f_1} - \tau_l). \tag{15}$$

The bar in $\bar{R}_{n'}(\tau_{f_1}, \tau_{f_2})$ and $\bar{y}_d(\tau_{f_1})$ represents averaging over the codes.

As it can be seen, the expressions obtained involve a great deal of computation.

Making vector $\mathbf{w}$ and $\mathbf{h}$ out of the y_d ($\mathbf{h}$ includes the power of the signal), the SNR is computed as

$$SNR = \frac{\mathbf{w}^H \mathbf{h} \mathbf{h}^H \mathbf{w}}{\mathbf{w}^H \mathbf{R}_u \mathbf{w}}, \tag{16}$$

where $\mathbf{R}_u$ is the sum of R_{ISI}, R_{MAI}, $\bar{R}_{n'}$ weighted with their respective powers. The only problem with this approach is that it considers the complex quantity $\mathbf{w^H h}$ instead of just the real part (necessary because of the correlator), as in [17], [33], and [36]. For MRC and other special cases, $\mathbf{w^H h}$ is in fact real, but the denominator of (16) becomes double for not using the real parts, but this factor is indeed considered when obtaining the BER. Also, R_{ISI} fails to consider self-interference that comes from the desired bit but from different paths as in [33]; nonetheless, this shortcoming can be easily fixed.

In most aspects, the approach of [33] is very similar to that in [10] and with the appropriate modifications, it arrives to equivalent expressions for the reverse link.

In the absence of MAI and using MRC, Sun and Cox in [64] compare analytical performance results with and without simplifications and simulation results. The waveform used is the sinc function and the MAI is ignored (signal in the presence of noise).

In [15], a comparison is presented between the performance of orthogonal codes and random codes. The system uses rectangular pulse shaping. The channel is assumed to be composed of L propagation paths spaced by multiples of a chip period. The desired signal at each path only comes from the path a RAKE finger is synchronized; for orthogonal codes, only the MAI interference synchronized to each RAKE finger is cancelled. These two assumptions are correct for the pulse shaping and channel model used, but real systems do not operate under these conditions.

In [31], almost the same approach is undertaken, although the analysis includes only BPSK, square pulse shaping, and SMRC for a system with one user with a RAKE receiver in the presence of noise.

In [8], channel delay profiles are explored where the paths and the RAKE fingers have sub-chip spacings for complex-spreading systems, but the rectangular pulse shaping is used and there is no maximum ratio combining. The weight for each RAKE is that of SMRC.

On the other hand, there are a few ways to calculate the (conditional) probability of error when the decision variable Z is assumed (conditionally) Gaussian and $L = F$. In [33],

Z is written as

$$Z = \mathrm{Re}\left\{\sum_{l=1}^{L} x_l y_l^*\right\} = x_l y_l^* + x_l^* y_l = \mathbf{z}^* \mathbf{Q} \mathbf{z}^{\mathbf{T}}, \tag{17}$$

where $\mathbf{z} = [\mathbf{x}\,\mathbf{y}]$, $\mathbf{x} = [x_1\, x_2 \ldots x_L]$ is the output of each finger without the weight, $\mathbf{y} = [y_1\, y_2 \ldots y_L]$ is the particular weight for each finger, and for $\mathbf{I}$ an $(L \times L)$ identity matrix

$$\mathbf{Q} = \begin{bmatrix} 0 & \mathbf{I} \\ \mathbf{I} & 0 \end{bmatrix}. \tag{18}$$

Using the characteristic function of Z as in [57],

$$P_e = \mathrm{Prob}\left[\mathbf{z}^* \mathbf{Q} \mathbf{z}^{\mathbf{T}} < 0\right] = \sum_{\lambda_i < 0} \prod_{\substack{l=1 \\ l \neq i}}^{2L} \frac{1}{1 - \lambda_l / \lambda_i}, \tag{19}$$

where for $i = 1, 2, \ldots 2L$, the set of λ_i is the set of eigenvalues of $\mathbf{RQ}$, $\mathbf{R} = \mathrm{E}[\mathbf{z}^{\mathbf{T}} \mathbf{z}^*]$.

Kuo in [36] has an alternative way of calculating (the conditional) P_e:

$$P_e = \frac{1}{2\pi j} \int_{s=\sigma - j\infty}^{\sigma + j\infty} \frac{\phi(s)}{s} \mathrm{d}s = \begin{cases} -\sum\limits_{right\, plane\, poles} \mathrm{Residue}\left[\dfrac{\phi(s)}{s}\right] \\ \sum\limits_{left\, plane\, poles \bigcup 0} \mathrm{Residue}\left[\dfrac{\phi(s)}{s}\right], \end{cases} \tag{20}$$

where $\phi(s)$ is the characteristic function of Z and $0 < \sigma <$ Re[first right plane pole of $\phi(s)$]:

$$\phi(s) = \mathrm{E}[\mathrm{e}^{-sZ}] = \frac{1}{\det(\mathbf{I} + s\mathbf{C_z Q})} \cdot \exp\left(-\mathrm{E}[\mathbf{z}]^H \mathbf{C_z^{-1}} [\mathbf{I} - (\mathbf{I} + \mathbf{sC_z Q})^{-1}] \mathrm{E}[\mathbf{z}]\right),$$
$$\mathbf{C_z} = \mathrm{E}[(\mathbf{z} - \mathrm{E}[\mathbf{z}])(\mathbf{z} - \mathrm{E}[\mathbf{z}])^H]. \tag{21}$$

The more common and straightforward way to obtain the (conditional) probability of error when Z is a (conditionally) Gaussian-distributed variable is by using the formula $Q(\sqrt{SNR})$, where SNR is $\mathrm{E}^2[Z]/\mathrm{Var}[Z]$. It should be noted that all these methods are equivalent. The unconditional probability is of course obtained from the conditional probability of error by averaging the latter over the conditional variables (such as phase and Rayleigh coefficients).

Geraniotis and Pursley in [20] use the method of characteristic functions, which does not assume Gaussianity in the calculation of P_e. For a single BPSK user with time-limited pulse (rectangular or sine) in the presence of noise, a receiver is synchronized to the first

(main) path of a τ-model channel. Modelling the output of the receiver as $Z = \eta_0 + \sqrt{\frac{1}{2}PT}\sum_{l=1}^{L} \cdot \alpha_l F_l$, where η is zero-mean Gaussian noise with mean $N_0T/4$ and F_l is similar to (5):

$$F_l = T^{-1}[d_{-1}^{(i)} R(\tau_l) + d_0^{(i)} \hat{R}(\tau_l)] \cos\phi_l, \tag{22}$$

then the probability of error given α_1 is shown to be

$$Q(\sigma^{-1}) + \pi^{-1} \int_0^{\infty} u^{-1} \sin(u) \phi_\eta [1 - \tilde{\phi}_0(u)\tilde{\phi}(u)] \mathrm{d}u, \quad \sigma^2 = (2E_b/N_o)^{-1}, \tag{23}$$

where ϕ_η, $\tilde{\phi}_0(u)$, $\tilde{\phi}(u)$ are the characteristic function of $\eta = \eta_0/(\sqrt{\frac{1}{2}PT})$, $\alpha_1 F_1$, and $\sum_{l=2}^{L} \alpha_l F_l$, respectively. These characteristic functions involve a great deal of computation.

Also, for one user in the presence of noise, transmitting in a T_c-model channel with L Rayleigh-distributed paths (having different powers), the work in [52, pg. 847] presents a well-known benchmark expression for the BER using BPSK (can be used for balanced QPSK):

$$P_2 = \frac{1}{2} \sum_{k=1}^{L} \pi_k \left[1 - \sqrt{\frac{\bar{\gamma}_k}{1 + \bar{\gamma}_k}} \right], \quad \pi_k = \prod_{\substack{i=1 \\ i \neq k}}^{L} \frac{\bar{\gamma}_k}{\bar{\gamma}_k - \bar{\gamma}_i}, \tag{24}$$

where for the nomenclature used, $\bar{\gamma}_k = \frac{\mathcal{E}}{N_o} \mathrm{E}[\alpha_k^2]$ is referred as the average SNR for finger k and $\gamma_b = \frac{\mathcal{E}}{N_o} \sum_{k=1}^{L} \alpha_k^2 = \gamma_k$ is referred as the SNR per bit.

The work by Geraniotis and Ghaffari in [18] extends the study to MAI for both BPSK and QPSK systems using random codes in the forward and reverse link. The forward link channel is assumed to be one path.

In [58], the study further extends to include concatenated orthogonal codes, SMRC, MAI, T_c-model, and rectangular pulse shaping. The Gaussian approximation is compared with results obtained using the characteristic function approach [20] and simulations. It is concluded that the Gaussian approximation is justified.

1.2.2 Orthogonality Factor

In the estimation of the system-level performance of novel architectures and schemes, usually some assumptions are made about the link level. Sometimes the effect of using orthogonal

codes is not considered as in [34]. Other times, the combined effect of using orthogonal codes, a particular waveform, chip rate, processing gain, RAKE receiver scheme, and modulation for a particular channel is modelled by a single parameter called orthogonality factor, which ranges between 0 and 1; its value is rather arbitrarily chosen as in [56], [65], and [42]. Qiu et al. in [55] estimate the performance of the forward link in CDMA for the typical urban (TU) channel assuming a value of 0.65 for the orthogonality factor, as obtained in [41]. Mehta et al. in [41] and [40] compare two expressions for the SNR at the output of the RAKE receiver. The expression

$$SNR = \frac{N P^{(k)} |\sum^{F} \bar{G}_f^* \bar{\alpha}_f|}{(\beta_o \sum_{\substack{i=1 \\ i \neq k}}^{K} P^{(i)} \sum^{L} |\bar{\alpha}_l^*| + I_{oc} + N_o) \sum_{f=1}^{F} |\bar{G}_f^*|^2} \tag{25}$$

is made equal to an actual SNR that is the ratio of the power of the desired signal at the output of the RAKE and the power of all the other sources (noise, out-of-cell users, same-cell users); then the equation is solved for β_o. In other words, a value for β_o is derived such that the expression above is equal to the actual SINR at the output of the RAKE. The actual SNR is obtained using an approach close to that in [17] and, as a result, it has similar shortcomings; the difference consisted in simulating RRC waveforming with roll-off factor of 0.22, and the study of both the traditional MRC ($\bar{G}_f = \alpha_f$) assignment and one that accounts for the difference in interference power that each finger observes in the absence of out-of-cell interference. This last assignment is not used by 3G mobile handsets; besides, a mechanism is needed to estimate the out-of-cell interference.

A value where β_o is averaged over the phases of the multipaths is also obtained. One of the peculiarities of this work is that although on average β_o is in the range from 0 to 1, instantaneously it can be greater than 1, which would go against the normal physical intuition that random codes can never perform better than orthogonal codes; this seems to suggest that the value obtained is instead an error factor to compensate the above expression to become the actual SNR. The phase-averaged value of β_o is given as

$$\mathrm{E}_\phi[\beta_o] = \frac{\sum_{f=1}^{F} \sum_{l=1}^{L} |\alpha_l|^2 |\alpha_f|^2 (|\hat{R}_{gg}(\tau'_{lf})|^2 + R_{gg}(\tau'_{lf})|)}{\left(\sum_{f=1}^{F} |\alpha_f|^2\right) \left(\sum_{l=1}^{L} |\alpha_l|^2\right)}, \tag{26}$$

where $\hat{R}_{gg}(\tau') = \int_{-\infty}^{\infty} g(t) g(t - \tau') \mathrm{d}t$ and $R_{gg}(\tau') = \int_{-\infty}^{\infty} g(t) g(t + T_c - \tau') \mathrm{d}t$.

In [48], the orthogonality factor is given as $\alpha = 1 - \frac{E_b}{I_o}(\frac{E_b}{N_o})^{-1}$, where $\frac{E_b}{N_o}$ is the figure required in the presence of intercell interference and $\frac{E_b}{I_o}$ is the figure required in the presence of same-cell interference; these figures are obtained from computer simulations.

Hunukumbure et al. in [26] and [25] study the orthogonality factor for wideband CDMA and MRC RAKE receiver based on the work in [5].

In [50], using SMRC and work in [52], the orthogonality factor is given as the complement of a "multipath loss factor" ($MPL = 1 - \alpha$):

$$MPL^{-1} = \sum_{f=1}^{F} \frac{|\alpha_f|^2}{\sum_{l \neq f} |\alpha_l|^2}. \tag{27}$$

1.2.3 Efficient and Accurate Performance Estimation for Reverse Link

In the estimation of the BER of the reverse link of binary CDMA, the Central Limit Theorem (CLT) is invoked to approximate the interference as being Gaussian in distribution; this approach, used in [54] and other articles, is generally known as Standard Gaussian Approximation (SGA). In this method, the average probability of error is determined by the average signal-to-noise ratio (SNR):

$$\bar{P}_e = Q(\sqrt{\mathrm{E}(SNR)}). \tag{28}$$

It has been shown that the BER obtained in system simulations departs from the BER obtained from SGA for low BER values [43] (in the order of 10^{-4} or less), which occurs when the number of users is much smaller than the processing gain.

In [39], an expression for the interference is derived for a particular code, phase, and delay of each interfering user; this work is used in [43] to obtain the probability density function (pdf) of Ψ, the variance of the MAI. Then, the average probability of error becomes

$$\bar{P}_e = E\left[Q\left(\frac{N}{\sqrt{\Psi}}\right)\right] = \int_0^\infty Q\left(\frac{N}{\sqrt{\Psi}}\right) f_{\Psi'}(\psi)\mathrm{d}\psi, \tag{29}$$

where the pdf of Ψ is obtained from convolution of the pdf for the variance of the interference for each user; the work was then improved in [44]. These last two works make the observation that for a large spreading gain N, a given set of delays and phases of the

interfering users, Ψ can be approximated as Gaussian. This approach (Eq. 2) is called Improved Gaussian Approach (IGA), but is computationally intensive. Consequently, another approach was devised that is simple without compromising the estimation: The Simplified Gaussian Approximation (SIGA) [24], which uses the work in [39] and [43], and a result from [23]. The SIGA approach was further simplified in [45] at a negligible impact on the estimation. These works have all assumed rectangular pulse shaping, which has a one chip duration. The work in [7] uses RRC pulses and assumes SGA, which was shown in [68] to be inaccurate, as in the rectangular case, for low BER situations. In [69], the SIGA approach is obtained for RRC pulses; the SIGA approach in this work presents a non-closed form that requires a great deal of computation.

All the previous works have only considered BPSK, but present spread-spectrum systems use offset QPSK (OQPSK); Song and Leung in [62], based on [69], present OQPSK BER expressions for bandlimited pulses, yet not in closed form either. Above all, none of these works present the effect of multiple paths from the same user and a RAKE receiver; neither they consider the effect of adjacent channel interference (ACI).

A closed form for SIGA for RRC pulses, based on and in inspired in the work in [45], is proposed.

1.3 Proposed Approach

The objective of the proposed research is to obtain analytical expressions to calculate the performance of 3G CDMA when applying SMRC and AMRC, τ-model channel, balanced and complex-spreading QPSK, RRC with any roll-off factor, variable chip rate, processing gain, and data rate for concatenated orthogonal codes, random codes, and noise. Quasi-Orthogonal codes and systems using Multicodes and Variable Spreading Factor are also to be considered. The results are to be accurate and computationally efficient to obtain. The so-called Orthogonality Factor, used in system simulations, is also to be studied.

We first demonstrate what part of $Z^{(i)}$ corresponds to Z_{Des}. It is then shown that $Z_{\substack{\text{Self} \\ \text{Interf}}}$, Z_{MAI}, and $\mathcal{I}_o$ are independent. The weights for SMRC and AMRC are obtained. For SMRC, the conditional variance of Z is obtained over the codes, data bits, and phases;

for AMRC, the conditional variance of Z is obtained only over codes and data bits. For SMRC, the interference is assumed conditionally Gaussian; for AMRC, it is shown to be conditionally Gaussian. The performance is obtained from $Q(\sqrt{SNR})$ and then Monte-Carlo averaging over the conditional variables.

In the calculation of the variance of the interference, the approach taken did not consider the discrete aperiodic cross-correlation function and the continuous-time partial croscorrelation functions from [54] as it is customary in many studies in the field. Rather, an approach was taken that is similar to that in [16], where a straight evaluation of expressions in the form $\mathrm{E}[c_{n_1}c_{a_1}c_{n_2}c_{a_2}]$ for random and orthogonal codes is performed.

In the expansion of the variance of Z we encounter terms in the form

$$\mathrm{E}_c\left[\sum_{n_1=0}^{N-1}\sum_{a_1=-\infty}^{\infty}\sum_{n_2=0}^{N-1}\sum_{a_2=-\infty}^{\infty} c^{(k)}_{\mathcal{C}_1,n_1} d^{(i)}_{\lfloor\frac{a_1}{N}\rfloor} c^{(i)}_{\mathcal{C}_2,a_1} c^{(k)}_{\mathcal{C}_3,n_2} d^{(i)}_{\lfloor\frac{a_2}{N}\rfloor} c^{(i)}_{\mathcal{C}_4,a_2}\right], \quad \mathcal{C}_1,\mathcal{C}_2,\mathcal{C}_3,\mathcal{C}_4 \,\epsilon\, \{\mathrm{I},\mathrm{Q}\}.$$

In the evaluation of $\mathrm{Var}[Z]$, the pairs of integrals that together contain only one code with a $\mathcal{C}$ equal to I or Q, are statistically orthogonal and do need to be evaluated; otherwise, depending on whether $i = k$ or $i \neq k$, we show the cases that need to be considered; for $k \neq i$ and all the $\mathcal{C}$ equal, the variance is nonzero when $n_1 = n_2$ and $a_1 = a_2$. All the nonzero cases are added. In the evaluation of the variance of Z, not only the variance of each finger, but also the covariance between fingers are derived.

The expressions obtained for SMRC are simpler than those for AMRC not only because of the choice of weights, but also because of the averaging over the ensemble of phases.

Also, following the approach in [16], where the sampling theorem is used to attain (10) for the sinc function, an adjustment to the sampling theorem (for functions that result in aliasing) and functional series were used to obtain expressions in closed form for an arbitrary roll-off factor:

$$\sum_{n=-\infty}^{\infty} g_2^2(nT_c-\tau) = 1-\frac{\beta}{2}\sin^2(\frac{\pi\tau}{T_c}),$$

$$\sum_{N=-\infty}^{\infty} g_2(nT_c-\tau)g_2(nT_c+\tau) = \mathrm{Sg}(\tau,-\tau) = g_2(2\tau)+\frac{1}{2}g_2(\tau)\sin(\frac{\tau\pi}{T_c})\sin(\frac{\beta\pi\tau}{T_c}),$$

$$\sum_{n=-\infty}^{\infty} g_2(nT_c-\tau_1)g_2(nT_c-\tau_2) = g_2(d)-\frac{\sin(\beta(d/T_c)\pi)}{2\pi(d/T_c)(1-\beta^2(d/T_c)^2)}\sin(\frac{\pi\tau_1}{T_c})\sin(\frac{\pi\tau_2}{T_c}),$$

where $d = \tau_1 - \tau_2$. It was subsequently observed that this adjustment in the Sampling Theorem is consistent with the Poisson Summation Formula [29, 49]:

$$\sum_{n=-\infty}^{\infty} x(t + nT_c) = \frac{1}{T_c} \sum_{m=-\infty}^{\infty} e^{j2\pi m f_c t} X(m f_c), \qquad f_c = \frac{1}{T_c}, \tag{30}$$

where T_c is an arbitrary constant and $X(f)$ is the Fourier transform of $x(t)$: $X(f) = \int_{-\infty}^{\infty} x(t) e^{-j2\pi f t} \mathrm{d}t$, provided that $x(t)$ satisfies some mild analytic conditions: for instance, that it be differentiable and it and its derivative decay reasonably rapidly at infinity.

The Orthogonality Factor is obtained from the expressions for random codes and orthogonal codes as the ratio of the carrier-to-interference ratio (CIR) values for orthogonal and random codes necessary to achieve 10^{-3} BER. The analysis of the performance can also be used for the ratio of the CIR values for orthogonal codes and Gaussian noise. Nevertheless, the expressions obtained for performance are simple, accurate, and fast to compute, thus eliminating the need to use the orthogonality factor.

CHAPTER II

FORWARD LINK PERFORMANCE

2.1 Simple MRC Model

2.1.1 Balanced Quaternary Transmitter

Following the nomenclature in the Background Section and referring to Figs. 1 and 2, the output of the RAKE receiver is given as

$$Z = \frac{1}{2}\mathrm{Re}\left[\int_{-\infty}^{\infty} r(t)\cdot \mathrm{conj}\left\{\sum_{f=1}^{F}\bar{G}_f\cdot(s_{N,I}^{(k)}(t-\tau_f)-js_{N,Q}^{(k)}(t-\tau_f))\right\}\right]\mathrm{d}t$$

$$=\sum_{i=1}^{K}\sum_{l=1}^{L}\sum_{f=1}^{F}G_f\alpha_l\sqrt{P^{(i)}}\frac{1}{2}\Big(\int_{-\infty}^{\infty}s_{N,I}^{(k)}(t)\tilde{s}_I^{(i)}(t-\tau_{lf})+s_{N,Q}^{(k)}(t)\tilde{s}_Q^{(i)}(t-\tau_{lf})\mathrm{d}t\cdot$$

$$\cos(\theta_l-\theta_f)+\int_{-\infty}^{\infty}s_{N,I}^{(k)}(t)\tilde{s}_Q^{(i)}(t-\tau_{lf})-s_{N,Q}^{(k)}(t)\tilde{s}_I^{(i)}(t-\tau_{lf})\mathrm{d}t\cdot\sin(\theta_l-\theta_f)\Big), \qquad (31)$$

where the parameter τ_{lf} is defined as $\tau_l-\tau_f$ (τ_f is the time the f-th finger is synchronized to). The effect of of $I(t)$ is treated in Appendix C. The chip waveform $g_1(t)$ is assumed not to be truncated; as a result, it is not necessary to consider partial aperiodic correlations of $g_1(t)$. The N subscript in $s_{N,I}^{(k)}(t)$ and $s_{N,Q}^{(k)}(t)$ is to emphasize that the received signal is correlated with a spreading waveform consisting of N chips; the subscript is going to be dropped from now on. The expression (31) can therefore be expanded as

$$Z=\frac{1}{2}\sum_{i=1}^{K}\sum_{l=1}^{L}\sum_{f=1}^{F}G_f\alpha_l\sqrt{P^{(i)}}\sum_{n=0}^{N-1}\sum_{a=-\infty}^{\infty}\Big(\Big[c_{I,n}^{(k)}d_{\lfloor\frac{a}{N}\rfloor}^{(i)}c_{I,a}^{(i)}g_2((n-a)T_c-\tau_{lf})+$$

$$c_{Q,n}^{(k)}d_{\lfloor\frac{a}{N}\rfloor}^{(i)}c_{Q,a}^{(i)}g_2((n-a)T_c-\tau_{lf})\Big]\cdot\cos(\theta_l-\theta_f)+$$

$$\Big[c_{Q,n}^{(k)}d_{\lfloor\frac{a}{N}\rfloor}^{(i)}c_{I,a}^{(i)}g_2((n-a)T_c-\tau_{lf})-c_{I,n}^{(k)}d_{\lfloor\frac{a}{N}\rfloor}^{(i)}c_{Q,a}^{(i)}g_2((n-a)T_c-\tau_{lf})\Big]\cdot\sin(\theta_l-\theta_f)\Big), \qquad (32)$$

where $g_2(t)=g_1(t)*g_1(t)$, namely, the raised cosine (RC) function with roll-off factor β [52, p. 560] (see also (8)). First, a system using only PN codes is going to be assumed. Each user is assigned unique in-phase and quadrature PN sequences (a total of $2K$ different PN codes) whose periods are assumed much larger than N. This system is called here random-codes system. Systems using Walsh (orthogonal) codes will be considered in section 2.1.4.

If PN sequences whose period is much greater than N are used, we have the code property

$$\mathrm{E}_c[c_{I,n}^{(i)}c_{I,a}^{(k)}] = \mathrm{E}_c[c_{Q,n}^{(i)}c_{Q,a}^{(k)}] = \delta_{na}\delta_{ik}, \tag{33}$$

where δ is the Kronecker delta. Moreover,

$$\mathrm{E}_c[c_{I,n}^{(k)}c_{Q,a}^{(i)}] = 0 \tag{34}$$

for any i and k, and the expectation of partial correlations (correlation over N chips) between different shifts of a PN sequence is zero. It is important to mention that although the mean of the correlation of two different sequences is zero, the variance is not.

On the other hand, if the Doppler fading is negligible, that is $f_dT \ll 1$, the α_l coefficients and the θ_l phases do not change significantly during a bit period.

We need to determine the desired signal and the appropriate finger weights. The terms multiplied by $\sin(\theta_l - \theta_f$ in (32) do not add to the desired signal; they add to the self-interference and the MAI. Using the remaining terms in (31), for finger f and user $i = k$,

$$\frac{1}{2}\sum_{l=1}^{L} G_f\alpha_l\sqrt{P^{(k)}}\sum_{n=0}^{N-1}\sum_{a=-\infty}^{\infty} d_{\lfloor\frac{a}{N}\rfloor}^{(k)}(c_{I,n}^{(k)}c_{I,a}^{(k)} + c_{Q,n}^{(k)}c_{Q,a}^{(k)})\cdot g_2((n-a)T_c - \tau_{lf})\cos(\theta_l - \theta_f). \tag{35}$$

If the weight G_f is temporarily ignored and the analysis in [52, pp. 554-555] is applied to our spread spectrum signal, the output of each finger can be reformulated as ($y_a = R_f$ without G_f)

$$y_a = d_{\lfloor\frac{a}{N}\rfloor}^{(k)}x_o +$$
$$\frac{1}{2}\sum_{l=1}^{L}\alpha_l\sqrt{P^{(k)}}\sum_{\substack{n=0\\n\neq a}}^{N-1}\sum_{a=-\infty}^{\infty} d_{\lfloor\frac{a}{N}\rfloor}^{(k)}(c_{I,n}^{(k)}c_{I,a}^{(k)} + c_{Q,n}^{(k)}c_{Q,a}^{(k)})g_2((n-a)T_c - \tau_{lf})\cos(\theta_l - \theta_f),$$
$$x_o = \frac{1}{2}\sqrt{P^{(k)}}\sum_{n=0}^{N-1}\sum_{\substack{a=-\infty\\a=n}}^{\infty}(c_{I,n}^{(k)}c_{I,a}^{(k)} + c_{Q,n}^{(k)}c_{Q,a}^{(k)}) = \sum_{l=1}^{L}\alpha_l\sqrt{P^{(k)}}Ng_2(\tau_{lf})\cos(\theta_l - \theta_f).$$

In [52], it is explained that the first term of y_a represents the desired signal (for each finger and without G_f) and the second, ISI. Notice that due to chip pulse shaping, signal multipath for the reference user does contribute to its signal power (when $a = n$) and also contributes to the ISI (when $a \neq n$). The closer a second path is to the one the finger is synchronized

to (smaller τ_{lf}), the less it contributes to the interference and the more it contributes to the mean. Then in our case, setting $d^{(k)} = 1$ without a loss in generality,

$$Z_{\text{Des}} = \sum_{f=1}^{F} G_f \sum_{l=1}^{L} \alpha_l \sqrt{P^{(k)}} N g_2(\tau_{lf}) \cos(\theta_l - \theta_f). \tag{36}$$

Ignoring $\sqrt{P^{(k)}}$ and N in x_o, which are common to all fingers, it can be seen that the signal for finger f is proportional to $\sum_{l=1}^{L} \alpha_l g_2(\tau_{lf}) \cos(\theta_l - \theta_f)$, that is, a particular finger f synchronized to the path arriving at τ_f actually perceives a composite of paths: The pulse-shaping tends to smear the different paths together [66]. Therefore, if each finger experiences the same interference, for MRC it is necessary to set

$$\bar{G}_f = \sum_{l=1}^{L} \bar{\alpha}_l g_2(\tau_{lf}) \tag{37}$$

(these conditions for G_f and θ_f are called here appropriate MRC model, AMRC, which will be considered in section 2.2); for a finger f synchronized to path l_1, $G_f e^{j\theta_f}$ is usually picked to be the complex conjugate of $\alpha_l e^{j\theta_l}$ (this simple MRC model is called SMRC). The two models converge as the paths become more separated; the models are equal when the paths are spaced by exact multiples of T_c. For this section, SMRC is followed:

$$\bar{G}_f = \bar{\alpha}_f \quad \text{when } f = l. \tag{38}$$

The mean of $Z^{(k)}$, considering the code properties presented above, becomes (subscript c for codes)

$$\mathrm{E}_c[Z^{(k)}] = N \sum_{l=1}^{L} \sum_{f=1}^{F} \alpha_f \alpha_l d_0^{(k)} \sqrt{P^{(k)}} g_2(\tau_{lf}) \cos(\theta_l - \theta_f). \tag{39}$$

Whenever finger f is locked to path l, and there is another path l_2 nearby, because of fading l_2 occasionally might be strong enough to make the phase of G_f for SMRC be off by more than $\pi/2$ with respect to the phase of G_f AMRC. This problem is remedied by making $\bar{G}_f = -\bar{\alpha}_f$ in this situation. More on the finger selection process is considered in the numerical results section.

The desired signal (same as mean of Z) becomes

$$Z_{\text{Des}} = \mathrm{E}_c[Z] = \mathrm{E}_c[Z_{n=a}^{(k)}] = \sum_{l=1}^{L} \sum_{f=1}^{F} \alpha_f \alpha_l \sqrt{P^{(k)}} N d_0^{(k)} g_2(\tau_{lf}) \cos(\theta_l - \theta_f). \tag{40}$$

Each of the factors α_l, θ, d, and $P^{(k)}$ are dependent on time and assumed independent of one another. The parameter of importance in calculating the SNR is the average power of $Z_{\rm Des}$. It is assumed that Z is Gaussian conditioned on the set of fading coefficients $\boldsymbol{\alpha} = \{\alpha_1, \alpha_2, ..., \alpha_L\}$ as in [37]; then, the average BER is

$$P_e = \int Q(\sqrt{SNR_{\boldsymbol{\alpha}}})\mathrm{p}(\boldsymbol{\alpha})\mathrm{d}\boldsymbol{\alpha}, \qquad \mathrm{SNR}_{\boldsymbol{\alpha}} = \frac{\mathrm{E}[Z_{\rm Des}^2|\boldsymbol{\alpha}]}{\sum_{f=1}^{F}\Big\{\mathrm{Var}[R_f|\boldsymbol{\alpha}] + \sum_{\substack{f_1=1\\f_1\neq f}}^{F}\mathrm{Cov}[R_f, R_{f_1}|\boldsymbol{\alpha}]\Big\}}. \quad (41)$$

Expanding $Z_{\rm Des}^2$ results

$$\mathrm{E}[Z_{\rm Des}^2] = N^2\sum_{f_1=1}^{F}\sum_{f_2=1}^{F}\sum_{l_1=1}^{L}\sum_{l_2=1}^{L}\alpha_{f_1}\alpha_{f_2}\alpha_{l_1}\alpha_{l_2}P^{(k)}g_2(\tau_{l_1f_1})g_2(\tau_{l_2f_2})\cdot \quad (42)$$

$$\cos(\theta_{l_1}-\theta_{f_1})\cos(\theta_{l_2}-\theta_{f_2}). \quad (43)$$

When the expectation is taken with respect to the phases, there are the following cases:

a) $l_1 = f_1$, $l_2 = f_2$ results in $N\sum_{f_1=1}^{F}\sum_{f_2=1}^{F}\alpha_{f_1}^2\alpha_{f_2}^2$, $F \leq L$,

b) $l_1 = l_2$, $f_1 = f_2$ results in $\frac{N}{2}\sum_{l_1=1}^{L}\sum_{f_1=1}^{F}\alpha_{l_1}^2\alpha_{f_1}^2 g_2^2(\tau_{l_1f_1})$,

c) $l_1 = f_2$, $l_2 = f_1$ results in $\frac{N}{2}\sum_{f_1=1}^{F}\sum_{f_2=1}^{F}\alpha_{f_1}^2\alpha_{f_2}^2 g_2^2(\tau_{f_2f_1})$, and

d) $l_1 = l_2 = f_1 = f_2$ results in $N\sum_{f}^{F}\alpha_f^4$.

Adding the first three cases and considering that the last case is common to all of the previous three, the following mean conditioned on $\boldsymbol{\alpha}$ is reached:

$$\mathrm{E}[Z_{\rm Des}|\boldsymbol{\alpha}] = N^2P^{(k)}\sum_{f_1=1}^{F}\alpha_{f_1}^2\Big\{\sum_{f_2=1}^{F}\alpha_{f_2}^2\Big(1+\frac{1}{2}g_2^2(\tau_{f_2f_1})\Big) + \frac{1}{2}\sum_{l_1=1}^{L}\alpha_{l_1}^2 g_2^2(\tau_{l_1f_1}) - \alpha_{f_1}^2\Big\}. \quad (44)$$

On the other hand, when expanding Z^2 in (32), 10 summation signs are obtained (let's called them summations in i_1, i_2, l_1, l_2, f_1, f_2, n_1, n_2, a_1, and a_2). In the derivation of $E_c[Z^2]$ from (32), observe that terms with factors in the form

$$\mathrm{E}_c\left[\sum_{n_1=0}^{N-1}\sum_{a_1=-\infty}^{\infty}\sum_{n_2=0}^{N-1}\sum_{a_2=-\infty}^{\infty}c_{\mathcal{C}_1,n_1}^{(k)}d_{\lfloor\frac{a_1}{N}\rfloor}^{(i_1)}c_{\mathcal{C}_2,a_1}^{(i_1)}c_{\mathcal{C}_3,n_2}^{(k)}d_{\lfloor\frac{a_2}{N}\rfloor}^{(i_2)}c_{\mathcal{C}_4,a_2}^{(i_2)}\right], \quad \mathcal{C}_1,\mathcal{C}_2,\mathcal{C}_3,\mathcal{C}_4\,\epsilon\,\{I,Q\} \quad (45)$$

are obtained. They reduce to zero if $i_1 \neq i_2$ and as a result, $\mathrm{Var}[Z|\boldsymbol{\alpha}] = \mathrm{Var}[\sum_{i=1}^{K}Z^{(i)}|\boldsymbol{\alpha}] = \sum_{i=1}^{K}\mathrm{Var}[Z^{(i)}|\boldsymbol{\alpha}]$. Because $Z = \sum_{f=1}^{F}R_f$,

$$\mathrm{Var}[Z|\boldsymbol{\alpha}] \;=\; E[Z^2|\boldsymbol{\alpha}] - E^2[Z|\boldsymbol{\alpha}] = \sum_{f_1=1}^{F}\sum_{f_2=1}^{F}\mathrm{E}[R_{f_1}R_{f_2}|\boldsymbol{\alpha}] - \sum_{f_1=1}^{F}\sum_{f_2=1}^{F}\mathrm{E}[R_{f_1}|\boldsymbol{\alpha}]\mathrm{E}[R_{f_2}|\boldsymbol{\alpha}]$$

$$= \sum_{f=1}^{F} \mathrm{Var}[R_f|\boldsymbol{\alpha}] + \sum_{f_1=1}^{F} \sum_{\substack{f_2=1 \\ f_2 \neq f_1}}^{F} \mathrm{Cov}[R_{f_1}, R_{f_2}|\boldsymbol{\alpha}]$$

$$= \sum_{f=1}^{F} \Big(\mathrm{Var}[R_f^{(k)}|\boldsymbol{\alpha}] + \mathrm{Cov}[R_f^{(k)}|\boldsymbol{\alpha}] \Big) + \sum_{\substack{i=1 \\ i \neq k}}^{K} \Big(\sum_{f=1}^{F} \mathrm{Var}[R_f^{(i)}|\boldsymbol{\alpha}] + \sum_{f_1=1}^{F} \sum_{\substack{f_2=1 \\ f_2 \neq f_1}}^{F} \mathrm{Cov}[R_{f_1}^{(i)} R_{f_2}^{(i)}|\boldsymbol{\alpha}] \Big)$$

$$= \mathrm{Var}[Z_{\substack{\mathrm{Self} \\ \mathrm{Interf}}}|\boldsymbol{\alpha}] + \mathrm{Var}[Z_{\mathrm{MAI}}|\boldsymbol{\alpha}]. \tag{46}$$

It will be observed later that the P_e obtained by averaging the numerator and denominator over the phases is only accurate for a channel where paths are separated by T_c or more.

2.1.2 Self-Interference

It can be seen that expanding Z^2 from (31) and (32) for $i = k$, double sums in l and f are obtained, and are called here sums in l_1, l_2, f_1, and f_2. This expansion results in factors in the form $y_{l_1,f_1} \cdot y_{l_2,f_2}$, where $y_{l,f} \, \epsilon \, \{\cos(\theta_l - \theta_f), \sin(\theta_l - \theta_f)\}$. For $f_1 = f_2$ (variance of R_{f_1}), these terms reduce to zero when averaged over the phase unless $l_1 = l_2$; for $f_1 \neq f_2$ (covariance of R_{f_1} and R_{f_2}), these factors reduce to zero unless

a) $f_1 = l_1$ and $f_2 = l_2$ or

b) $f_1 = l_2$ and $f_2 = l_1$

The first case results in the factor $g_2((n_1 - a_1)T_c)g_2((n_2 - a_2)T_c)$, which is nonzero for $n_1 = a_1$ and $n_2 = a_2$, and thus belongs to the mean (and therefore Z_{Des}), but not the variance (self-interference). Additionally, for $i = k$ in (31), the correlation (over the codes) between the first and second terms is nonzero; the same applies to the third and fourth terms; any other pairs are statistically orthogonal (with respect to codes); for instance,

$$\mathrm{E}_c[\int_{-\infty}^{\infty} s_I^{(k)} \tilde{s}_I^{(k)}(t - \tau_{lf})\mathrm{d}t \int_{-\infty}^{\infty} s_I^{(k)} \tilde{s}_Q^{(k)}(t - \tau_{lf})\mathrm{d}t] =$$

$$\mathrm{E}_c\Big\{ \sum_{n_1=0}^{N-1} \sum_{a_1=0}^{\infty} \sum_{n_2=0}^{N-1} \sum_{a_2=0}^{\infty} d_{\lfloor \frac{a_1}{N} \rfloor}^{(k)} d_{\lfloor \frac{a_2}{N} \rfloor}^{(k)} c_{I,n_1}^{(k)} c_{I,a_1}^{(k)} c_{I,n_2}^{(k)} c_{Q,a_2}^{(k)} \cdot$$

$$g_2((n_1 - a_1)T_c - \tau_{lf})g_2((n_2 - a_2)T_c - \tau_{lf}) \Big\} = 0 \tag{47}$$

for the first and third terms because $E_c[c_{I,n_1}^{(k)} c_{I,a_1}^{(k)} c_{I,n_2}^{(k)} c_{Q,a_2}^{(k)}] = 0$.

$$\text{Then,} \quad \mathrm{E}_c[R_f^2 | i=k] = \frac{1}{4}\sum_{l=1}^{L} \alpha_f^2 \alpha_l^2 P^{(k)} \mathrm{E}_c\Big\{ \Big[\Big(\int_{-\infty}^{\infty} s_I^{(k)}(t)\tilde{s}_I^{(k)}(t-\tau_{lf})\mathrm{d}t \Big)^2 + \Big(\int_{-\infty}^{\infty} s_Q^{(k)}(t)\tilde{s}_Q^{(k)}(t-\tau_{lf})\mathrm{d}t \Big)^2 + 2\int_0^T s_I^{(k)}(t)\tilde{s}_I^{(k)}(t-\tau_{lf})\mathrm{d}t \cdot \int_{-\infty}^{\infty} s_Q^{(k)}(t)\tilde{s}_Q^{(k)}(t-\tau_{lf})\mathrm{d}t \Big] \cos^2(\theta_l - \theta_f) + \Big[\Big(\int_{-\infty}^{\infty} s_I^{(k)}(t)\tilde{s}_Q^{(k)}(t-\tau_{lf})\mathrm{d}t \Big)^2 + \Big(\int_{-\infty}^{\infty} s_Q^{(k)}(t)\tilde{s}_I^{(k)}(t-\tau_{lf})\mathrm{d}t \Big)^2 - 2\int_{-\infty}^{\infty} s_I^{(k)}(t)\tilde{s}_Q^{(k)}(t-\tau_{lf})\mathrm{d}t \cdot \int_{-\infty}^{\infty} s_Q^{(k)}(t)\tilde{s}_I^{(k)}(t-\tau_{lf})\mathrm{d}t \Big] \sin^2(\theta_l - \theta_f) \Big\}. \tag{48}$$

Because of the independence of the variables d_m ($m = \lfloor \frac{n}{N} \rfloor$), the expectation of the first term with respect to the data bits (d) becomes

$$\begin{aligned} \mathrm{E}_d\left[\left(\int_{-\infty}^{\infty} s_I^{(k)}(t)\tilde{s}_I^{(k)}(t-\tau_{lf})\mathrm{d}t \right)^2 \right] &= \mathrm{E}_d\left[\left(\sum_m d_m^{(k)} \rho_m^{(k)}(\tau_{lf}) \right)^2 \right] \\ &= \mathrm{E}_d\left[\sum_m \left(\rho_m^{(k)}(\tau_{lf}) \right)^2 \right] \\ = \sum_m \sum_{n_1=0}^{N-1} \sum_{a_1=mN}^{(m+1)N-1} \sum_{n_2=0}^{N-1} \sum_{a_2=mN}^{(m+1)N-1} & c_{I,n_1}^{(k)} c_{I,a_1}^{(k)} c_{I,n_2}^{(k)} c_{I,a_2}^{(k)} \cdot \\ & g_2((n_1-a_1)T_c - \tau_{lf}) \cdot g_2((n_2-a_2)T_c - \tau_{lf}), \end{aligned} \tag{49}$$

where partial correlation $\rho_m^{(i)}(\tau_{lf})$ is defined as

$$\rho_m^{(i)}(\tau_{lf}) = \int_{-\infty}^{\infty} s_T^{(k)}(t) s_{T,m}^{(i)}(t-\tau_{lf})\,\mathrm{d}t, \qquad s_{T,m}^{(i)} = \sum_{a=mN}^{(m+1)N-1} c_a^{(i)} g_1(t-aT_c). \tag{50}$$

The expectation $\mathrm{E}_c[c_{I,n_1}^{(k)} c_{I,a_1}^{(k)} c_{I,n_2}^{(k)} c_{I,a_2}^{(k)}]$ is nonzero for the code cases

i) $n_1 = a_1$ and $n_2 = a_2$,

ii) $n_1 = n_2$ and $a_1 = a_2$,

iii) $n_1 = a_2$ and $a_1 = n_2$,

iv) $n_1 = n_2 = a_1 = a_2$.

Case i belongs to the mean; for case ii, making $n = n_1 - a_1 = n_2 - a_2$, $N\sum_{n=-\infty}^{\infty} g_2^2(nT_c - \tau_{lf})$; for iii, making $n = n_1 - n_2 = a_2 - a_1$, $\sum_{n=-(N-1)}^{N-1}(N-|n|) g_2(nT_c + \tau_{lf}) g_2(nT_c - \tau_{lf})$. Both cases ii and iii include case iv, which yields $N g_2^2(\tau_{lf})$ and is also part of the mean when case i is possible.

To calculate the variance of R_f (for $i = k$), it can observed that the first integral results in cases ii and iii; the second integral, in cases ii and iii; the third integral, in (2 times) case i (and then does not add to the variance); the fourth, in case ii; the fifth, in case iii; the sixth, in (-2 times) case iii. The expectation of the cases is independent of the integral they come from (all cases iii for instance result in the same expression). Adding all the cases together yields (4 times) case ii. Using the relation (101), derived in Chapter 3, and remembering to subtract case iv,

$$\mathrm{Var}[R_f|i=k,\boldsymbol{\alpha}] = \frac{1}{2}\sum_{l=1}^{L}\alpha_f^2\alpha_l^2 P^{(k)} N\Big\{1-\frac{\beta}{2}\sin^2(\frac{\pi\tau_{lf}}{T_c}) - g_2^2(\tau_{lf})\Big\}. \tag{51}$$

When $f_1 \neq f_2$, it was mentioned above that the covariance between the outputs of the fingers due to self interference can be obtained by applying case b) $f_1 = l_2$ and $f_2 = l_1$:

$$\begin{aligned}
&\mathrm{Cov}[R_{f_1}R_{f_2}|i=k,\boldsymbol{\alpha}] = \\
&\frac{1}{4}\alpha_{f_1}^2\alpha_{f_2}^2 P^{(k)}\Big\{\Big[\int_{-\infty}^{\infty} s_I^{(k)}(t)\tilde{s}_I^{(k)}(t-\tau_{f_2f_1})\mathrm{d}t\cdot\int_{-\infty}^{\infty} s_I^{(k)}(t)\tilde{s}_I^{(k)}(t-\tau_{f_1f_2})\mathrm{d}t + \\
&\qquad\int_{-\infty}^{\infty} s_Q^{(k)}(t)\tilde{s}_Q^{(k)}(t-\tau_{f_2f_1})\mathrm{d}t\cdot\int_{-\infty}^{\infty} s_Q^{(k)}(t)\tilde{s}_Q^{(k)}(t-\tau_{f_1f_2})\mathrm{d}t + \\
&2\int_{-\infty}^{\infty} s_I^{(k)}(t)\tilde{s}_I^{(k)}(t-\tau_{f_2f_1})\mathrm{d}t\cdot\int_{-\infty}^{\infty} s_Q^{(k)}(t)\tilde{s}_Q^{(k)}(t-\tau_{f_1f_2})\mathrm{d}t\Big]\cos^2(\theta_{f_1}-\theta_{f_2}) \\
&\qquad-\Big[\int_{-\infty}^{\infty} s_I^{(k)}(t)\tilde{s}_Q^{(k)}(t-\tau_{f_2f_1})\mathrm{d}t\cdot\int_{-\infty}^{\infty} s_I^{(k)}(t)\tilde{s}_Q^{(k)}(t-\tau_{f_1f_2})\mathrm{d}t + \\
&\qquad\int_{-\infty}^{\infty} s_Q^{(k)}(t)\tilde{s}_I^{(k)}(t-\tau_{f_2f_1})\mathrm{d}t\cdot\int_{-\infty}^{\infty} s_Q^{(k)}(t)\tilde{s}_I^{(k)}(t-\tau_{f_1f_2})\mathrm{d}t \\
&-2\int_{-\infty}^{\infty} s_I^{(k)}(t)\tilde{s}_Q^{(k)}(t-\tau_{f_2f_1})\mathrm{d}t\cdot\int_{-\infty}^{\infty} s_Q^{(k)}(t)\tilde{s}_I^{(k)}(t-\tau_{f_1f_2})\mathrm{d}t\Big]\sin^2(\theta_{f_1}-\theta_{f_2})\Big\}
\end{aligned} \tag{52}$$

instead of (48). Again, considering code cases i, ii, iii, and iv results in 4 times case iii; case i belongs to the mean. Particularly, for the first integral above, when using the relation

$$\mathrm{E}_d\left[\left(\sum_m d_m^{(k)}\rho_m^{(k)}(\tau_{lf})\right)\left(\sum_m d_m^{(k)}\rho_m^{(k)}(-\tau_{lf})\right)\right] = \sum_m p_m^{(i)}(\tau_{lf})p_m^{(i)}(-\tau_{lf}), \tag{53}$$

it becomes

$$\begin{aligned}
&\frac{1}{8}\alpha_{f_1}^2\alpha_{f_2}^2 P^{(k)}\mathrm{E}_c\Big[\sum_m\sum_{n_1=0}^{N-1}\sum_{a_1=mN}^{(m+1)N-1}\sum_{n_2=0}^{N-1}\sum_{a_2=mN}^{(m+1)N-1} c_{n_1}^{(k)}c_{a_1}^{(k)}c_{n_2}^{(k)}c_{a_2}^{(k)}\cdot \\
&\qquad g_2((n_1-a_1)T_c+\tau_{lf})g_2((n_2-a_2)T_c-\tau_{lf})\Big]
\end{aligned} \tag{54}$$

after taking the expectation with respect to the phases and then,

$$\mathrm{Cov}[R_{f_1}, R_{f_2}|i=k,\boldsymbol{\alpha}] = \frac{1}{2}\alpha_{f_1}^2\alpha_{f_2}^2 P^{(k)} \left[\sum_{\substack{n=-N \\ n\neq 0}}^{N} (N-|n|) g_2(nT_c - \tau_{f_2 f_1}) g_2(nT_c - \tau_{f_2 f_1})\right]. \quad (55)$$

Notice that because of the choice of $\bar{G}_f$, $\mathrm{Cov}[R_{f_1}, R_{f_2}]$ does not tend to $\mathrm{Var}[R_{f_1}]$ for $f_1 = f_2$.

2.1.3 Multi-Access Interference

To calculate the variance of the MAI interference, note that for $i \neq k$, (31), all the terms are statistically orthogonal with one another, and thus the variance of the output of the finger f due to MAI is given by

$$\mathrm{Var}_c[R_f|i\neq k] = \frac{1}{4}\sum_{\substack{i=1 \\ i\neq k}}^{K}\sum_{l=1}^{L} \alpha_f^2\alpha_l^2 P^{(i)} \Big\{ \mathrm{E}_c\Big[\Big(\int_{-\infty}^{\infty} s_I^{(k)}(t)\tilde{s}_I^{(i)}(t-\tau_{lf})\mathrm{d}t\Big)^2 + \Big(\int_{-\infty}^{\infty} s_Q^{(k)}(t)\tilde{s}_Q^{(i)}(t-\tau_{lf})\mathrm{d}t\Big)^2\Big] \cdot \cos^2(\theta_l - \theta_f) + \mathrm{E}_c\Big[\Big(\int_{-\infty}^{\infty} s_I^{(k)}(t)\tilde{s}_Q^{(i)}(t-\tau_{lf})\mathrm{d}t\Big)^2 + \Big(\int_{-\infty}^{\infty} s_Q^{(k)}(t)\tilde{s}_I^{(i)}(t-\tau_{lf})\mathrm{d}t\Big)^2\Big] \sin^2(\theta_l - \theta_f)\Big\}. \quad (56)$$

Taking the inner expectations and noticing that $\mathrm{E}[(\int_{-\infty}^{\infty} s_I^{(k)}(t) d_m^{(k)} s_I^{(i)}(t-\tau_{lf})\mathrm{d}t)^2]$, the expectation of the other three terms are all equal to $(1 - \frac{\beta}{2}\sin^2(\frac{\pi\tau_{lf}}{T_c}))$ since they involve factors in the form $\mathrm{E}_c[c_{I,n_1}^{(k)} c_{I,a_1}^{(i)} c_{I,n_2}^{(k)} c_{I,a_2}^{(i)}]$, which reduce to zero unless $n_1 = n_2$ and $a_1 = a_2$ (case ii). Therefore, the above expression results in

$$\mathrm{Var}[R_f|i\neq k,\boldsymbol{\alpha}] = \frac{1}{2}\sum_{\substack{i=1 \\ i\neq k}}^{K}\sum_{l=1}^{L} \alpha_f^2\alpha_l^2 P^{(i)} N\Big\{1 - \frac{\beta}{2}\sin^2(\frac{\pi\tau_{lf}}{T_c})\Big\}. \quad (57)$$

Notice that case iv is not substracted here since case i is not possible.

On the other hand, the covariance between two different fingers, which for MAI only is the same as the correlation, is obtained in a very similar way as for the self-interference. The difference now is that the case that makes a contribution is a)$f_1 = l_1$ and $f_2 = l_2$. Case b)$f_1 = l_2$ and $f_2 = l_1$ reduces to zero after averaging over the phases. Therefore, the covariance between the fingers due to MAI is simply

$$\mathrm{Cov}[R_{f_1}, R_{f_2}|i\neq k,\boldsymbol{\alpha}] = \frac{1}{2}\alpha_{f_1}^2\alpha_{f_2}^2 \sum_{\substack{i=1 \\ i\neq k}}^{K} P^{(i)} N. \quad (58)$$

2.1.4 Orthogonal Codes

For the IS-95 system, each user is assigned a unique Walsh code $c_W^{(i)}$; this code is multiplied by a shared (common to all users) PN code for the in-phase channel $c_{PN,I}$ and a shared PN code for the quadrature channel $c_{PN,Q}$. Therefore, the resulting code for the in-phase channel for user k ($c_W^{(k)} \cdot c_{PN,I}$) is orthogonal to the one for user $i \neq k$ ($c_W^{(i)} \cdot c_{PN,I}$); the same applies to the quadrature channel; nevertheless, $c_W^{(k)} \cdot c_{PN,I}$ is not orthogonal to $c_W^{(i)} \cdot c_{PN,Q}$ for any i or k, but assumed to appear random to one another. A RAKE finger is synchronized to a particular delay-path; when using orthogonal codes, multiuser interference arriving through that path is going to be cancelled; moreover, interference from paths slightly asynchronous to this RAKE finger, especially paths offset less than a chip period, are going go be partially cancelled.

The variance of the self-interference has the same form as that for the random codes. To calculate the variance of R_f due to MAI, we look again at (56) and take into account that $\sum_{n=0}^{N-1} c_{W,n}^{(k)} c_{W,n}^{(i)} = 0$ (thus substracting case i from each of the first two terms); we also see that each term results in case ii. Besides (56), we also need to consider

$$-2\mathrm{E}_c\Big[\int_{-\infty}^{\infty} s_I^{(k)}(t)\tilde{s}_Q^{(i)}(t-\tau_{lf})\mathrm{d}t \int_{-\infty}^{\infty} s_Q^{(k)}(t)\tilde{s}_I^{(i)}(t-\tau_{lf})\mathrm{d}t\Big] = -2g_2^2(\tau_{lf}), \tag{59}$$

which is nonzero since $\mathrm{E}_c[c_{W,n_1}^{(k)} c_{I,n_1} c_{W,a_1}^{(i)} c_{Q,a_1} c_{W,n_2}^{(k)} c_{Q,n_2} c_{W,a_2}^{(i)} c_{I,a_2}] = 1$ when $n_1 = n_2 = a_1 = a_2$, which is not the case for random codes ($\mathrm{E}_c[c_{I,n_1}^{(k)} c_{Q,a_1}^{(i)} c_{Q,n_2}^{(k)} c_{I,a_2}^{(i)}] = 0$). Putting it all together,

$$\mathrm{Var}_{ortho}[R_f^2 | i \neq k, \boldsymbol{\alpha}] = \sum_{\substack{i=1,\\ i\neq k}}^{K} \sum_{\substack{l=1\\ l\neq f}}^{L} \alpha_f^2 \alpha_l^2 P'_m N[1 - \frac{\beta}{2}\sin^2(\frac{\pi\tau_{lf}}{T_c}) - g_2^2(\tau_{lf})]. \tag{60}$$

The covariance between the fingers due to MAI reduces to zero for orthogonal codes.

2.1.5 Orthogonality Factor

The orthogonality factor Θ is defined here as the ratio of the in-cell CIR (in the absence of thermal noise and out-of-cell interference) required to achieve an uncoded BER of 10^{-3} for Random Codes to the respective in-cell CIR for orthogonal codes codes:

$$\Theta = \frac{CIR_{rnd}}{CIR_{ortho}}. \tag{61}$$

The in-cell CIR means that I_o, the sum of AWGN noise and out-of-cell interference, is excluded. The Θ is a figure of merit for the amount of in-cell interference that is produced; notice that for a channel that has only one path, Θ is equal to zero since there is no in-cell interference; a channel with many multipaths would have a Θ value close to 1.

In [60], the effective interference at the output of the RAKE is composed of the thermal noise, the out-of-cell interference $\mathcal{I}_{oc}$, and the product of the in-cell interference and an orthogonality factor Θ (our Θ and their a_j add to 1); all of this interference is divided by the processing gain. Since the thermal noise is negligible in comparison with the $\mathcal{I}_{oc}$, in obtaining Θ, we would really want to compare the in-cell interference with $\mathcal{I}_{oc}$ with the same power $KP_m \sum_{l=1}^{L} \alpha_l^2$. The codes from other cells appear as random codes to a user in the reference cell since they are multiplied by different PN codes. The channel profile is different for each cell and we can thus average over the path delay and get a $1 - \frac{\beta}{4}$ factor instead of $1 - \frac{\beta}{2}\sin^2(\frac{\pi\tau_{lf}}{T_c})$. Putting all together, we obtain an SNR-based orthogonality factor:

$$\begin{aligned}\Theta_{\mathrm{SNR}} &= \frac{\sum_{f=1}^{F} Var_{ortho}[R_f]}{KP_mN \sum_{l=1}^{L} \alpha_l^2 \sum_{f=1}^{F} \alpha_f^2 (1 - \frac{\beta}{4})} \\ &\approx \frac{\sum_{l=1}^{L}\sum_{f=1}^{F} \alpha_f^2\alpha_l^2[1 - \frac{\beta}{2}\sin^2(\frac{\pi\tau_{lf}}{T_c}) - g_2^2(\tau_{lf})]}{\sum_{l=1}^{L}\alpha_l^2 \sum_{f=1}^{F}\alpha_f^2(1-\frac{\beta}{4})}.\end{aligned} \tag{62}$$

2.1.6 Complex-Spreading Quaternary Transmitter

The received signal is modelled as follows:

$$r(t) = \sum_{i=1}^{K/2}\sum_{l=1}^{L} \hat{\alpha}_l \sqrt{P^{(i)}} \left\{ [\tilde{s}_{II}^{(i)}(t-\tau_l) - \tilde{s}_{QQ}^{(i)}(t-\tau_l)] - j[\tilde{s}_{QI}^{(i)}(t-\tau_l) + \tilde{s}_{IQ}^{(i)}(t-\tau_l)] \right\} + \mathcal{I}(t) \tag{63}$$

where $\tilde{s}_{\mathcal{C}_1\mathcal{C}_2}^{(i)}(t) = \sum_n d_{\mathcal{C}_1,\lfloor\frac{n}{N}\rfloor}^{(i)} c_{\mathcal{C}_1\mathcal{C}_2,n}^{(i)} g_1(t - nT_c)$, for $\mathcal{C}_1$, $\mathcal{C}_2 \in \{I, Q\}$. Data streams $d_I^{(i)}$ and $d_Q^{(i)}$ are different, but belong to the same user i; there are $K/2$ users (K even). For a random-code system, $c_{II}^{(i)}$, $c_{IQ}^{(i)}$, $c_{QI}^{(i)}$, $c_{QQ}^{(i)}$ are all different PN codes (for a total of $2K$ PN codes).

To obtain the in-phase and the quadrature data, the received signal is correlated with

$\bar{G}_f(s_{II}(t-\tau_f) - js_{IQ}(t-\tau_f))$ and $\bar{G}_f(-s_{QQ}(t-\tau_f) - js_{QI}(t-\tau_f))$. Since this system is symmetric in the in-phase and quadrature components, we can look at the performance from the point of view of the in-phase data; therefore,

$$\begin{aligned} Z_I &= \frac{1}{2}\mathrm{Re}\left[r(t)\,\mathrm{conj}\left(\bar{G}_f(S_{II} - jS_{IQ})\right)\right] \\ &= \sum_{i=1}^{K/2}\sum_{l=1}^{L}\sum_{f=1}^{F} G_f\alpha_l\sqrt{P^{(i)}}\frac{1}{2}\Big(\int_0^T s_{II}^{(k)}(t)\tilde{s}_{II}^{(i)}(t-\tau_{lf}) - s_{II}^{(k)}(t)\tilde{s}_{QQ}^{(i)}(t-\tau_{lf}) + \\ &\qquad s_{IQ}^{(k)}(t)\tilde{s}_{QI}^{(i)}(t-\tau_{lf}) + s_{IQ}^{(k)}(t)\tilde{s}_{IQ}^{(i)}(t-\tau_{lf})\mathrm{d}t\cdot\cos(\theta_l-\theta_f) + \\ &\qquad \int_0^T s_{II}^{(k)}(t)d_{Q,m}^{(i)}s_{QI}^{(i)}(t-\tau_{lf}) + s_{II}^{(k)}(t)d_{I,m}^{(i)}s_{IQ}^{(i)}(t-\tau_{lf}) \\ &\qquad -s_{IQ}^{(k)}(t)d_{I,m}^{(i)}s_{II}^{(i)}(t-\tau_{lf}) + s_{IQ}^{(k)}(t)d_{Q,m}^{(i)}s_{QQ}^{(i)}(t-\tau_{lf})\mathrm{d}t\cdot\sin(\theta_l-\theta_f)\Big). \end{aligned} \tag{64}$$

Only the first and the fourth terms in the integrand of the first integral contribute to the mean. The mean of Z_I turns out to be the same as in the BPSK and balanced QPSK case since:

$$\mathrm{E}_c[Z_I^{(k)}] = \sum_{l=1}^{L}\sum_{f=1}^{F}\alpha_f\alpha_l\sqrt{P^{(k)}}\frac{1}{2}\cdot 2Ng_2(\tau_{lf})\cos(\theta_l-\theta_f). \tag{65}$$

The instantaneous variance of the interference caused by each user $i \neq k$ reduces to

$$\begin{aligned} \mathrm{Var}_c[R_{f_I}|i\neq k] &= \frac{1}{4}\sum_{l=1}^{L}\alpha_f^2\alpha_l^2P'_m\Big\{\mathrm{E}_c\Big[\Big(\int_0^T s_{II}^{(k)}(t)\tilde{s}_{II}^{(i)}(t-\tau_{lf})\mathrm{d}t\Big)^2 + \\ &\qquad \Big(\int_0^T s_{II}^{(k)}(t)\tilde{s}_{QQ}^{(i)}(t-\tau_{lf})\mathrm{d}t\Big)^2 + \\ &\Big(\int_0^T s_{IQ}^{(k)}(t)\tilde{s}_{QI}^{(i)}(t-\tau_{lf})\mathrm{d}t\Big)^2 + \Big(\int_0^T s_{IQ}^{(k)}(t)\tilde{s}_{IQ}^{(i)}(t-\tau_{lf})\mathrm{d}t\Big)^2\Big]\cos^2(\theta_l-\theta_f) + \\ &\qquad \mathrm{E}_c\Big[\Big(\int_0^T s_{II}^{(k)}(t)\tilde{s}_{QI}^{(i)}(t-\tau_{lf})\mathrm{d}t\Big)^2 + \Big(\int_0^T s_{II}^{(k)}(t)\tilde{s}_{IQ}^{(i)}(t-\tau_{lf})\mathrm{d}t\Big)^2 + \\ &\Big(\int_0^T s_{IQ}^{(k)}(t)\tilde{s}_{II}^{(i)}(t-\tau_{lf})\mathrm{d}t\Big)^2 + \Big(\int_0^T s_{IQ}^{(k)}(t)\tilde{s}_{QQ}^{(i)}(t-\tau_{lf})\mathrm{d}t\Big)^2\Big]\sin^2(\theta_l-\theta_f). \end{aligned} \tag{66}$$

Each of these integrals contributes a case code ii for a total of eight. Therefore, the variance of the interference contributed by each of the other users becomes

$$\mathrm{Var}[R_{f_I}|i\neq k,\boldsymbol{\alpha}] = \sum_{l=1}^{L}\alpha_f^2\alpha_l^2P^{(i)}N\Big\{1-\frac{\beta}{2}\sin^2(\frac{\pi\tau_{lf}}{T_c})\Big\}. \tag{67}$$

With regards to the variance of the self-interference, $\mathrm{Var}[R_f|i=k]$, we obtain the same terms as in (66) and

$$-2\Big(\int_0^T s_{II}^{(k)}(t)\tilde{s}_{IQ}^{(i)}(t-\tau_{lf})\int_0^T s_{IQ}^{(k)}(t)\tilde{s}_{II}^{(i)}(t-\tau_{lf})\mathrm{d}t\Big)\sin^2(\theta_l-\theta_f), \quad i=k. \tag{68}$$

The term $2\Big(\int_0^T s_{II}^{(k)}(t)\tilde{s}_{II}^{(k)}(t-\tau_{lf})\int_0^T s_{IQ}^{(k)}(t)\tilde{s}_{IQ}^{(k)}(t-\tau_{lf})\mathrm{d}t\Big)\cos^2(\theta_l-\theta_f)$ does not add to the variance. The first integral and the fourth integral in (66) each contribute a code case iii ($n_1 = a_2$ and $n_2 = a_1$), which cancel out with the 2 cases iii in (68). In (66), we have 8 cases iv; two of those contribute to the mean but not the variance; (68) contributes 2 with negative sign:

$$\mathrm{Var}[R_{f_I}|i=k,\boldsymbol{\alpha}] = \sum_{l=1}^{L}\alpha_f^2\alpha_l^2 P^{(k)}N\Big\{1-\frac{\beta}{2}\sin^2(\frac{\pi\tau_{lf}}{T_c})-\frac{1}{2}g_2^2(\tau_{lf})\Big\}. \tag{69}$$

For an orthogonal system, we have $c_{\mathcal{C}_1\mathcal{C}_2}^{(i)} = c_{W\mathcal{C}_1}^{(i)}c_{PN\mathcal{C}_2}$, that is, the product of the Walsh-code for the $\mathcal{C}_1$ component (in-phase or quadrature) of user i, and the PN code for the C_2 component. The Walsh-code is different for the quadrature and in-phase of user i, and also different for each user; the in-phase PN code is common to all users; the same applies to the quadrature PN code. The variance of the self-interference is the same as in the random case. For the variance due to MAI, we obtain 8 times case ii and 2 times case iii from (66); for instance, for the first integral we get $\mathrm{E}_c[c_{WI,n_1}^{(k)}c_{I,n_1}c_{WI,a_1}^{(i)}c_{I,a_1}c_{WI,n_2}^{(k)}c_{I,n_2}c_{WI,a_2}^{(k)}c_{I,a_2}]$ is nonzero only if ii) $n_1 = n_2$, $a_1 = a_2$ or iii) $n_1 = a_2$, $n_2 = a_1$. Additionally, for the first, fourth, fifth, and eight integrals case iv ($n_1 = a_1 = n_2 = a_2$) is cancelled when counted in the deterministic property $\sum_{n=0}^{N-1}c_{W,I_n}^{(k)}c_{W,I_n}^{(i)} = \sum_{n=0}^{N-1}c_{W,I_n}^{(k)}c_{W,Q_n}^{(i)} = 0$ of the orthogonal codes used. We also get -2 times case ii from (68) for $i \neq k$; moreover, we get another -2 times case ii from

$$-2\Big(\int_0^T s_{II}^{(k)}(t)\tilde{s}_{QQ}^{(k)}(t-\tau_{lf})\int_0^T s_{IQ}^{(k)}(t)\tilde{s}_{IQ}^{(k)}(t-\tau_{lf})\mathrm{d}t\Big)\sin^2(\theta_l-\theta_f). \tag{70}$$

Putting all together,

$$\mathrm{Var}[R_{f_I}|i\neq k,\boldsymbol{\alpha}] = \sum_{l=1}^{L}\alpha_f^2\alpha_l^2 P^{(k)}N\Big\{1-\frac{\beta}{2}\sin^2(\frac{\pi\tau_{lf}}{T_c})-g_2^2(\tau_{lf})\Big\}. \tag{71}$$

It can be seen that the expressions obtained are the same as in the balanced QPSK case if we consider each $d_I^{(i)}$ and $d_Q^{(i)}$ as coming from a different user; following this observation and applying the code cases, the respective expressions for the covariance between the fingers of the RAKE receiver can be shown to be the same as (55), (57), (58), and (60).

2.2 Appropriate MRC Model

2.2.1 Quaternary Transmitter

In this section, we obtain the SNR and the BER of CDMA systems when the more accurate form of G_f (37) is used.

From Monte Carlo simulations, it was observed that, unlike for the simple finger weight model, the interference due to either orthogonal codes or random codes deviated heavily from the Gaussian distribution even for fixed fading coefficients. Nevertheless, when both the fading coefficients and the phases were fixed, the sample distribution can be assumed Gaussian for all practical reasons (see Figs. 3 and 4 for 10,000 points). Therefore, we reuse all the results for expectations with respect to codes (code case i through iv and correlation between terms in Z), but we use the complex form of G_f and do not average over the phases.

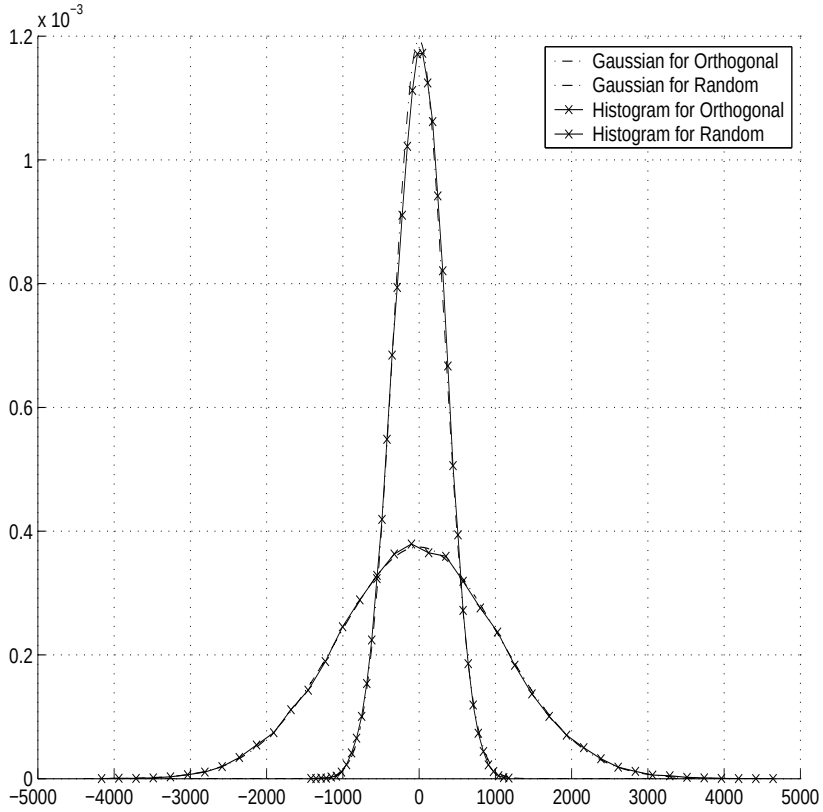

Figure 3: Comparison of interference in output of RAKE for AMRC model with the Gaussian distribution ($\beta = 0.00$).

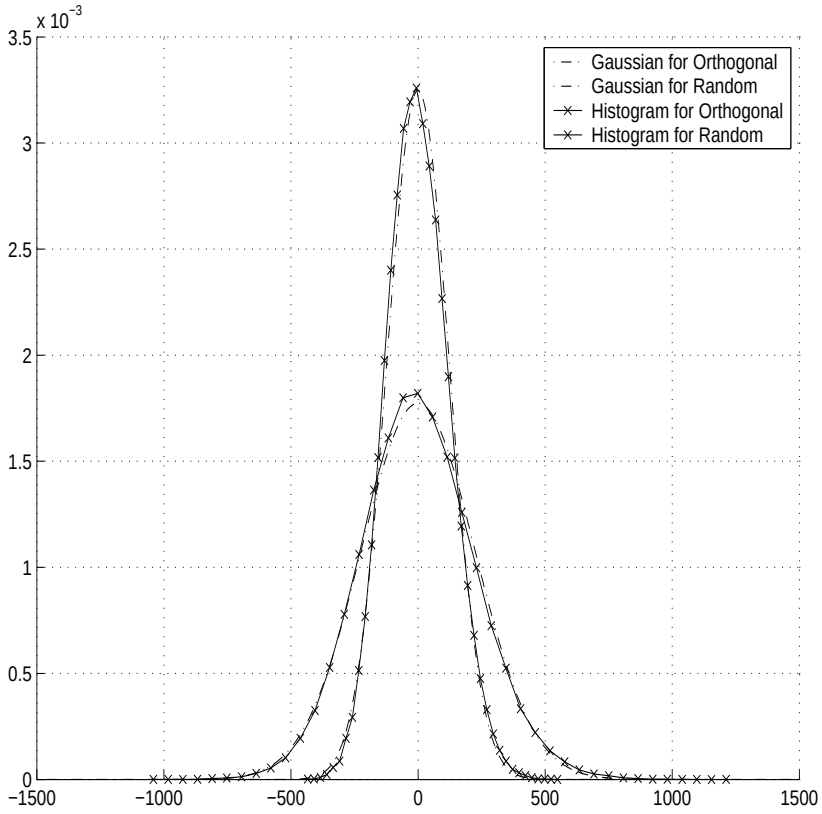

Figure 4: Comparison of interference in output of RAKE for AMRC model with the Gaussian distribution ($\beta = 1.00$).

The total interference perceived by finger f_1 of user k due to user i is

$$R_f^{(i)} = \frac{1}{2}\mathrm{Re}\Bigg\{ \sum_{l=1}^{L} \sqrt{P^{(i)}}\bar{\alpha}_l \left(\int_{-\infty}^{\infty} \tilde{s}_I^{(i)}(t-\tau_l) s_I^{(k)}(t-\tau_f) + \tilde{s}_Q^{(i)}(t-\tau_l) s_Q^{(k)}(t-\tau_l) \right.$$
$$\left. + j\,\tilde{s}_Q^{(i)}(t-\tau_l) s_I^{(k)}(t-\tau_f) - j\,\tilde{s}_I^{(i)}(t-\tau_l) s_Q^{(k)}(t-\tau_f)\mathrm{d}t \right) \bar{G}_f^* \Bigg\}. \qquad (72)$$

We then set up an equation similar to (56) and (48) and define the parameters

$$A(l_1, l_2, f) = \frac{1}{2}\mathrm{Re}\Big\{ \sum_{l_1=1}^{L} \bar{\alpha}_{l_1} \cdot \bar{G}_f^* \Big\} = \frac{1}{2} \sum_{l_1=1}^{L} \sum_{l_2=1}^{L} \Big(\alpha_{l_1,I}\,\alpha_{l_2,I} \; + \alpha_{l_1,Q}\,\alpha_{l_2,Q} \Big) g_2(\tau_{l_2 f}),$$
$$B(l_1, l_2, f) = \frac{1}{2}\mathrm{Re}\Big\{ \sum_{l_1=1}^{L} j\bar{\alpha}_{l_1} \cdot \bar{G}_f^* \Big\} = \frac{1}{2} \sum_{l_1=1}^{L} \sum_{l_2=1}^{L} \Big(\alpha_{l_1,I}\,\alpha_{l_2,Q} - \alpha_{l_1,Q}\,\alpha_{l_2,I} \Big) g_2(\tau_{l_2 f}). \qquad (73)$$

This expression is in the same form as (31); for $i \neq k$ the four integrals are uncorrelated of

one another; therefore, in obtaining $\mathrm{E}_c[R_{f_1}^{(i)} R_{f_2}^{(i)} | i \neq k]$, we encounter the terms

$$A_2 = A(l_1, l_2, f_1) A(l_3, l_4, f_2) [N \,\mathrm{Sg}(\tau_{l_1 f_1}, \tau_{l_3 f_2})] \quad \text{and}$$

$$B_2 = B(l_1, l_2, f_1) B(l_3, l_4, f_2) [N \,\mathrm{Sg}(\tau_{l_1 f_1}, \tau_{l_3 f_2})]. \tag{74}$$

The infinite sum $\mathrm{Sg}(\tau_1, \tau_2) = \sum_{m=-\infty}^{\infty} g_2(mT_c - \tau_1) g_2(mT_c - \tau_2)$ comes from case ii of the expectation with respect to the codes; a closed form has been derived in Chapter 3 (see Eq. 100.)

Expanding,

$$\begin{aligned}\mathrm{Cov}[R_{f_1}, R_{f_2} | \bar{\boldsymbol{\alpha}}] = \sum_{\substack{i=1 \\ i \neq k}}^{K} \sum_{l_1=1}^{L} \sum_{l_2=1}^{L} \sum_{l_3=1}^{L} \sum_{l_4=1}^{L} \frac{N P^{(i)}}{2} [&\alpha_{l_1,I} \alpha_{l_2,I} \alpha_{l_3,I} \alpha_{l_4,I} + \alpha_{l_1,Q} \alpha_{l_2,Q} \alpha_{l_3,I} \alpha_{l_4,I} \\ &+ \alpha_{l_1,Q} \alpha_{l_2,I} \alpha_{l_3,Q} \alpha_{l_4,I} - \alpha_{l_1,I} \alpha_{l_2,Q} \alpha_{l_3,Q} \alpha_{l_4,I} - \alpha_{l_1,Q} \alpha_{l_2,I} \alpha_{l_3,I} \alpha_{l_4,Q} + \alpha_{l_1,I} \alpha_{l_2,Q} \alpha_{l_3,I} \alpha_{l_4,Q} \\ &+ \alpha_{l_1,I} \alpha_{l_2,I} \alpha_{l_3,Q} \alpha_{l_4,Q} + \alpha_{l_1,Q} \alpha_{l_2,Q} \alpha_{l_3,Q} \alpha_{l_4,Q}] \,\mathrm{Sg}(\tau_{l_1 f_1}, \tau_{l_3 f_2}) g_2(\tau_{l_2 f_1}) g_2(\tau_{l_4 f_2}). \end{aligned} \tag{75}$$

Rearranging the terms,

$$\begin{aligned}\mathrm{Cov}[R_{f_1}, R_{f_2} | \bar{\boldsymbol{\alpha}}] = \sum_{\substack{i=1 \\ i \neq k}}^{K} \frac{N P^{(i)}}{2} \Bigg[&\sum_{l_1=1}^{L} \sum_{l_3=1}^{L} (\alpha_{l_1,I} \alpha_{l_3,I} + \alpha_{l_1,Q} \alpha_{l_3,Q}) \mathrm{Sg}(\tau_{l_1 f_1}, \tau_{l_3 f_2}) \cdot \\ &\sum_{l_2=1}^{L} \sum_{l_4=1}^{L} (\alpha_{l_2,I} \alpha_{l_4,I} + \alpha_{l_2,Q} \alpha_{l_4,Q}) g_2(\tau_{l_2 f_1}) g_2(\tau_{l_4 f_2}) + \\ &\sum_{l_1=1}^{L} \sum_{l_3=1}^{L} (\alpha_{l_1,I} \alpha_{l_3,Q} - \alpha_{l_1,Q} \alpha_{l_3,I}) \mathrm{Sg}(\tau_{l_1 f_1}, \tau_{l_3 f_2}) \cdot \\ &\sum_{l_2=1}^{L} \sum_{l_4=1}^{L} (\alpha_{l_2,I} \alpha_{l_4,Q} - \alpha_{l_2,Q} \alpha_{l_4,I}) g_2(\tau_{l_2 f_1}) g_2(\tau_{l_4 f_2}) \Bigg], \end{aligned} \tag{76}$$

where $\bar{\boldsymbol{\alpha}}$ is a vector corresponding to the set of $\boldsymbol{\alpha}_l$ complex fading coefficients. With this rearrangement, the first pair of summations in l are independent from the second pair of summations in l, which improves the computation efficiency.

For the self interference, $\mathrm{Sg}(\tau_{l_1 f_1}, \tau_{l_3 f_2})$ is replaced by $\mathrm{Sg}(\tau_{l_1 f_1}, \tau_{l_3 f_2}) - g_2(\tau_{l_1 f_1}) g_2(\tau_{l_3 f_2})$

in (76) for user k:

$$\mathrm{Cov}_{SI,A}[R_{f_1}, R_{f_2}|\bar{\boldsymbol{\alpha}}] = \frac{NP^{(k)}}{2}\left[\sum_{l_1=1}^{L}\sum_{l_3=1}^{L}(\alpha_{l_1,I}\alpha_{l_3,I}+\alpha_{l_1,Q}\alpha_{l_3,Q})\cdot\right.$$
$$(\mathrm{Sg}(\tau_{l_1 f_1},\tau_{l_3 f_2})-g_2(\tau_{l_1 f_1},\tau_{l_3 f_2}))\cdot\sum_{l_2=1}^{L}\sum_{l_4=1}^{L}(\alpha_{l_2,I}\alpha_{l_4,I}+\alpha_{l_2,Q}\alpha_{l_4,Q})g_2(\tau_{l_2 f_1})g_2(\tau_{l_4 f_2})+$$
$$\sum_{l_1=1}^{L}\sum_{l_3=1}^{L}(\alpha_{l_1,I}\alpha_{l_3,Q}-\alpha_{l_1,Q}\alpha_{l_3,I})(\mathrm{Sg}(\tau_{l_1 f_1},\tau_{l_3 f_2})-g_2(\tau_{l_1 f_1},\tau_{l_3 f_2}))\cdot$$
$$\left.\sum_{l_2=1}^{L}\sum_{l_4=1}^{L}(\alpha_{l_2,I}\alpha_{l_4,Q}-\alpha_{l_2,Q}\alpha_{l_4,I})g_2(\tau_{l_2 f_1})g_2(\tau_{l_4 f_2})\right] \quad (77)$$

There is an additional expression to consider for the self-interference: As in the case for SMRC, where we expand $\mathrm{Cov}[R_{f_1}, R_{f_2}]$, we get additional cases. From (72), the 1st and 2nd term in the integrand result additionally in 2 time case iii, the third and the fourth terms in the integrand (the terms multiplied by j) are correlated and correspond additionally to code case iii; adding at these case iii terms, we call the sum

$$\mathrm{Cov}_{SI,B}[R_{f_1}, R_{f_2}|\bar{\boldsymbol{\alpha}}] =$$
$$\frac{P^{(k)}}{2}\left[\sum_{l_1=1}^{L}\sum_{l_3=1}^{L}(\alpha_{l_1,I}\alpha_{l_3,I}-\alpha_{l_1,Q}\alpha_{l_3,Q})\sum_{n=0}^{N-1}(N-|n|)g_2(nT_c-\tau_{l_1 f_1})g_2(nT_c+\tau_{l_3 f_2})\cdot\right.$$
$$\sum_{l_2=1}^{L}\sum_{l_4=1}^{L}(\alpha_{l_2,I}\alpha_{l_4,I}-\alpha_{l_2,Q}\alpha_{l_4,Q})g_2(\tau_{l_2 f_1})g_2(\tau_{l_4 f_2})+$$
$$\sum_{l_1=1}^{L}\sum_{l_3=1}^{L}(\alpha_{l_1,I}\alpha_{l_3,Q}+\alpha_{l_1,Q}\alpha_{l_3,I})\sum_{n=0}^{N-1}(N-|n|)g_2(nT_c-\tau_{l_2 f_1})g_2(nT_c+\tau_{l_4 f_2})\cdot$$
$$\left.\sum_{l_2=1}^{L}\sum_{l_4=1}^{L}(\alpha_{l_2,I}\alpha_{l_4,Q}+\alpha_{l_2,Q}\alpha_{l_4,I})g_2(\tau_{l_2 f_1})g_2(\tau_{l_4 f_2})\right]. \quad (78)$$

The covariance between fingers f_1 and f_2 due to self-interference becomes

$$\mathrm{Cov}_{SI}[R_{f_1}, R_{f_2}|\bar{\boldsymbol{\alpha}}] = \mathrm{Cov}_{SI,A}[R_{f_1}, R_{f_2}|\bar{\boldsymbol{\alpha}}] + \mathrm{Cov}_{SI,B}[R_{f_1}, R_{f_2}|\bar{\boldsymbol{\alpha}}]. \quad (79)$$

For orthogonal codes, the expressions for the self-interference remain the same, but to get the expressions for the MAI, $\mathrm{Sg}(\tau_{l_1 f_1},\tau_{l_3 f_2})$ is replaced by $\mathrm{Sg}(\tau_{l_1 f_1},\tau_{l_3 f_2})-g_2(\tau_{l_1 f_1})g_2(\tau_{l_3 f_2})$ in (76).

With regards to the desired signal, the expectation of the output of finger f_1 with respect to the codes becomes

$$\mathrm{E}_c[R_{f_1}] = \sum_{l_1}\sum_{l_2} N\sqrt{P^{(k)}}\, g_2(\tau_{l_1 f_1}) g_2(\tau_{l_2 f_1}) \Big\{ \alpha_{l_1,I}\alpha_{l_2,I} + \alpha_{l_1,Q}\alpha_{l_2,Q} \Big\}. \tag{80}$$

Therefore,

$$\mathrm{E}^2\left[Z|\boldsymbol{\alpha},\boldsymbol{\theta}\right] = N^2 P^{(k)} \left[\sum_{f=1}^{F}\sum_{l_1=1}^{L}\sum_{l_2=1}^{L} g_2(\tau_{l_1 f_1}) g_2(\tau_{l_2 f_1}) \Big\{ \alpha_{l_1,I}\alpha_{l_2,I} + \alpha_{l_1,Q}\alpha_{l_2,Q} \Big\} \right]^2 \tag{81}$$

Notice that if we multiply the expressions (76), (78), and (80) by $\delta_{f_1 l_2}\delta_{f_2 l_4}$, which is the same as replacing l_2 and l_4 by f_1 and f_2, respectively, we will obtain the expressions for $G_f = \alpha_f$ without phase averaging.

2.2.2 Variable Spreading Factor and Quasi-Orthogonal Codes

When data rate beyond that of the basic service is required, two approaches are possible; one is to assign multiple codes per user; the other is to use a variable spreading factor, where each bit comprises $2^n \leq N$ chips. To maintain the orthogonality between users, the tree structure proposed in [4] is used; if a user is allocated a code, the other users cannot use its branches (if $c_{4,1}$ is used, $c_{8,1}$ and $c_{8,2}$ cannot be used). Following this scheme, codes of different length (for different rate) are orthogonal (this is a "window" property of Walsh codes).

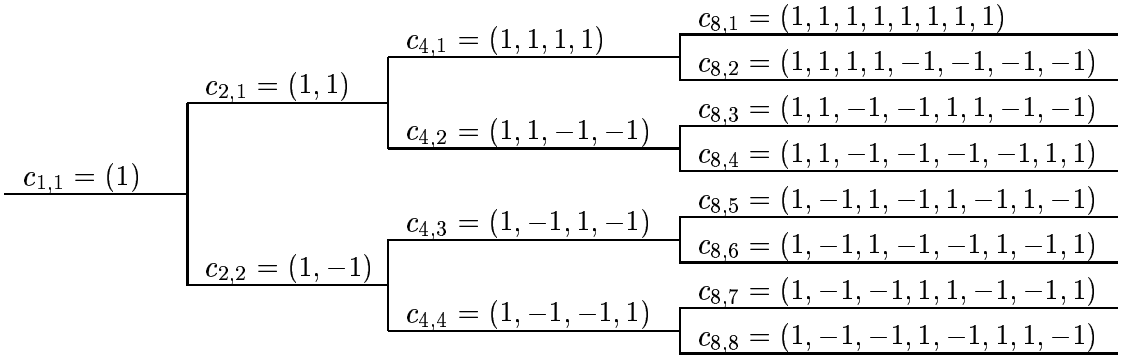

Figure 5: Construction of orthogonal spreading codes for different spreading factors

Table 3: Masking functions for QOS codes.

Function	Masking Function	
	Hexadecimal Representation of QOF_{sign}	$Walsh_{rot}$
0	00000000000000000000000000000000 00000000000000000000000000000000	W_0^{256}
1	7228d7724eebebb1eb4eb1ebd78d8d28 278282d81b41be1b411b1bbe7dd8277d	W_{130}^{256}
2	1724bd71b28118d48ebddb172b187eb2 e7d4b27ebd8ee82481b22be7dbe871bd	W_{47}^{256}

$$(4,4)c_N = \begin{pmatrix} c_{N,1} \\ c_{N,2} \\ \vdots \\ c_{N,N} \end{pmatrix} = \begin{pmatrix} \begin{pmatrix} c_{N/2,1} & c_{N/2,1} \\ c_{N/2,1} & -c_{N/2,1} \end{pmatrix} \\ \vdots \\ \begin{pmatrix} c_{N/2,N/2} & c_{N/2,N/2} \\ c_{N/2,N/2} & -c_{N/2,N/2} \end{pmatrix} \end{pmatrix} \tag{82}$$

On the other hand, the number of Walsh codes might not be enough. The cdma2000 standard [2] has introduced three sets of Quasi-Orthogonal (QOS) codes. They are constructed by applying a particular mask and a rotation to the set of Walsh codes. Within each resulting set, the properties of Walsh codes are preserved (window property as well as the property that within each set all the codes are mutually orthogonal). Simulations show that when we take one of these 256x256 QOS matrices and correlate the codes (rows of the matrix) from any of the resulting four 128x128 submatrices with codes (rows) from a 128x128 Walsh matrix, the correlation is in the form $\sqrt{128}\exp(j\theta)$, where $\theta = \pi/4, 3\pi/4, 5\pi/4, 7\pi/4$ with equal probability; when correlating a code from one of the resulting sixteen 64x64 submatrices with a code from a 16x16 Walsh matrix, the correlation is in the form $\sqrt{128}\exp(j\theta)$, where $\theta = 0, \pi/2, \pi, 3\pi/2$. In general, when we take any code from one of the $(256/N)^2$ NxN ($N = 2^n$, n integer) resulting submatrices with a code from a NxN Walsh matrix, the result is of the form $\sqrt{128}\exp(j\theta)$, where $\theta = \pi/4, 3\pi/4, 5\pi/4, 7\pi/4$ with equal probability for n odd and $\theta = 0, \pi/2, \pi, 3\pi/2$ with equal probability for n even. Therefore, if we use Walsh codes for the in-phase and quadrature, the average of the sum of their correlations

with a QOS code is $\sqrt{N}$ (same as correlating with a random code in the in-phase or quadrature) . Since both the Walsh codes and the QOS codes are concatenated with PN codes, the asynchronous correlations between the two sets will have the same statistical properties as those between Walsh and random codes.

In conclusion, we can use the formulas for orthogonal codes for the MAI interference between different QOS codes and we can use the formulas for random codes for the MAI interference between a QOS code and a Walsh code.

2.2.2.1 Voice Activity

During a cellphone conversation, one party is not talking continuously; it was observed in [12] that a speaker is active between 35% and 40% of the time; we will assume the speaker is active 37.5% of the time as in [21]. This effect could be modelled with a voice activity factor $\nu^{(i)}$ [66] multiplying $P^{(i)}$ in the MAI expressions:

$$P(\nu^{(i)} = 1) = 3/8, \quad P(\nu^{(i)} = 0) = 5/8. \tag{83}$$

When considering the effect of voice activity and code rate of 1/2, the length of the Walsh Hadamard code (and the number of WH codes) is halved: If the processing gain is 128, a bit of information becomes two coded bits, and each of these two coded bit is spread by a WH code with length of 64. Even without considering the coding gain, just the gain through interleaving (in the presence of fading), under some channel conditions (one main path and a second smaller path at subchip spacing from the first), the number of WH codes is not going to be sufficient. The mathematical expressions could be adjusted and still be used under these conditions.

2.3 Comparison with Previous Work

Usually in the literature, square pulse shaping is assumed, and the fingers are spaced by T_c or more. Defining $g_s(t)$ as a square function of duration T_c, then the triangular function $g_t(t) = g_s(t) * g_s(t) = 1 - |t|/T_c$ (for t between $-T_c$ and T_c) and $g_t(t) = 0$ (for t elswhere).

Instead of $\sum_{N=-\infty}^{\infty} g_2^2(nT_c - \tau_{lf}) = 1 - \frac{\beta}{2}\sin^2(\frac{\pi\tau_{lf}}{T_c})$, it is better to define

$$S_t(\tau_{lf}) = \sum_{N=-\infty}^{\infty} g_t^2(nT_c - \tau_{lf}) = (1 - \frac{\tau'}{T_c})^2 + (\frac{\tau'}{T_c})^2 = 1 - \frac{\tau_{lf}^2}{T_c^2} - 2\frac{\tau_{lf}}{T_c}, \tag{84}$$

where τ' is $\mathrm{mod}(\tau_{lf}, T_c)$ for any value of τ_{lf}. The above expression is usually averaged over τ_{lf}, yielding $\frac{2}{3}$; such average for $1 - \frac{\beta}{2}\sin^2(\frac{\pi\tau_{lf}}{T_c})$ is $1 - \frac{\beta}{4}$, a value already obtained in [7] and [61].

When using $g_s(t)$ and $\tau_{lf} \geq T_c$, the equivalent expression for (44) is

$$\mathrm{E}[E_c^2[Z]|\boldsymbol{\alpha}] = N^2 P \sum_{f_1=1}^{F}\sum_{f_2=1}^{F} \alpha_{f_1}^2 \alpha_{f_2}^2 = N^2 P \left(\sum_{f=1}^{F} \alpha_f\right)^2. \tag{85}$$

For random codes, when the path is synchronized to the finger

$$\mathrm{Var}[R_f|\boldsymbol{\alpha}] = \frac{1}{2}\sum_{l=1}^{L} \alpha_f^2 \alpha_l^2 P_m N(KS_t(\tau_{lf}) - g_2(\tau_{lf})), \tag{86}$$

which after averaging over τ_{lf} and observing that $S_t(0) = 1$, becomes $\frac{1}{2}\alpha_f^4 P_m N(K-1) + \frac{1}{3}\sum_{\substack{l=1,\\ l\neq f}}^{L} \alpha_f^2 \alpha_l^2 P_m NK$. For orthogonal codes, averaging over the path delays, $\mathrm{Var}[R_f|\boldsymbol{\alpha}] = \frac{1}{3}\sum_{\substack{l=1\\ l\neq f}}^{L} \alpha_f^2 \alpha_l^2 P_m KN$ is obtained. The expression for the covariance between two fingers for random codes is still valid; for orthogonal codes, the covariance can be assumed to be zero.

Making $E_b = NP_m g_2(0) = NP_m$ ($g_2(t)$ has time units since $g_1(t)$ is unitless), for a synchronous system using random codes with a channel model containing only one path, the SNR becomes

$$\frac{NE_b\alpha_f^2}{\frac{1}{2}\alpha_f^4 E_b(K-1) + N\alpha^2\frac{I_o}{2}} = \left(\frac{K-1}{2N} + \left(\frac{2E_b}{I_o}\right)^{-1}\right)^{-1}; \tag{87}$$

see the Appendix C for the effect of $I_o(t)$. For an asynchronous random-code system,

$$\left(\frac{K-1}{3N} + \left(\frac{2E_b}{I_o}\right)^{-1}\right)^{-1}. \tag{88}$$

is obtained. Keeping in mind how the SNR is defined in this paper and in other sources, the last two expressions agree with the binary DS/SSMA system expressions in [18] and [53]. Also they match the Quaternary DS/SSMA without offset cases, which differ from the balanced-mode in that each I and Q has different data, when N is replaced by $2N$ –keeping in mind that in our case the data is carried by $2N$ chips (the I and Q sequences).

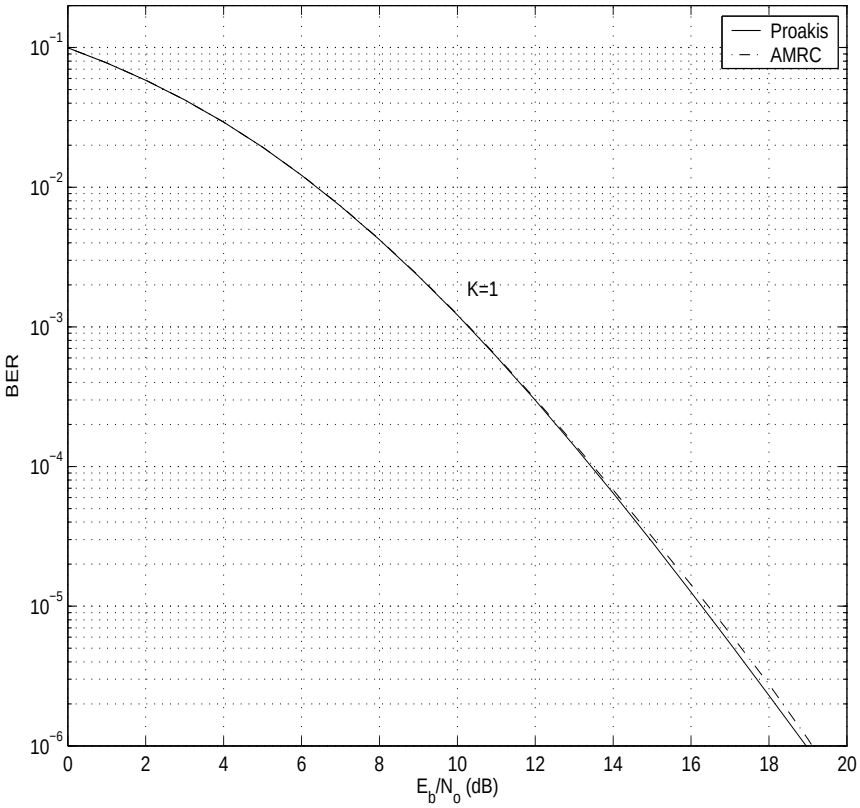

Figure 6: BER vs. E_b/I_o for AMRC and [52].

Also, in Fig. 6, the AMRC expressions were compared with (24) for a T_c-model channel with 4 Rayleigh-distributed paths with power 0, -1.5, -3.0, and -4.5 dB, respectively.

Fig. 7 shows the BER vs. number of orthogonal-code users for the AMRC expressions and (16) for a fixed T_c-model channel having 4 paths with powers 0, -1.5, -3.0, and -4.5 dB, respectively and phases 0, 60, 120, and 180 degrees, respectively. In [10], the R_{ISI} for the same bit is mistakenly omitted; if it is considered for a T_c-channel model, then it is equal to the R_{MAI} due to one user with the same power, so R_{ISI} was lumped into R_{MAI}; basically, the number of users for R_{MAI} included the reference user and R_{ISI} was omitted. An exact fit was obtained in the absence of noise for E_b/N_o= 5 dB and 10 dB.

In this study, two wideband CDMA forward-link performance model sets of expressions were derived that were general enough to apply to different channel models, chip rates, roll-off factors, spreading gain, number of users, for QPSK and MRC, using orthogonal codes, quasi-orthogonal codes, or noise as the source of interference. Moreover, the expressions

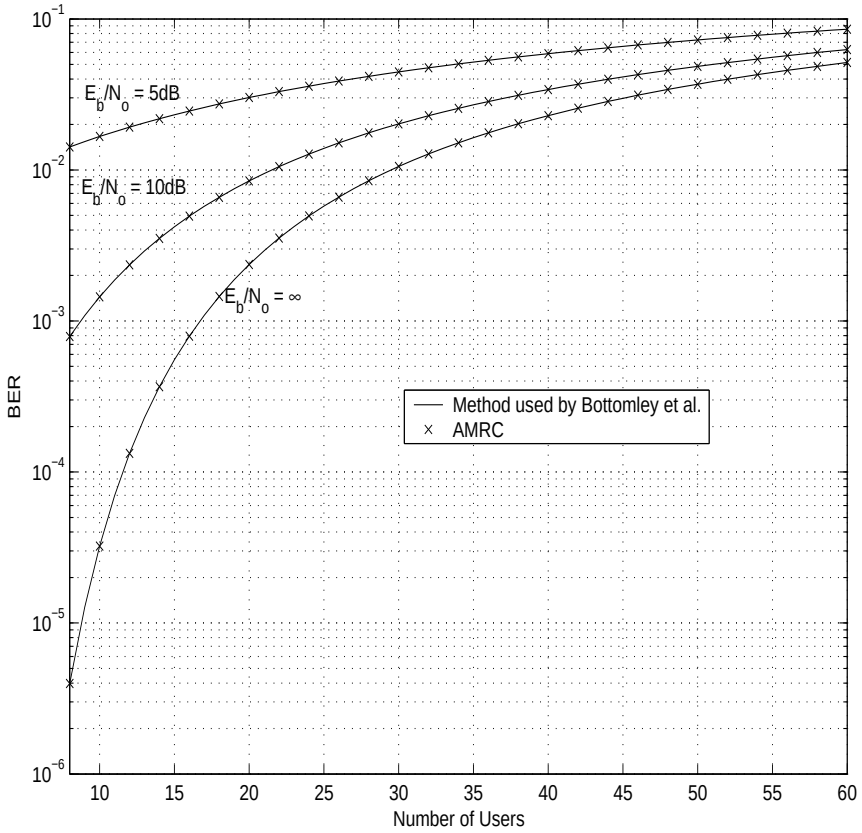

Figure 7: BER vs. number of users for AMRC and [10].

resulted in great saving of computational processing with respect to system simulations.

The loss of the orthogonality of the forward link was also obtained; it was shown that the roll-off factor, the chip rate, channel, and the model for the finger weight can have a significant impact on this orthogonality and therefore performance of the link.

2.4 Impact of Work

The analysis obtained here applies to real systems; it applies to variable data rate, chip rate, processing gain, any channel model, RRC waveshaping with arbitrary roll–off factor; it takes into account properties of random codes, orthogonal codes, quasi-orthogonal codes, and Gaussian noise. The analysis can be used with Variable Spreading Factor and Multicode proposed systems for 3G CDMA.

For a fixed channel model, the expressions are in closed-form. To obtain the BER, the expressions only require Monte-Carlo Integration over the probability distribution of the

paths; the net effect is a reduction of the computation by several orders of magnitude. At the same time, the analysis is very accurate and works not only for special channel cases and finger spacings, but very general types of channels and any finger spacing.

The analysis provides insight into the importance of each variable and can be used for further studies; it can be used for related fields in CDMA such as novel architectures, multi-user detection, and wireless networks. The analysis provides a very good tool for predicting the performance of 3G systems. We have shown that an increase in bandwidth does not necessarily result in better spectral efficiency for those users close to the Base Station. Also, we have shown that depending on the roll-off factor used, the performance can be significantly different from that obtained by assuming square pulse shaping.

Above all, the work makes it possible to have joint link and system–level simulations without making any assumptions. Otherwise, it is usually necessary to run separate simulations to obtain the average values of link-level parameters such as required E_b/N_o and orthogonality factor, which would result in the loss of estimation accuracy. The required E_b/N_o changes not only with the power delay profile, but also with the location of the mobile in the cell. Also, the BER depends more on the instantaneous orthogonality rather than the average value; the study presented here bypasses the need to estimate the orthogonality factor, in effect making it obsolete.

The work shows analytic expressions using RRC pulse shaping. Most CDMA books are written using square pulse shaping. We expect the work presented here to help change this literature.

2.5 Numerical Results and Conclusions

It is necessary to validate the SMRC and AMRC conditional SNR expressions derived. System simulations were performed for the simple MRC model for two channels: The ITU-R M.1225 Vehicular Test Environment Channel A and the COST 207 CODIT Macrocell Channel (referred from now on as channel 1 and channel 4 respectively) for a rate of 1.2288 Mcps; these and other channels used in this work can be found in [1] and [51]). Channels 1 and 4 were modified as follows: The delay of the paths in the two channel models were

adjusted to the nearest $0.1T_c$; the fading coefficients were set to their average values. The chip wave shaping was limited to the window $[-10T_c, 10T_c]$ (a length of $20T_c$) and sampled 10 times per chip. The values were set to $K = 16$, $N = 16$. For the AMRC model, additionally, the phases were set to constant but arbitrary values.

In Table 4, we see the fingers assigned for the

Table 4: Path numbers assigned to fingers

Channel	Chip Rate			
	1.2288 Mcps	3.6864 Mcps	5.0 Mcps	10 Mcps
1	1, 3, 5, 6	all	all	all
2	1, 3, 5, 6	all	all	all
3	1, 3, 5, 6	all	all	all
4	1, 6	1, 4, 5, 7, 8	1, 4, 5, 7, 8, 10	1, 2, 3, 4, 5, 7, 8, 10

Table 5: Table of Channels. Delay is in msec. and Power is dB.

Path	Channel 1		Channel 2		Channel 3		Channel 4	
	Delay (msec)	Power (dB)	Delay	Power	Delay	Power	Delay	Power
1	0	0.0	0	-2.5	0	0.0	100	-32
2	310	-1.0	300	0.0	380	10.0	200	-5.0
3	710	-9.0	8900	-12.8	930	-22.7	500	-4.5
4	1090	-10.0	12900	-10.0	1940	-24.7	600	-3.6
5	1730	-15.0	17100	-25.2	2290	-20.7	900	0.0
6	2510	-20.0	20000	-16.0	2910	-22.1	1050	-3.0
7							1050	-3.0
8							1350	-1.2
9							1450	-5.0
10							1500	-3.5

The reason for selecting these two was that channel 1 has a main path and a few other smaller paths; channel 4 has many paths at about the same power and they are closely spaced in time. The other channels mentioned in the figure are the ITU-R M.1225 Vehicular Test Environment Channel B (channel 2) and the Outdoor/Indoor/Pedestrian Environment Channel B (channel 3). For all the channels we assigned a fixed finger to the path with the most average power when there were two or more paths within a chip ($\mathrm{E}[\alpha_1] > \mathrm{E}[\alpha_2]$), even though sometimes $\alpha_2 > \alpha_1$ because of the Rayleigh distribution. The selection of the fingers of the RAKE receiver were also such that they were spaced by approximately one chip or more.

The conditional SNR values obtained were virtually the same as those predicted by the theoretical formulas.

The next step in the validation of our formulas was to determine the accuracy of the models when including the statistics of the unconditional variables; namely, the Rayleigh coefficients were allowed to change for both models and the phases were allowed to change for AMRC; this way the average of the conditional SNR over the conditioning variables was obtained; this is tantamount to Monte Carlo integration for the theoretical expressions.

Simulations were done for the simple MRC model, where the users were assigned orthogonal codes and random codes ($K = 32$, $N = 32$) and arbitrary phases for the paths (the phases varied with the path but not the user); the process was repeated $M_{inner} = 1000$ times and each of these times, the PN codes (those for random codes on one hand and those concatenated with the orthogonal codes on the other hand) and phase of each path changed (following the uniform distribution), but the randomly generated fading coefficients remained the same. The results were used to obtain an SNR conditioned to the given set of fading coefficients (as in the previous validation step). The process was repeated $M_{outer} = 1000$ times (each time the fading coefficients changed), and the values obtained were used to obtain the average SNR (Table 6 in the Tables and Figures section). Additionally, we generated Gaussian noise that had the power of K interfering users within the frequency band of the users (but we did not count the self-interference caused by the reference user); the noise sample function changed every single time ($M_{inner} \cdot M_{outer}$).

Moreover, an alternative scheme (orthoV) was attempted ($a'_f = a_f / (\sum_{l=1, l \neq f}^{L} a_l)$, that is, each original weight is divided by the sum of all *path coefficients* except the one corresponding to that finger) to take into account that each finger in an orthogonal code scheme perceives a different amount of interference.

Simulations were also performed for the AMRC model, with the same parameters, but for each event in M_{inner} only the codes changed, and for each M_{outer}, both the phase and fading coefficients changed. For the orthoV scheme, this time we experimented with $G'_f = G_f / (\sum_{g=1, g \neq f}^{F} G_f)$, that is, each original weight divided by the sum of all *finger weights* except itself.

Table 6: Conditional SNR (dB) Comparison for SMRC Model, Channel 1 and a Chip Rate of 1.2288 Mcps

	System				Theoretical			
β	Ortho	OrthoV	Rnd	Noise	Ortho	OrthoV	Rnd	Noise
0.00	6.74	7.52	0.64	1.08	6.90	7.80	0.68	1.29
0.12	7.19	8.08	0.75	1.11	7.13	7.94	0.76	1.25
0.22	7.38	8.31	0.81	1.11	7.32	8.24	0.82	1.30
0.35	7.61	8.59	0.88	1.08	7.56	8.56	0.89	1.27
0.50	7.87	8.90	0.96	1.05	7.82	8.81	0.97	1.19
1.00	8.70	9.94	1.21	0.91	8.66	9.80	1.23	1.02
Ch4								
0.00	1.97	2.20	-1.31	-0.87	2.07	2.33	-1.29	-0.85
0.12	2.19	2.44	-1.21	-0.85	2.25	2.50	-1.21	-0.85
0.22	2.34	2.60	-1.15	-0.86	2.39	2.64	-1.14	-0.86
0.35	2.50	2.78	-1.06	-0.89	2.56	2.80	-1.06	-0.87
0.50	2.70	3.03	-0.98	-1.07	2.73	3.05	-0.98	-0.93
1.00	3.17	3.54	-0.73	-1.13	3.22	3.53	-0.73	-1.13

In the forward link, the same-cell interference travels through the same channel as the signal for the intended user; therefore it can be expected that the power of the desired signal is correlated with the power of the interference. For orthogonal codes, we are able to reduce some same-cell interference and this correlation is expected to be smaller in general. For Gaussian noise, the correlation is expected to be even smaller. The effect of these observations is that it is necessary to use a greater number of points for the value of the SNR due noise to converge. We used $M_{inner} = 2000$ and $M_{outer} = 1500$.

The IS-95 waveform (the same as the one used for cdma2000) was investigated and it turned out to be very close to a raised cosine function with roll-off factor of 0.12. The β factor used for W-CDMA is 0.22; we also investigated β values of 0 (sinc function), 0.35 (as in IS-54), and 1.

The results were compared with the theoretical ones (10000 points were generated for Monte Carlo integration) and it can be observed that they match very well (Tables 6 and 7). These Monte Carlo integrations to obtain the theoretical values were several orders of magnitude faster to obtain than the Monte Carlo simulations of the system; more about the efficiency of computation will be mentioned below.

The accuracy of the theoretical formulas just for self-interference was also compared

Table 7: Conditional SNR (dB) Comparison for AMRC Model, Channel 1 an d Chip Rate = 1.2288 Mcps

	System				Theoretical			
β	Ortho	OrthoV	Rnd	Noise	Ortho	OrthoV	Rnd	Noise
Ch1								
0.00	9.03	9.91	1.77	2.96	9.21	10.24	1.78	2.76
0.12	9.51	10.71	1.85	2.96	9.42	10.57	1.83	2.72
0.22	9.67	11.04	1.89	2.90	9.54	10.86	1.87	2.73
0.35	9.83	11.44	1.93	2.80	9.71	11.33	1.93	2.66
0.50	10.01	11.89	1.96	2.68	9.90	11.81	1.95	2.62
1.00	10.58	13.04	2.04	2.18	10.38	12.83	2.03	2.19
Ch4								
0.00	6.24	6.42	0.72	1.64	6.49	6.68	0.72	1.56
0.12	6.67	6.88	0.80	1.64	6.61	6.81	0.80	1.50
0.22	6.81	7.06	0.81	1.61	6.74	6.95	0.84	1.49
0.35	6.97	7.24	0.88	1.55	6.97	7.15	0.87	1.43
0.50	7.10	7.41	0.91	1.45	7.15	7.34	0.92	1.35
1.00	7.46	7.81	0.98	1.02	7.44	7.67	0.98	0.90

with system simulations results for ($\beta = 0.00, 0.50, 1.00$) and $K = N = 8$; the difference was 0.02, 0.00, and 0.01 dB for SMRC and the difference was 0.23, 0.06, and 0.06 dB for the AMRC. For both system simulations we used $M_{outer} = 4000$ and $M_{inner} = 1000$.

An immediate observation is that the SNR for both random and orthogonal codes increases with roll-off factor β. It can be explained by observing that as β increases, the value of the waveform outside $|t| \leq T_c$ becomes small (reducing interchip interference). The improvement in SNR with roll-off can also be explained in terms of effective processing gain (with higher roll-off, higher is the bandwidth and thus the spreading).

A simulation of a system using a square pulse shaping function was also undertaken and the results obtained were 2.37 dB for random codes and 8.28 dB orthogonal codes (SMRC); also, we obtained 3.19 dB for random codes and 9.18 dB for orthogonal codes (AMRC). These results point out that the common assumption of square pulse shaping yields optimistic results compared to the IS-95 pulse shape.

For SMRC, the component due to interference at the output of the RAKE receiver was assumed unconditionally Gaussian in distribution; simulations showed it departed somewhat for SMRC; simulations also showed that this component was essentially Gaussian in

distribution for the AMRC model (see Figures 3 and 4). Essentially, at the RAKE output, the component due to other codes is Gaussian in distribution conditioned on the fading coefficients and phases. The SMRC formulas were obtained by taking the variances of the interference due to orthogonal codes, random codes, and Gaussian noise at the output of the RAKE receiver (and the signal power) with respect to not only codes but also phases; this was the cause of the small deviation from the Gaussian distribution. Consequently, we compared simulations of the SMRC formulas (case I) on one hand with AMRC formulas with the same finger weights as SMRC (case II). Case II essentially results in formulas for SMRC without phase averaging the variances and signal power. It was discovered that the averaging over the phases did not pose a problem for channels 1, 2, and 3 when using rates of 3.6864 Mcps and higher; the reason for this effect is that under those circumstances, the paths become well separated (and the output of each finger uncorrelated).

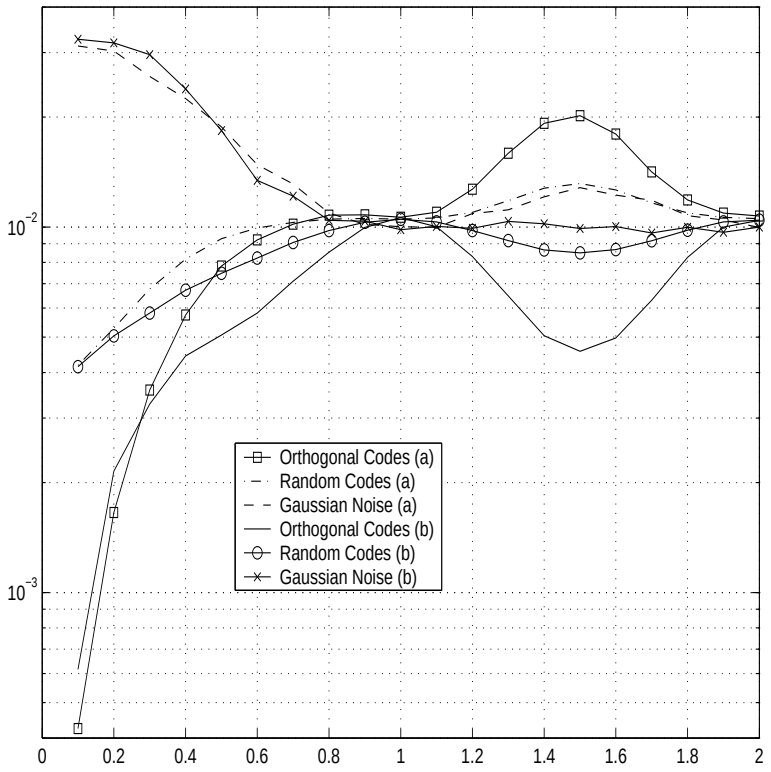

Figure 8: Performance with 2 paths for AMRC.

From now on, we are going to discuss the AMRC model. For this model, there is no

need to assign a finger to coincide exactly with a path; the model can easily take care of this by changing the time location of the finger. In Figure 8, we tested a channel with two paths (first at 0 and the second at t, which varied from $0.1T_c$ and $2T_c$) with two different finger location schemes: a) three fingers (at 0, T_c, and $2T_c$), b) two fingers (at 0 and τ) always time-alligned with the paths. The β factor was set to 0.50, $N = 128$ (constant), and each path was Rayleigh-distributed. The number of users was 128 for orthogonal codes, 36 for random codes; for noise, there were 18 users transmitting Gaussian noise (no self-interference). The experiment becomes also a test for bandwidth and spectral efficiency, if it is interpreted as the paths remaining at constant separation and the chips reducing their length (therefore increasing data rate as well).

It can be seen that scheme b) is better and that the relative delays of the paths impact the performance. For scheme b, the performance when the second path is located between $1.1T_c$ and $1.9T_c$ is clearly better that when it is located at $2T_c$; if we realize that for a fixed two-path channel, the separation of the paths increases with rate (and bandwidth), this figure has an important implication: A system with a lower chip rate (and bandwidth) can have sometimes a better spectral efficiency than a system with higher chip rate (and bandwidth) for both orthogonal and random codes for a particular power delay profile (with both schemes using same number of fingers). This situation where the interference from same-cell orthogonal codes or random codes is predominant for mobiles close to the base station.

With regards to Gaussian noise, we modelled the user as subjected to Gaussian noise with a power of K users in the bandwidth (we have desired signal and noise yet no self-interference). When the paths are increasingly separated, the two fingers become increasingly decorrelated and provide more diversity. It is not altogether clear that one scheme is superior to the other for a path separation of T_c or less: Although scheme a) has more decorrelated fingers ($\mathrm{Cov}(R_{f_1}, R_{f_2})$ is smaller), scheme b) captures better the energy in the desired signal. Clearly, scheme b) is superior. The performance for scheme b) should remain approximately constant for high path separation; the small deviation from a line in the figure can only be attributed to the sample number in the Monte Carlo simulation.

Looking again at the curve of scheme b) for noise, it is essentially a monotonically decreasing function for both schemes for τ in $[0, T_c]$. For τ greater than T_c, scheme a) decreases performance as the second path becomes equidistant between the second and third fingers; scheme b) appears to reach an asymptote, but the curve wiggles around it, which implies that up to a certain point higher chip rate (and bandwidth) results in better performance when the number of fingers remains constant and tracking the paths, but after that point, the performance is going to vary a little around the ultimate asymptote; this effect can be easily understood by looking at (274).

Scheme b) was repeated (Figure 9) for 30, 15, and 5 users for orthogonal codes, random codes, and Gaussian noise respectively. For noise, using higher β resulted in some improvement in performance when the delays between the two paths were less than 1 chip; for delays greater than one chip, the same performance was obtained for β. Additional simulations were done with higher number of samples and it was observed that curve becomes straight for delays greater than a chip.

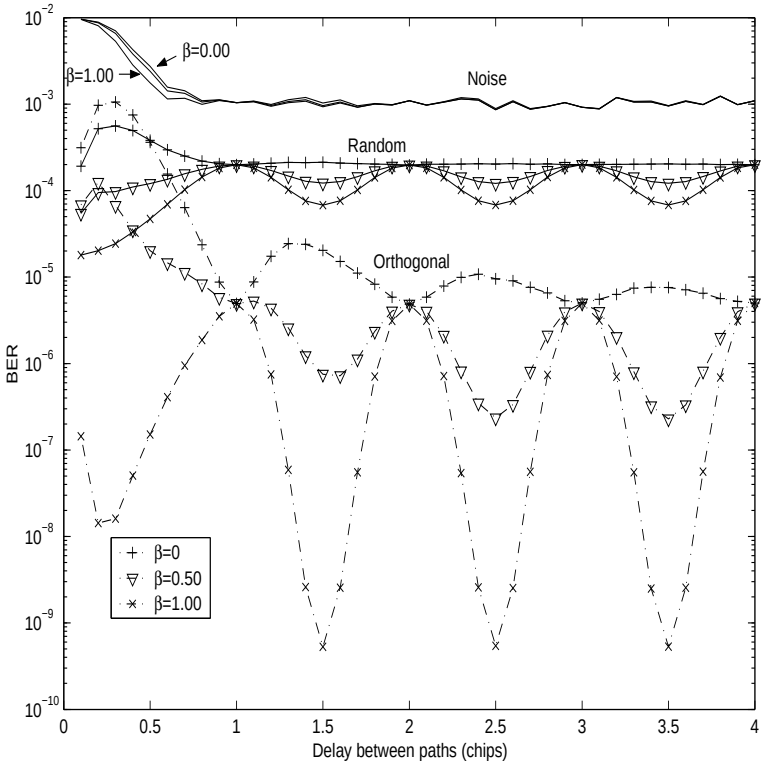

Figure 9: Performance for different roll-off factors.

For random and orthogonal codes, higher β resulted in better performance; there was also some periodicity over τ greater than a chip (except $\beta = 0$ for random codes).

On the other hand, the performance was obtained (not shown) for separations less than 0.1 chips and it was observed that as expected, the interference indeed approaches zero as the the two paths reduce to one path.

Next, we consider BER (Figs. 11 through 18), number of users (Figs. 19 through 22), and the required E_b/I_o (for BER of 10^{-3}) (Figs. 23 through 30) vs. roll-off factor and chip rate for orthogonal codes, random codes, and Gaussian noise using the AMRC scheme.

The results were obtained for different rates: cdma2000 uses 1.2288 and 3.6864 Mcps, W-CDMA uses 3.84 Mcps now, so this last value was omitted since it is very close to 3.6864. We also explored the possibility of using 5.0 and 10 Mcps in future systems. The processing gain and the number of users constants were set to 128 (therefore the data rate increased with chip rate).

The BER vs roll-off factor and chip rate was obtained for orthogonal codes, random codes, and Gaussian noise for channel 1 (K was set to 37 for orthogonal codes and 17 for random codes). For noise, a power equivalent to 17 users (same as random codes) was generated, no self-interference coming from the user. From now on, the path delays in the channel models are not rounded to the nearest $0.1T_c$.

Orthogonal codes result in a much better performance (taking into account more users are operational) than random codes. Notice that increasing the chip rate (increasing bandwidth) does not necessarily result in better performance; this was expected from the previous two figures. Two characteristics of orthogonal codes are i) the correlation between the desired signal and the interference is lower than that for random codes and ii) there is loss of orthogonality as paths very closely situated become separated. As you increase the rate, on one hand you increasingly lose the orthogonality between the codes, but on the other hand you can average over more paths.

For channels 1 through 3, we allocated a finger to each path for the rates 3.6864, 5.0, and 10.0 Mcps; it can be seen that for noise with increasing rate, the performance improves over virtually all values of β; the exception can be attributed to the randomness in the fading

simulations (more Monte Carlo samples). Overall, for all channels, the performance appears to improve with increasing chip rate. It can be easily understood since with increasing bandwidth, the paths can be distinguished better and the multipath of the reference signal can be combined better. Nevertheless, the performance does not improve with β, which is not difficult to see from [66, p. 27], where the variance of the noise depends on the absolute squared value of the Fourier Transform of the pulse-shaping function, which equals simply $g_2(0) = 1$ in our case.

For random codes, it was observed the power of the desired signal was very correlated with the power of the interference (correlation factor of approximately 0.99 and even close to unity). As a result, the increase in the number of fingers and the captured energy of the desired signal also results in the corresponding increase in the power of the interference. It then becomes difficult to predict whether the performance improves or deteriorates with increasing number of fingers; the only assurance is that the performance is going to be within a certain window of the best (as in Figure 9). Nevertheless, we can see that only at $\beta = 0.00$, the performance either improves or remains the same with increasing rate (for the same number of fingers); this is not easy to explain physically, but can be understood by looking at (76) ($\mathrm{Sg}(t_1, t_2) = g_2(2(t_2 - t_1))$ for $\beta = 0$) and taking into account that we have path separations greater or equal to T_c.

With regards to the maximum allowable number of users, it increases with β for random and orthogonal codes. The channel that allows the most users is 3. We can also see the same tendencies as in the BER figures with regards to rate. It is necessary to remember that the processing gain is kept constant at 128; therefore, the data rates for the various chip rates are different. As a result, the figures can be interpreted as spectrum efficiency in the presence of only same-cell interference.

The next set of figures present the E_b/N_o (the N_o here is either noise or MAI) required at the output of the RAKE receiver to achieve a BER of 10^{-3}. Again, these values are in the presence of only orthogonal codes, random codes, or noise.

It was mentioned already that the power of the desired signal is very correlated with the power of the interference coming from random codes; as a result, there is not going to

be much variation of the SNR and the value for E_b/N_o is going to be close to the value in the absence of fading (6.79 dB).

Many system level simulations assume that a certain fixed E_b/N_o is necessary to accomplish a BER of 10^{-3}. As a mobile moves around the cell, it is going to be subjected to different proportions of out-of-cell (modelled as noise) and in-cell (orthogonal or random codes) interference; the figures show clearly that the value of E_b/N_o would be dependent on the location of the mobile.

The last two tables present the values of the orthogonality factor Θ obtained. As the chip rate is increased, there should be a tendency for Θ to go up: the reason for this is that as the chip period becomes smaller (and the bandwidth of the system increases), it is easier to distinguish a path from another. Therefore, paths spaced very closely together that might have appeared before as being one path now are a manifold of paths. Some of this tendency can still be observed, but it is not very obvious because of other factors, such as relative paths delays and finger assignments.

Table 8: Orthogonality Factor for QPSK using Simplified Finger Weights

	Without Variance						With Variance					
	0.00	0.12	0.22	0.35	0.50	1.00	0.00	0.12	0.22	0.35	0.50	1.00
ch1												
1.2288	0.547	0.528	0.515	0.507	0.498	0.476	0.539	0.520	0.507	0.500	0.490	0.468
3.6864	0.364	0.359	0.353	0.348	0.342	0.320	0.341	0.337	0.332	0.327	0.322	0.303
5.0	0.364	0.354	0.347	0.338	0.328	0.291	0.341	0.330	0.325	0.315	0.305	0.270
10.0	0.371	0.367	0.366	0.363	0.360	0.352	0.348	0.344	0.344	0.341	0.338	0.331
ch2												
1.2288	0.783	0.781	0.772	0.740	0.742	0.705	0.790	0.788	0.779	0.746	0.748	0.709
3.6864	0.360	0.354	0.347	0.340	0.333	0.307	0.336	0.330	0.324	0.318	0.314	0.291
5.0	0.354	0.344	0.336	0.327	0.317	0.275	0.330	0.321	0.313	0.304	0.294	0.254
10.0	0.362	0.362	0.362	0.361	0.361	0.362	0.339	0.339	0.338	0.337	0.337	0.338
ch3												
1.2288	0.540	0.528	0.525	0.468	0.490	0.478	0.524	0.511	0.509	0.449	0.474	0.464
3.6864	0.300	0.288	0.281	0.268	0.259	0.217	0.271	0.260	0.253	0.240	0.232	0.194
5.0	0.310	0.304	0.299	0.295	0.289	0.271	0.280	0.276	0.271	0.269	0.263	0.249
10.0	0.309	0.304	0.300	0.296	0.286	0.264	0.279	0.276	0.272	0.269	0.259	0.240
ch4												
1.2288	0.691	0.693	0.676	0.662	0.660	0.657	0.697	0.699	0.682	0.668	0.665	0.663
3.6864	0.639	0.635	0.625	0.623	0.619	0.590	0.639	0.635	0.625	0.623	0.620	0.591
5.0	0.617	0.613	0.606	0.601	0.598	0.565	0.616	0.612	0.606	0.601	0.598	0.565
10.0	0.585	0.580	0.573	0.565	0.560	0.523	0.582	0.577	0.570	0.562	0.557	0.521

On the other hand, Θ decreases with roll-off factor; this can be easily understood if we

Table 9: Orthogonality Factor for QPSK and AMRC

	Without Variance						With Variance					
	0.00	0.12	0.22	0.35	0.50	1.00	0.00	0.12	0.22	0.35	0.50	1.00
ch1												
1.2288	0.466	0.434	0.406	0.390	0.378	0.348	0.417	0.385	0.362	0.349	0.340	0.315
3.6864	0.415	0.402	0.398	0.393	0.380	0.347	0.374	0.363	0.361	0.358	0.348	0.320
5.0	0.417	0.403	0.392	0.381	0.369	0.324	0.381	0.366	0.357	0.347	0.333	0.290
10.0	0.376	0.374	0.372	0.369	0.365	0.352	0.349	0.348	0.347	0.344	0.340	0.330
ch2												
1.2288	0.651	0.626	0.613	0.582	0.580	0.521	0.672	0.641	0.624	0.585	0.578	0.506
3.6864	0.362	0.356	0.349	0.345	0.334	0.307	0.338	0.333	0.327	0.323	0.313	0.290
5.0	0.370	0.358	0.347	0.335	0.318	0.270	0.348	0.337	0.325	0.313	0.296	0.248
10.0	0.359	0.360	0.359	0.358	0.358	0.357	0.336	0.336	0.335	0.335	0.334	0.334
ch3												
1.2288	0.428	0.401	0.374	0.368	0.358	0.367	0.400	0.371	0.344	0.338	0.322	0.327
3.6864	0.321	0.308	0.298	0.287	0.269	0.217	0.289	0.277	0.268	0.258	0.239	0.190
5.0	0.315	0.307	0.304	0.300	0.289	0.270	0.281	0.276	0.273	0.270	0.262	0.247
10.0	0.310	0.306	0.301	0.295	0.285	0.262	0.278	0.275	0.271	0.266	0.256	0.237
ch4												
1.2288	0.832	0.788	0.785	0.789	0.798	0.774	0.857	0.816	0.812	0.822	0.826	0.792
3.6864	0.539	0.528	0.530	0.516	0.516	0.494	0.513	0.500	0.500	0.488	0.487	0.465
5.0	0.523	0.513	0.513	0.502	0.493	0.471	0.500	0.491	0.490	0.479	0.471	0.450
10.0	0.530	0.523	0.517	0.513	0.507	0.490	0.520	0.511	0.506	0.500	0.493	0.477

consider the fact the chip waveform decays faster for higher roll-off factor: there is going to be less ICI for both random and orthogonal codes, but the orthogonal codes are going to experience the most increase in SNR since they already have lower interference. Notice also, how in some instances there is a meaningful variation in Θ depending on the roll-off selected.

Notice that high values of Θ are related to high values E_b/N_o: Same cell interference is composed of i) desired signals for other users, ii) their own self-interference. Low values for ii) means more correlation between one user's desired signal and the interference from other users, and thus less variability in the SNR.

Also notice that for channel 1 (10 Mcps), Channels 2 and 3 (3.6864, 5.0, and 10 Mcps), the values for orthogonality without variance for SMRC have similar values to AMRC; this implies that we can use the simpler method to come out with approximately the same result for channels with paths well separated.

The SNR-based orthogonality factor Θ_{SNR} was also obtained (see Table 10). Notice that Θ_{SNR} values are very different from the Θ values; also Θ_{SNR} decreases with increasing

β, but in general increases with chip rate.

	Without Variance					
	0.00	0.12	0.22	0.35	0.50	1.00
ch1						
1.2288	0.3336	0.3257	0.3152	0.3057	0.2985	0.2788
3.6864	0.3248	0.3290	0.3307	0.3345	0.3404	0.3558
5.0	0.3239	0.3199	0.3181	0.3128	0.3086	0.2849
10.0	0.3312	0.3377	0.3462	0.3530	0.3641	0.4104
ch2						
1.2288	0.4122	0.4022	0.3898	0.3734	0.3643	0.3318
3.6864	0.3134	0.3157	0.3165	0.3192	0.3227	0.3303
5.0	0.3083	0.3040	0.3020	0.2970	0.2933	0.2688
10.0	0.3161	0.3250	0.3356	0.3450	0.3600	0.4225
ch3						
1.2288	0.1523	0.1488	0.1436	0.1355	0.1337	0.1219
3.6864	0.1857	0.1842	0.1803	0.1758	0.1740	0.1556
5.0	0.1930	0.1943	0.1960	0.1987	0.2011	0.2173
10.0	0.1924	0.1946	0.1966	0.1993	0.1999	0.2106
ch4						
1.2288	0.5124	0.5051	0.5004	0.4944	0.4884	0.4810
3.6864	0.5561	0.5551	0.5521	0.5525	0.5546	0.5528
5.0	0.5410	0.5403	0.5387	0.5387	0.5409	0.5385
10.0	0.5211	0.5209	0.5188	0.5178	0.5187	0.5124

Table 10: SNR-based Orthogonality Factor for different channels, roll-offs and chip rate

The algorithm for AMRC is in the order $O(F^2 \cdot L^2)$: The sum over l_2 and l_4 can be obtained from reusing the sum over l_1 and l_3; the $\mathrm{Sg}(t_1, t_2)$ and $g2(t)$ functions need only be calculated once for each combination of the paths; there are other ways to simplify the algorithm even further (such as using the identity $\sum_{f_1=1}^{F} \sum_{f_2=1}^{F} a_{f_1} a_{f_2} = \sum_{f=1}^{N} a_f^2 + 2 \sum_{f_1=1}^{F} \sum_{f_2=f_1+1}^{F} a_{f_1} a_{f_2}$), but we chose not to use them for the sake of code simplicity. For N=128, the expressions for AMRC took 7.4 seconds to generate 10,000 points (each point a different fading situation) for channel 4, $\beta = 0.22$ and rate of 1.2288 Mcps; it takes 3.3 days to system-simulate 1 million points (which would be enough for estimate BER values up to 10^{-4}); it would take the same time to simulate the SMRC system (since only the weights change). The theoretical expression for SMRC takes 1.88 seconds. Under the same conditions, the values for channel 1 become respectively 11.05 seconds, 3.4 days, 2.83 seconds.

2.5.1 Tables and Figures

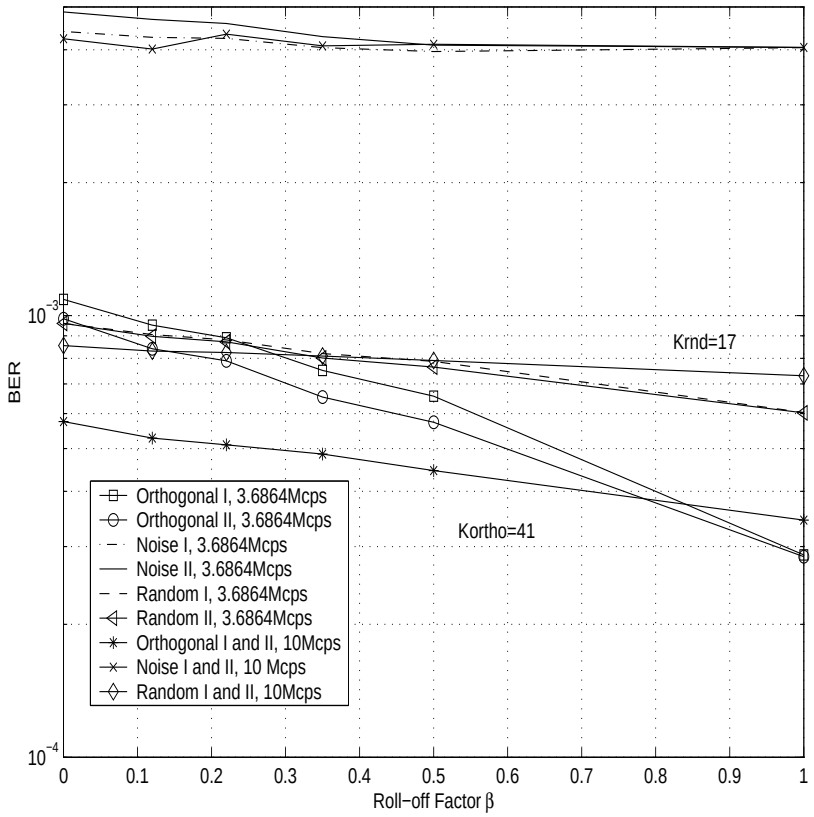

Figure 10: Comparison of Simple MRC models I and II for Channel 1.

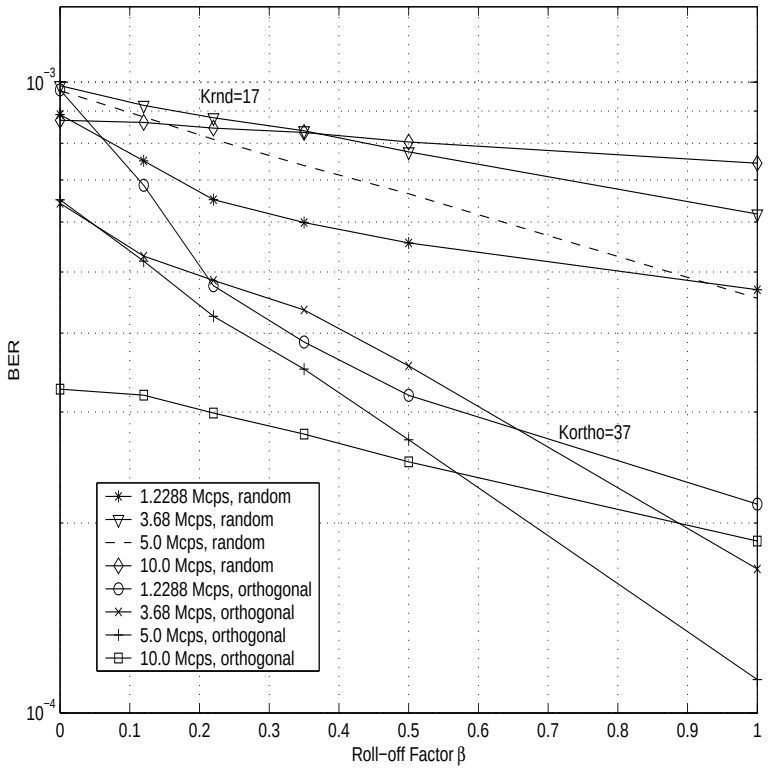

Figure 11: BER vs. Roll-off Factor for Channel 1 using different rates.

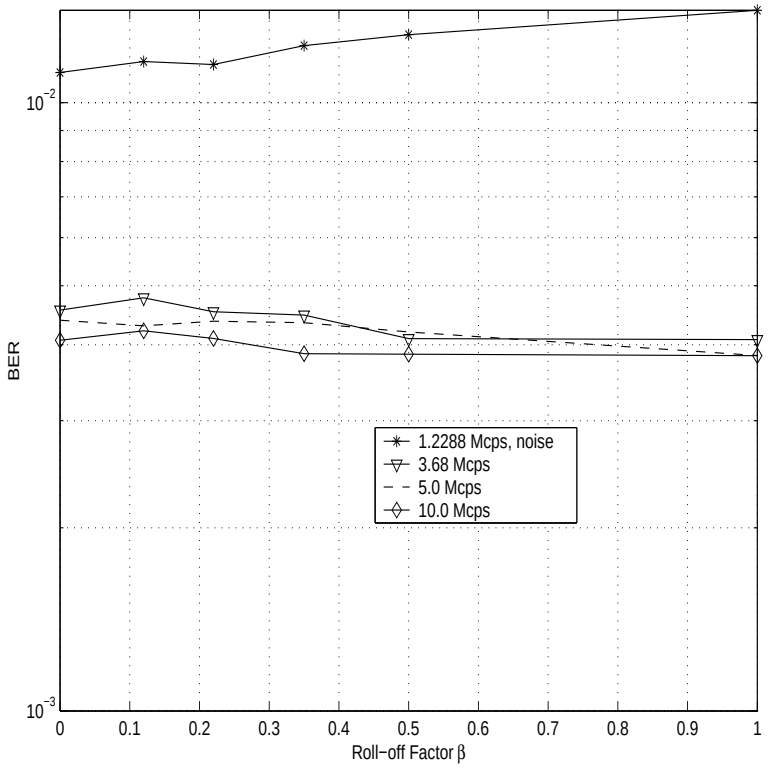

Figure 12: BER vs. Roll-off Factor for Channel 1 (Noise) using different rates.

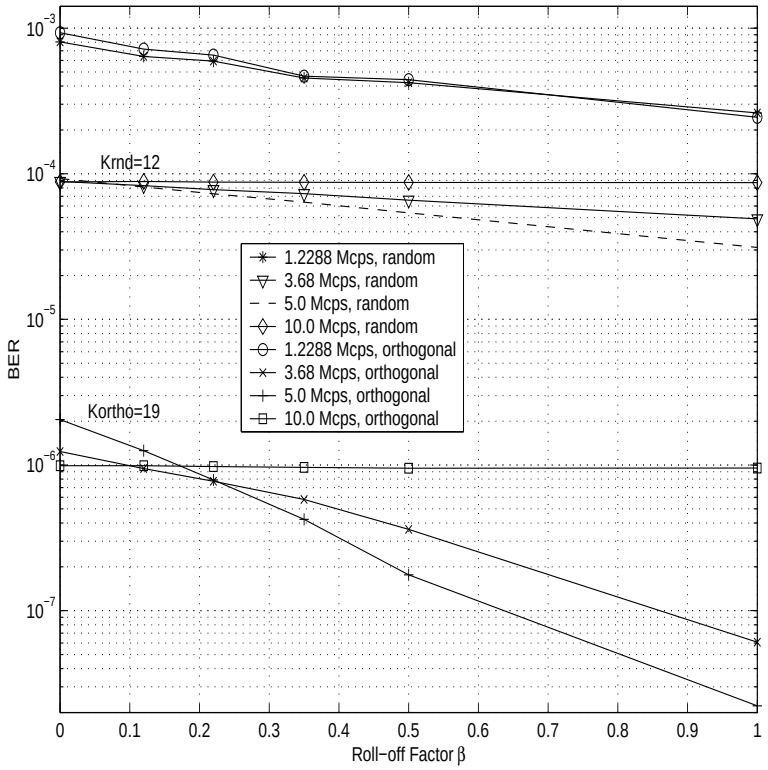

Figure 13: BER vs. Roll-off Factor for Channel 2 using different rates.

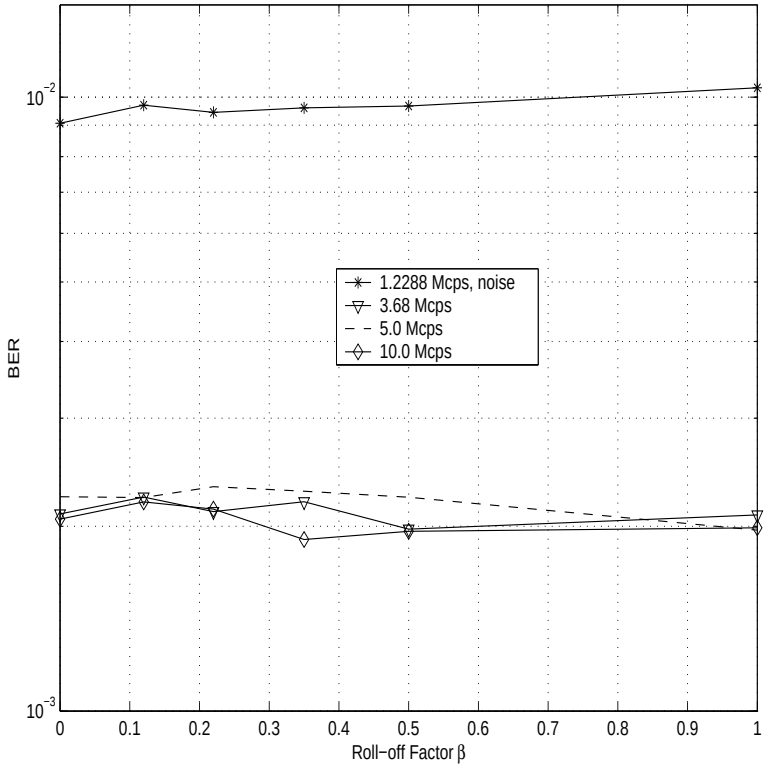

Figure 14: BER vs. Roll-off Factor for Channel 2 (Noise) using different rates.

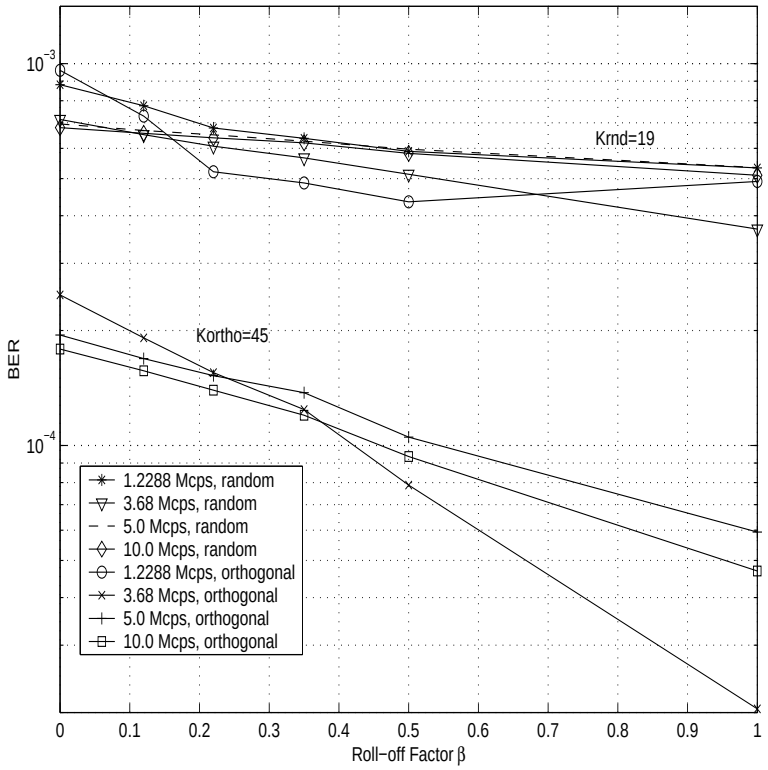

Figure 15: BER vs. Roll-off Factor for Channel 3 using different rates.

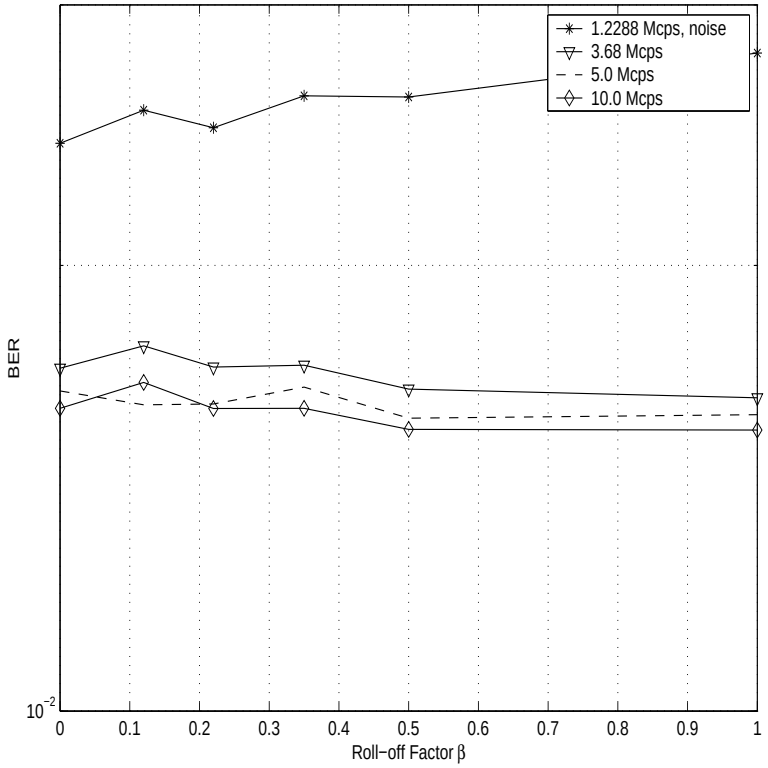

Figure 16: BER vs. Roll-off Factor for Channel 3 (Noise) using different rates.

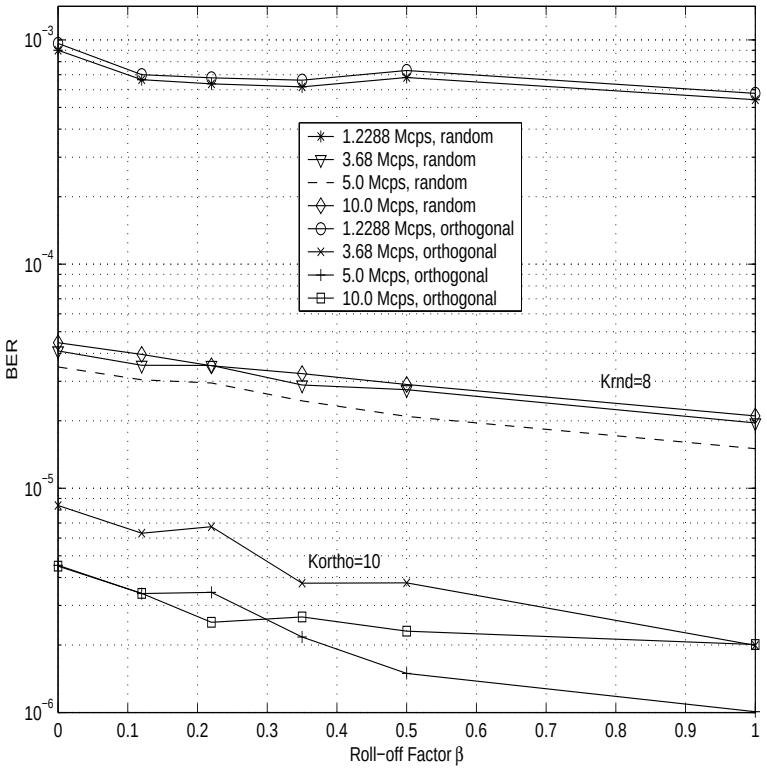

Figure 17: BER vs. Roll-off Factor for Channel 4 using different rates.

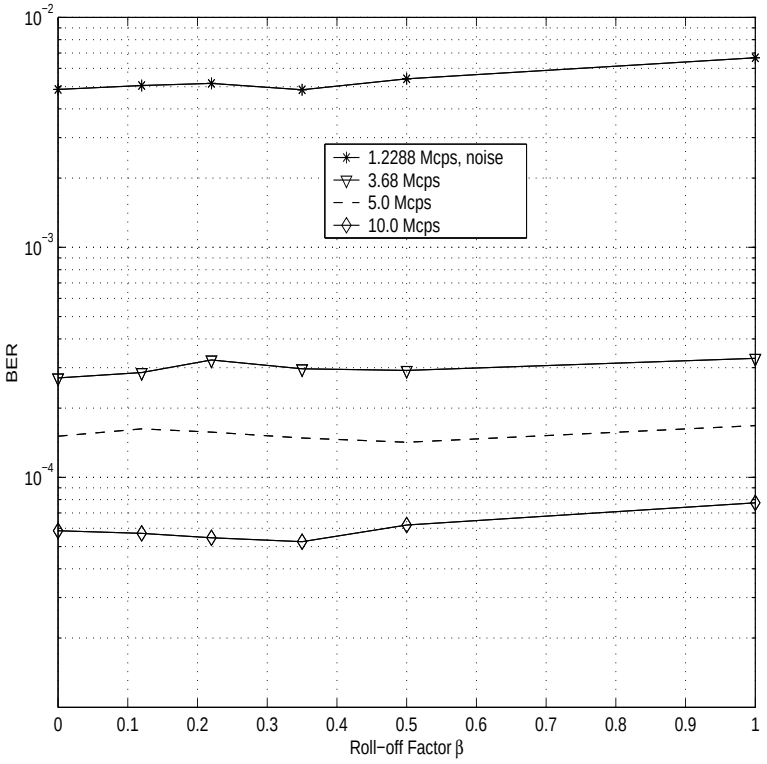

Figure 18: BER vs. Roll-off Factor for Channel 4 (Noise) using different rates.

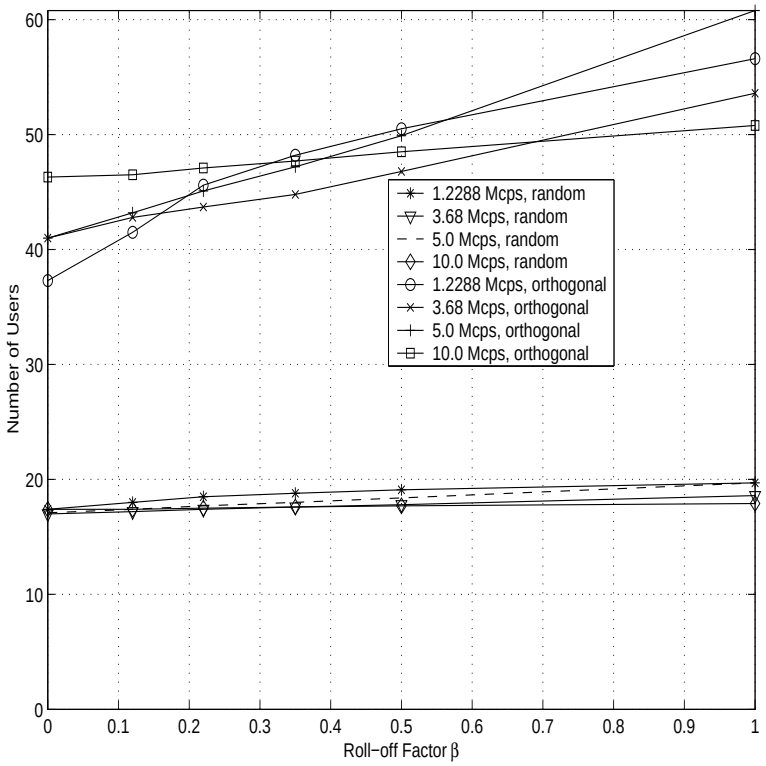

Figure 19: Number of Users vs. Roll-off Factor for Channel 1 using different rates.

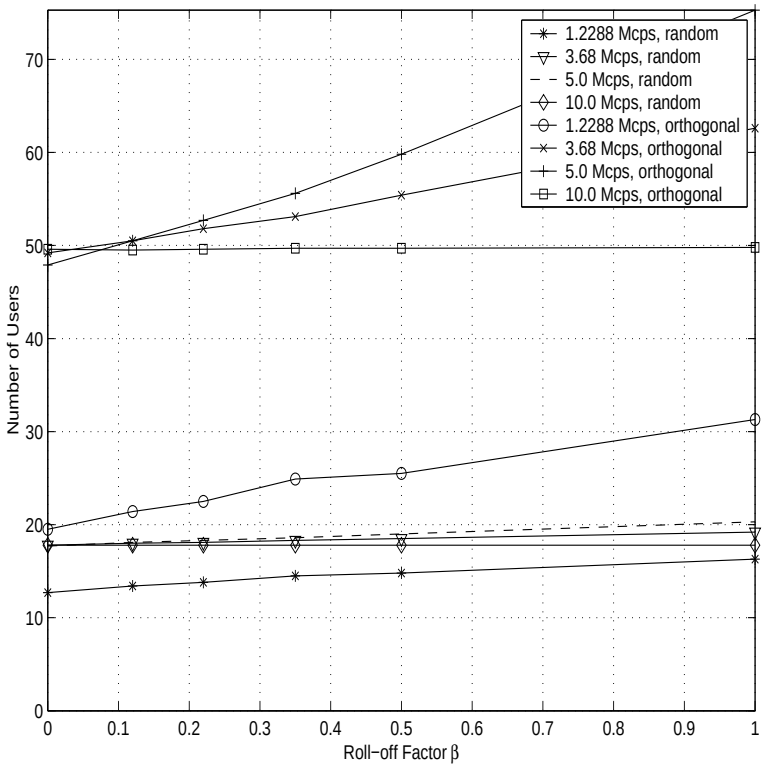

Figure 20: Number of Users vs. Roll-off Factor for Channel 2 using different rates.

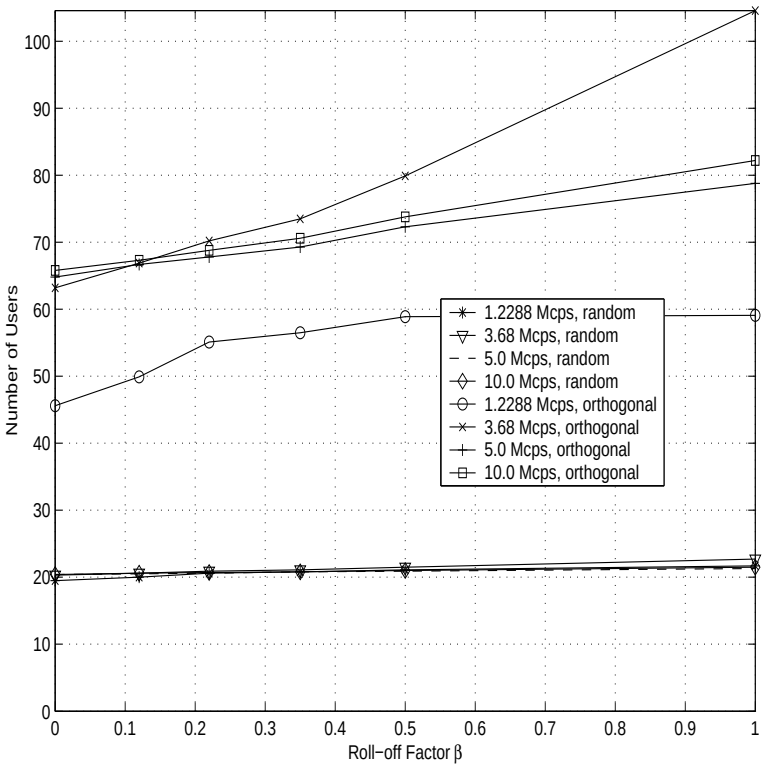

Figure 21: Number of Users vs. Roll-off Factor for Channel 3 using different rates.

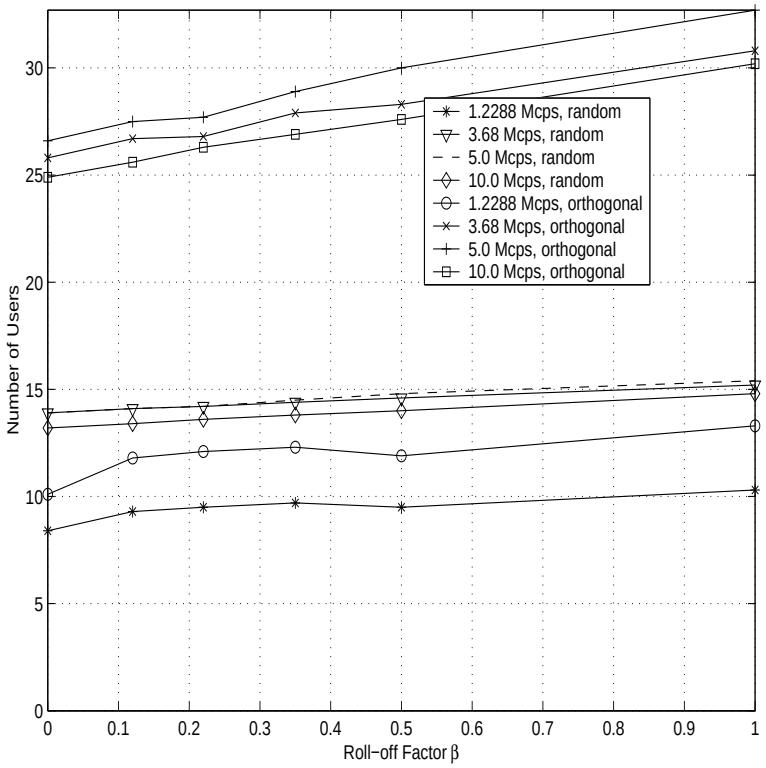

Figure 22: Number of Users vs. Roll-off Factor for Channel 4 using different rates.

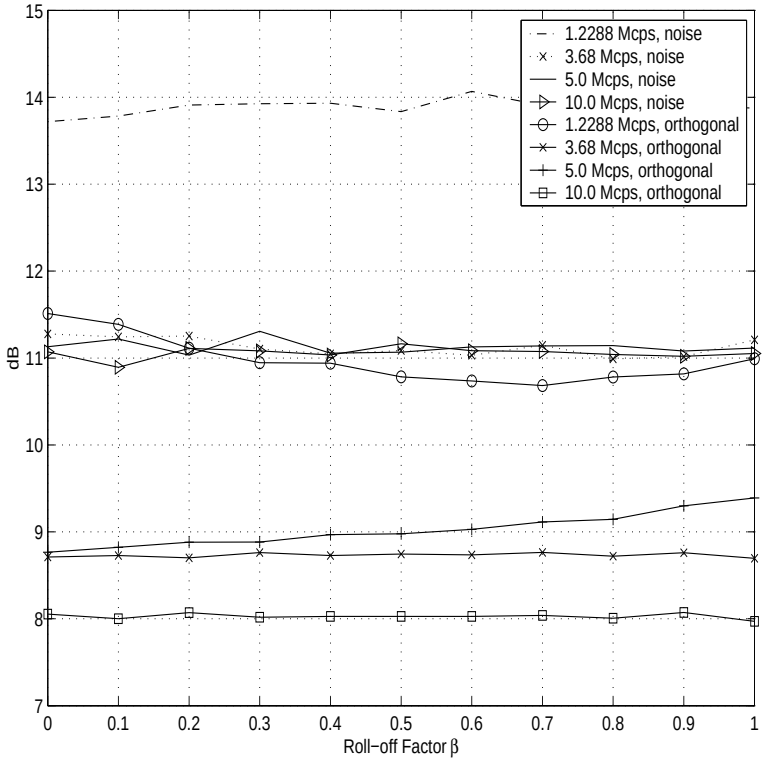

Figure 23: Output E_b/I_o vs. Roll-off Factor for Channel 1 using different rates.

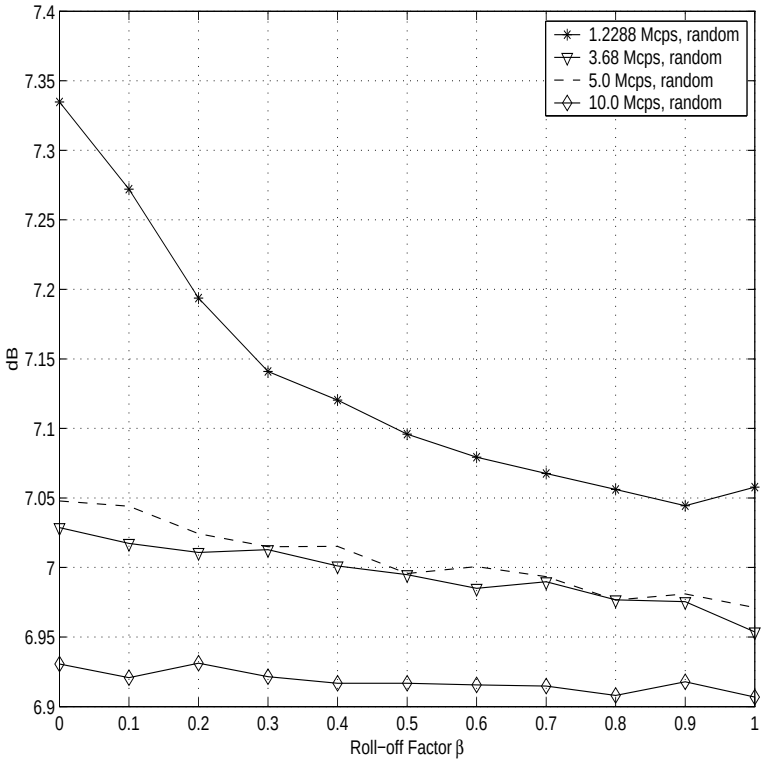

Figure 24: Output E_b/I_o vs. Roll-off Factor for Channel 1 using different rates.

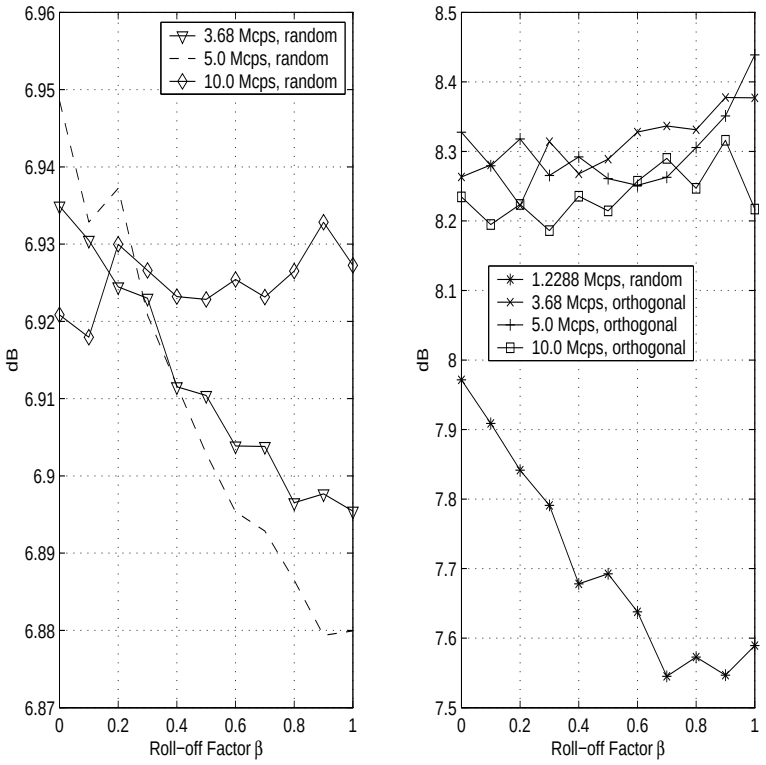

Figure 25: Output E_b/I_o vs. Roll-off Factor for Channel 2 using different rates.

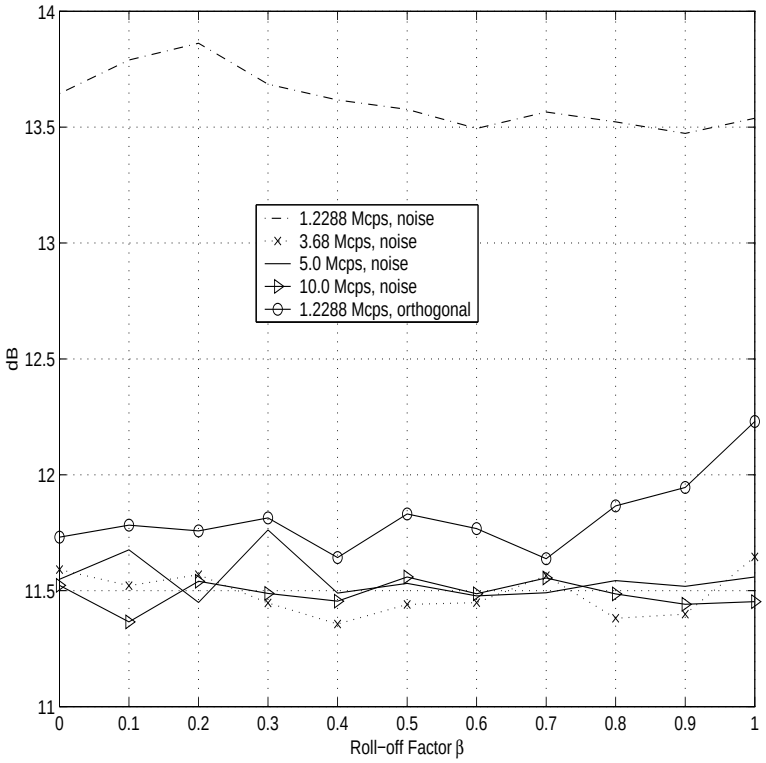

Figure 26: Output E_b/I_o vs. Roll-off Factor for Channel 2 using different rates.

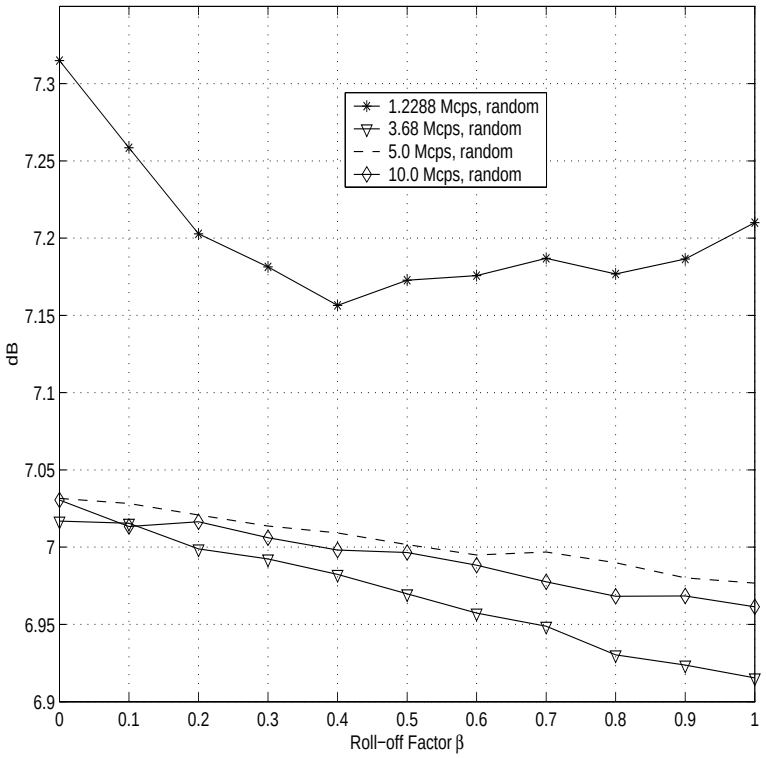

Figure 27: Output E_b/I_o vs. Roll-off Factor for Channel 3 using different rates.

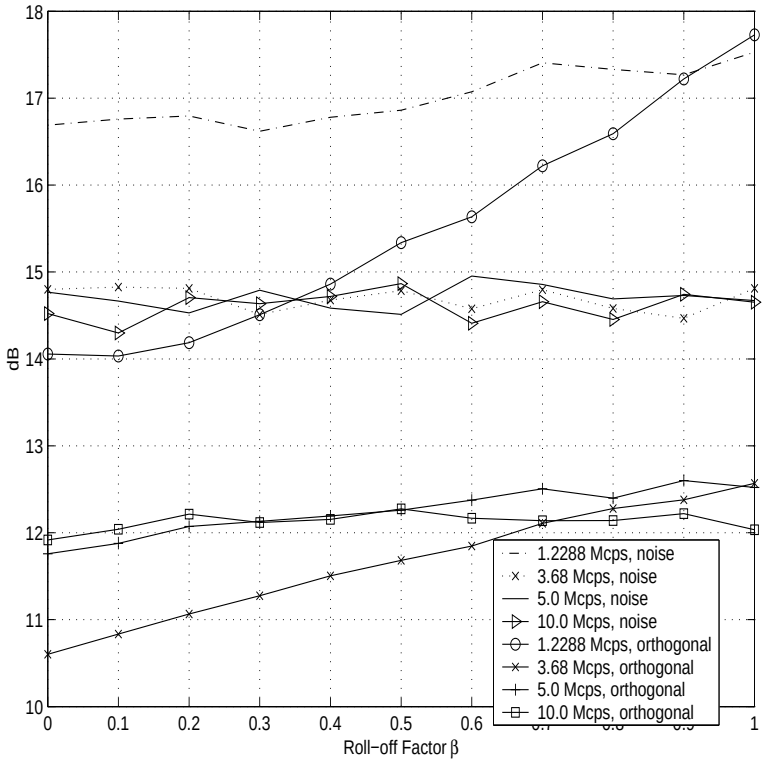

Figure 28: Output E_b/I_o vs. Roll-off Factor for Channel 3 using different rates.

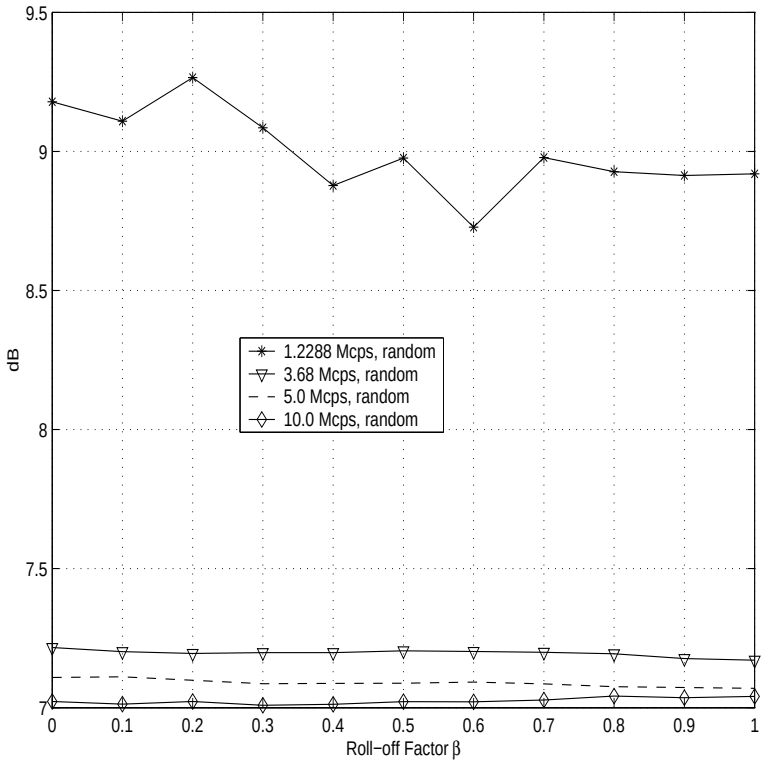

Figure 29: Output E_b/I_o vs. Roll-off Factor for Channel 4 using different rates.

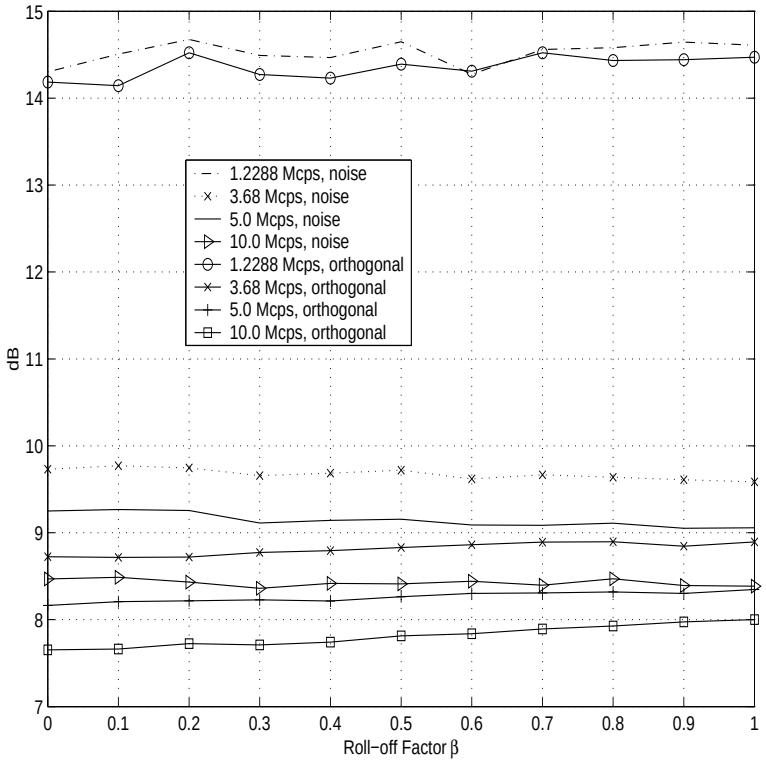

Figure 30: Output E_b/I_o vs. Roll-off Factor for Channel 4 using different rates.

CHAPTER III

CLOSED-FORM FOR INFINITE SUM OF NYQUIST FUNCTIONS

3.1 Raised Cosine Pulses

In the estimation of the performance of CDMA systems, many works assume rectangular pulse shaping to simplify the mathematical analysis. Some works do consider Root-Raised-Cosine (RRC) pulse shaping analysis ([7], [61], [16], [33], [69], [62]), usually in the reverse link, but leave the expressions for BER in terms of a variation ($t_1 = t_2$) of the following infinite sum form:

$$\sum_{n=-\infty}^{\infty} g_2(nT_c - t_1)g_2(nT_c - t_2), \tag{89}$$

where $g_2(t)$ is the RC function defined in (8).

While obtaining the expressions for the forward link of a CDMA system using RRC, the author ran into the more general form $t_1 \neq t_2$ form of the sum, which is presented in a closed form in this section.

Previously, Asano in [7] and Sibata et al. in [61] showed that

$$\sum_{n=-\infty}^{\infty} \frac{1}{T_c} \int_0^{T_c} g_2^2(nT_c + t)\mathrm{d}t = 1 - \frac{\beta}{4}. \tag{90}$$

DaSilva et al. [16] used the Sampling Theorem to show that $\sum_{n=-\infty}^{\infty} g_2^2(nT_c - t) = 1$ for $\beta = 0$ and any t. In trying to extend the result for arbitrary β, the author obtained (101) through curve-fitting; the expression matched very well the sum and it was decided to demonstrate it theoretically; a modification of the Sampling Theorem was used for this purpose (see A). Subsequently, functional series were used to derive the expression (102) for $t_1 = -t_2$ (see B). It was also observed that, for $\beta = 0$,

$$\sum_{n=\infty}^{\infty} g_2(nT_c - t_1)g_2(nT_c - t_2) = g_2(2(t_1 - t_2)), \quad \beta = 0. \tag{91}$$

These expressions ultimately shed light on the general expression.

3.1.1 Closed-Form Representation and Applications

Let $G_2(f)$ and $H(f)$ be the Fourier Transforms (FT) of $g_2(t)$ and $h(t) = g_2^2(t)$, respectively.

$$G_2(f) = \begin{cases} T_c & : \quad \left(0 \leq |f| \leq \frac{1-\beta}{2T_c}\right) \\ \frac{T_c}{2}\left\{1 + \cos\left[\frac{\pi T_c}{\beta}\left(|f| - \frac{1-\beta}{2T_c}\right)\right]\right\} & : \quad \left(\frac{1-\beta}{2T_c} \leq |f| \leq \frac{1+\beta}{2T_c}\right) \\ 0 & : \quad \left(|f| > \frac{1+\beta}{2T_c}\right) \end{cases} \tag{92}$$

A modification of the Sampling Theorem is used to take into account the aliasing when RRC with $\alpha \neq 0$ is sampled. The Fourier Transforms of $g_3(t) = g_2(t - \tau_1)$ and $g_4(t) = g_2(t-\tau_2)$ are respectively $G_2(f)e^{-j2\pi f\tau_1}$ and $G_2(f)e^{-j2\pi f\tau_2}$, where $G_2(F)$ is the FT of $g_2(t)$. Expressing convolution with an asterisk sign, the expression $\sum_{n=-\infty}^{\infty} g_2(nT_c-\tau_1)g_2(nT_c-\tau_2)$ can be rewritten as

$$\begin{aligned} &\int_{-\infty}^{\infty} g_3(t)g_4(t) \sum_{n=-\infty}^{\infty} \delta(t - nT_c)\mathrm{d}t \\ &= \frac{1}{T_c}\Big(\left[G_2(f)e^{-j2\pi f\tau_1}\right] * \left[G_2(f)e^{-j2\pi f\tau_2}\right] * \sum_{n=-\infty}^{\infty} \delta(f - \frac{n}{T_c})\Big)|_{f=0} \\ &= \frac{1}{T_c}\Big(\left[G_2(f')e^{-j2\pi f\tau_1}\right] * \left[\sum_{n=-\infty}^{\infty} G_2(f - \frac{n}{T_c})e^{-j2\pi(f-\frac{n}{T_c})\tau_2}\right] \Big)|_{f=0} \\ &= \frac{1}{T_c}\sum_{n=-\infty}^{\infty}\int_{-\infty}^{\infty} G_2(-\nu)e^{j2\pi\nu\tau_1}G_2(\nu - \frac{n}{T_c})e^{-j2\pi(\nu-\frac{n}{T_c})\tau_2}\mathrm{d}\nu \end{aligned} \tag{93}$$

Setting $\nu = -f'$ and considering that $G_2(f')$ is bandlimited ($|f'| > \frac{1+\beta}{2T_c}$, $0 \leq \beta \leq 1$), the values of n reduce to just -1, 0, and 1. Therefore, it becomes

$$\begin{aligned} \frac{1}{T_c}\Bigg(&\int_{-\infty}^{\infty} G_2^2(f')e^{-j2\pi f'(\tau_1-\tau_2)}\mathrm{d}f' + \int_{-\infty}^{\infty} G_2(f')G_2(\frac{1}{T_c} - f')e^{-j2\pi f'(\tau_1-\tau_2)}e^{-j\frac{2\pi\tau_2}{T_c}}\mathrm{d}f' \\ &+ \int_{-\infty}^{\infty} G_2(f')G_2(-\frac{1}{T_c} - f')e^{-j2\pi f'(\tau_1-\tau_2)}e^{j\frac{2\pi\tau_2}{T_c}}\mathrm{d}f'\Bigg) \end{aligned} \tag{94}$$

It was latter observed that this expression could have been alternatively obtained using the Poisson Summation Formula (30) and that it is in the form $z_1 + z_2e^{-j2\pi\tau_2/T_c} + z_3e^{j2\pi\tau_2/T_c}$,

where z_1, z_2, and z_3 can be shown to be respectively ($f' = f/T_c$, $d = (\tau_1 - \tau_2)/T_c$):

$$z_1 = \int_{\frac{1-\beta}{2}}^{\frac{1+\beta}{2}} e^{-j2\pi fd} \cos^4\left(\frac{\pi(2f-1+\beta)}{4\beta}\right) \mathrm{d}f + \int_{\frac{-1+\beta}{2}}^{\frac{1-\beta}{2}} e^{-j2\pi fd} \cos^4\left(\frac{\pi(-2f-1+\beta)}{4\beta}\right) \mathrm{d}f + \int_{\frac{-1+\beta}{2}}^{\frac{1-\beta}{2}} e^{-j2\pi fd} \mathrm{d}f$$
$$= \frac{j\,\left(3 - 3\,e^{2\,j\,(1+\beta)\,d\,\pi} + \left(-5 + 8\,\beta^2\,d^2\right)\,\left(e^{2\,j\,d\,\pi} - e^{2\,j\,\beta\,d\,\pi}\right)\right)}{16\,\pi\,d\,\left(1 - 5\,\beta^2\,d^2 + 4\,\beta^4\,d^4\right)\,e^{j\,(1+\beta)\,d\,\pi}}, \tag{95}$$

$$z_2 = \frac{1}{4}\int_{(1-\beta)/2}^{(1+\beta)/2} e^{-j2\pi fd}\left(1 + \cos\left[\frac{\pi}{\beta}(f - \frac{1-\beta}{2})\right]\right) \cdot \left(1 + \cos\left[\frac{\pi}{\beta}(-f + 1 - \frac{1-\beta}{2})\right]\right) \mathrm{d}f = \frac{j\,\left(-1 + e^{2\,j\,\beta\,d\,\pi}\right)}{16\,\pi\,d\,\left(-1+\beta\,d\right)\,\left(1+\beta\,d\right)\,e^{j\,(1+\beta)\,d\,\pi}}$$
$$= \frac{-2\,\cos(d\,\pi)\,\sin(d\pi\beta) + 2\,j\,\sin(d\,\pi)\,\sin(d\,\pi\,\beta)}{16\,\pi\,d\,((\beta\,d)^2 - 1)}, \tag{96}$$

$$z_3 = \frac{1}{4}\int_{-(1+\beta)/2}^{-(1-\beta)/2} e^{-j2\pi fd}\left(1 + \cos\left[\frac{\pi}{\beta}(-f - \frac{1-\beta}{2})\right]\right) \cdot \left(1 + \cos\left[\frac{\pi}{\beta}(f + 1 - \frac{1-\beta}{2})\right]\right) \mathrm{d}f = z_2^*. \tag{97}$$

Combining these three expressions, we obtain

$$z_1 + z_2 e^{-j2\pi\tau_2/T_c} + z_3 e^{j2\pi\tau_2/T_c} = \frac{\sin(d\,\pi\,\beta)(-2\,\cos(d\,\pi) + 2\,j\,\sin(d\,\pi))\,e^{-j2\pi\tau_2/T_c}}{16\,\pi\,d\,((\beta\,d)^2 - 1)} + \frac{\sin(d\,\pi\,\beta)(-2\,\cos(d\,\pi) - 2\,j\,\sin(d\,\pi))\,e^{j2\pi\tau_2/T_c}}{16\,\pi\,d\,((\beta\,d)^2 - 1)} + \frac{j\,\left(3 + \left(-5 + 8\,\beta^2\,d^2\right)\,e^{2\,j\,d\,\pi} + \left(5 - 8\,\beta^2\,d^2\right)\,e^{2\,j\,\beta\,d\,\pi} - 3\,e^{2\,j\,(1+\beta)\,d\,\pi}\right)}{16\,\pi\,d\,\left(1 - 5\,\beta^2\,d^2 + 4\,\beta^4\,d^4\right)\,e^{j\,(1+\beta)\,d\,\pi}}$$

The first two terms in the sum simplify to

$$\frac{\sin(\beta d\pi)\cos(\pi(\tau_1+\tau_2)/T_c)}{4\pi d(1-\beta^2 d^2)}, \tag{98}$$

and the third term to

$$\frac{3\sin((1-\beta)d\pi) + 3\sin((1+\beta)d\pi)}{8d\pi(1-4\beta^2d^2)(1-\beta^2d^2)} + \frac{2\sin(d\pi(1-\beta))}{4d\pi(1-\beta^2d^2)}. \tag{99}$$

After further simplification and redefining $d = (\tau_1 - \tau_2)$,

$$\mathrm{Sg}(\tau_1,\tau_2) = g_2(d) - \frac{\sin(\beta(d/T_c)\pi)}{2\pi(d/T_c)(1-\beta^2(d/T_c)^2)}\sin(\frac{\pi\tau_1}{T_c})\sin(\frac{\pi\tau_2}{T_c}), \tag{100}$$

which for $\tau_2 = \tau_1 = \tau$, $d = 0$, and applying the Rule of L'Hopital and simplifying, we obtain:

$$\sum_{n=-\infty}^{\infty} g_2^2(nT_c - \tau) = \mathrm{Sg}(\tau, \tau) = 1 - \frac{\beta}{2}\sin^2(\frac{\pi\tau}{T_c}). \tag{101}$$

If $\tau_1 = -\tau_2$,

$$\sum_{n=-\infty}^{\infty} g_2(nT_c - \tau)g_2(nT_c + \tau) = \mathrm{Sg}(\tau, -\tau) = g_2(2\tau) + \frac{1}{2}g_2(\tau)\sin(\frac{\tau\pi}{T_c})\sin(\frac{\beta\pi\tau}{T_c}). \tag{102}$$

For $\beta = 0$, (100) reduces to $g_2(d)$. The expression (101) is periodic in τ and its average is $1 - \frac{\beta}{4}$, a value obtained in [7] and [61]; the equivalent value for rectangular pulse shaping is $\frac{2}{3}$. An interesting property is that $\mathrm{Sg}(0, t) = \mathrm{Sg}(t, 0) = g_2(t)$.

Averaging $\mathrm{Sg}(t, t + d)$ over t in $[0, T_c]$ results in the convolution of $g_2(t)$ with itself:

$$\begin{aligned}\frac{1}{T_c}\int_0^{T_c}\sum_{n=-\infty}^{\infty} g_2(nT_c + t)g_2(nT_c + t + d)\mathrm{d}t &= \frac{1}{T_c}\int_{-\infty}^{\infty} g_2(\tau)g_2(\tau + d)\mathrm{d}\tau \\ = \frac{1}{T_c}\int_{-\infty}^{\infty} g_2(\tau)g_2(-\tau - d)\mathrm{d}\tau &= \frac{1}{T_c}g_2(-d) * g_2(-d) = \frac{1}{T_c}g_2(d) * g_2(d).\end{aligned} \tag{103}$$

Therefore,

$$\frac{1}{T_c}g_2(t) * g_2(t) = g_2(t) - \frac{\sin(\beta(t/T_c)\pi)}{4\pi(t/T_c)(1 - \beta^2(t/T_c)^2)}\cos(\frac{\pi t}{T_c}). \tag{104}$$

In Fig. 31, the expression derived (solid lines) was compared with the sum (dotted lines) for $\beta = 0.22$ and $T_c = 1$. The sum was done for $-10 \leq n \leq 10$. The values for τ_1 and τ_2 were multiple of 0.1 between -2 and 2.

This expression applies to the variance of the MAI in the reverse link of CDMA systems [33, eq. A7]. In [69, eq 21], the variance of the MAI is in the same form as (101); also, the infinite sum in [62, eqs. 9-10 and eqs. 19-23] are in the (101) form. Notice that in [10, eq. 26], collecting the i and m variables together and taking into account that $N = T/T_c$, we can obtain an equation in the form
$N\sum_{n=\infty}^{\infty} g_2(nT_c - t_1)g_2(nT_c - t_2) - Ng_2(t_1)g_2(t_2)$. In [36, eq. A2.6], the expression we derived is applicable to var_ρ; it can also be used to approximate res_ρ_a_1a_2 for large N_1 and N_2 and Δ much smaller than the bit duration.

We have thus presented a close-form expression for an infinite sum that often appears in CDMA systems analysis that include RRC pulse shaping with arbitrary roll-off factor.

Examples of the applications of this expression were also presented. It is expected as a result that new studies will not need to rely as much on rectangular pulse shaping from now on.

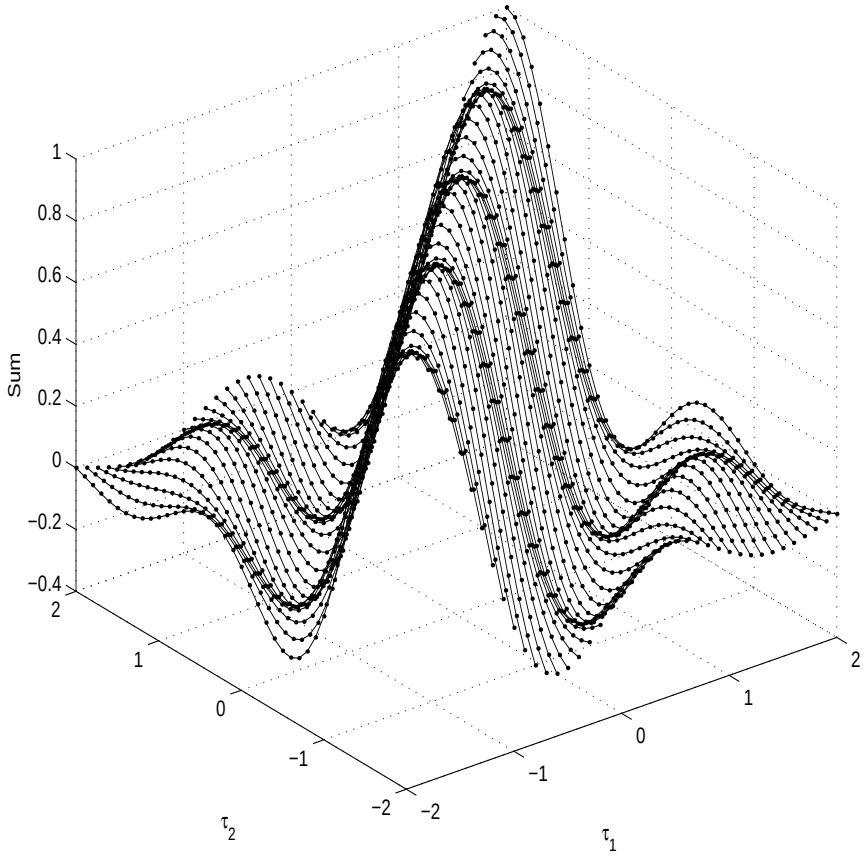

Figure 31: Comparison of Infinite Sum (dotted lines) and Derived Formula (solid lines) for $\beta = 0.22$

3.1.2 Detailed Proof

We can use the following identities to simplify the integrals in z_1:

$$\cos^4(x) = \frac{3 + 4\,\cos(2\,x) + \cos(4\,x)}{8}, \tag{105}$$

$$\int \cos(\frac{b\,x + c}{d}) e^{-j\,a\,x} \mathrm{d}x = \frac{j\,h\,\cos(\frac{b\,x}{h})\,\left(a\,h\,\cos(\frac{c}{h}) + j\,b\,\sin(\frac{c}{h})\right)}{e^{j\,a\,x}\,(-b + a\,h)\,(b + a\,h)} + \frac{h\,\left(-\left(b\,\cos(\frac{c}{h})\right) - j\,a\,h\,\sin(\frac{c}{h})\right)\,\sin(\frac{b\,x}{h})}{e^{j\,a\,x}\,(-b + a\,h)\,(b + a\,h)}. \tag{106}$$

For z_1, the first integral without the limits becomes

$$\frac{3\,j}{16\,\pi\,d\,e^{2\,j\,d\,f\,\pi}}+\frac{j\,\beta\,\cos(\frac{f\,\pi}{\beta})\,\left(2\,d\,\beta\,\cos(\frac{\pi\,(-1+\beta)}{2\,\beta})+j\,\sin(\frac{\pi\,(-1+\beta)}{2\,\beta})\right)}{2\,e^{2\,j\,d\,f\,\pi}\,\pi\,(-1+2\,d\,\beta)\,(1+2\,d\,\beta)}+$$
$$\frac{\beta\,\sin(\frac{f\,\pi}{\beta})\,\left(-\cos(\frac{\pi\,(-1+\beta)}{2\,\beta})-2\,j\,d\,\beta\,\sin(\frac{\pi\,(-1+\beta)}{2\,\beta})\right)}{2\,e^{2\,j\,d\,f\,\pi}\,\pi\,(-1+2\,d\,\beta)\,(1+2\,d\,\beta)}+$$
$$\frac{j\,\beta\,\cos(\frac{2\,f\,\pi}{\beta})\,\left(d\,\beta\,\cos(\frac{\pi\,(-1+\beta)}{\beta})+j\,\sin(\frac{\pi\,(-1+\beta)}{\beta})\right)}{16\,e^{2\,j\,d\,f\,\pi}\,\pi\,(-1+d\,\beta)\,(1+d\,\beta)}+$$
$$\frac{\beta\,\sin(\frac{2\,f\,\pi}{\beta})\,\left(-\cos(\frac{\pi\,(-1+\beta)}{\beta})-j\,d\,\beta\,\sin(\frac{\pi\,(-1+\beta)}{\beta})\right)}{16\,e^{2\,j\,d\,f\,\pi}\,\pi\,(-1+d\,\beta)\,(1+d\,\beta)}. \tag{107}$$

For z_1, the second integral without the limits becomes

$$\frac{3\,j}{16\,d\,e^{2\,j\,d\,f\,\pi}\,\pi}+\frac{j\,\beta\,\cos(\frac{f\,\pi}{\beta})\,\left(2\,\beta\,d\,\cos(\frac{(-1+\beta)\,\pi}{2\,\beta})-j\,\sin(\frac{(-1+\beta)\,\pi}{2\,\beta})\right)}{2\,(-1+2\,\beta\,d)\,(1+2\,\beta\,d)\,e^{2\,j\,d\,f\,\pi}\,\pi}+$$
$$\frac{j\,\beta\,\cos(\frac{2\,f\,\pi}{\beta})\,\left(\beta\,d\,\cos(\frac{(-1+\beta)\,\pi}{\beta})-j\,\sin(\frac{(-1+\beta)\,\pi}{\beta})\right)}{16\,(-1+\beta\,d)\,(1+\beta\,d)\,e^{2\,j\,d\,f\,\pi}\,\pi}-$$
$$\frac{\beta\,\left(\cos(\frac{(-1+\beta)\,\pi}{2\,\beta})-2\,j\,\beta\,d\,\sin(\frac{(-1+\beta)\,\pi}{2\,\beta})\right)\,\sin(\frac{f\,\pi}{\beta})}{2\,(-1+2\,\beta\,d)\,(1+2\,\beta\,d)\,e^{2\,j\,d\,f\,\pi}\,\pi}-$$
$$\frac{\beta\,\left(\cos(\frac{(-1+\beta)\,\pi}{\beta})-j\,\beta\,d\,\sin(\frac{(-1+\beta)\,\pi}{\beta})\right)\,\sin(\frac{2\,f\,\pi}{\beta})}{16\,(-1+\beta\,d)\,(1+\beta\,d)\,e^{2\,j\,d\,f\,\pi}\,\pi}. \tag{108}$$

For z_2, we have that

$$\left(1+\cos\left[\frac{\pi}{\beta}(f-\frac{1-\beta}{2})\right]\right)\left(1+\cos\left[\frac{\pi}{\beta}(-f+1-\frac{1-\beta}{2})\right]\right)=\frac{1}{2}+\frac{1}{2}\,\cos(\frac{\pi}{\beta}-\frac{2\,f\,\pi}{\beta}). \tag{109}$$

Therefore, without the limits, it is simply

$$\frac{j e^{-2\,j\,d\,f\,\pi}}{16\,d\,\pi}+\frac{j\,\beta\,\cos(\frac{2\,f\,\pi}{\beta})\,\left(\beta\,d\,\cos(\frac{\pi}{\beta})-j\,\sin(\frac{\pi}{\beta})\right)}{16\,\pi\,(-1+\beta\,d)\,(1+\beta\,d)\,e^{2\,j\,d\,f\,\pi}}-$$
$$\frac{\beta\,\left(\cos(\frac{\pi}{\beta})-j\,\beta\,d\,\sin(\frac{\pi}{\beta})\right)\,\sin(\frac{2\,f\,\pi}{\beta})}{16\,\pi\,(-1+\beta\,d)\,(1+\beta\,d)\,e^{2\,j\,d\,f\,\pi}}. \tag{110}$$

Replacing the limits for z_1,

$$\frac{j}{2\,\pi\,d}(e^{-j\,\pi\,(1-\beta)\,d}-e^{-j\,\pi\,(-1+\beta)\,d})-\frac{3\,j}{16\,d\,e^{j\,d\,\pi\,(-1-\beta)\,\pi}}-\frac{3\,j}{16\,d\,e^{j\,d\,\pi\,(1-\beta)\,\pi}}+$$
$$\frac{3\,j}{16\,d\,e^{j\,d\,\pi\,(-1+\beta)\,\pi}}+\frac{3\,j}{16\,d\,e^{j\,d\,\pi\,(1+\beta)\,\pi}}+$$
$$\left(\frac{-j\,\beta\,\cos(\frac{\pi\,(-1-\beta)}{2\,\beta})\,\left(2\,d\,\beta\,\cos(\frac{\pi\,(-1+\beta)}{2\,\beta})-j\,\sin(\frac{\pi\,(-1+\beta)}{2\,\beta})\right)}{e^{j\,d\,\pi\,(-1-\beta)}}+\right.$$
$$\frac{j\,\beta\,\cos(\frac{\pi\,(-1+\beta)}{2\,\beta})\,\left(2\,d\,\beta\,\cos(\frac{\pi\,(-1+\beta)}{2\,\beta})-j\,\sin(\frac{\pi\,(-1+\beta)}{2\,\beta})\right)}{e^{j\,d\,\pi\,(-1+\beta)}}-$$
$$\frac{j\,\beta\,\cos(\frac{\pi\,(1-\beta)}{2\,\beta})\,\left(2\,d\,\beta\,\cos(\frac{\pi\,(-1+\beta)}{2\,\beta})+j\,\sin(\frac{\pi\,(-1+\beta)}{2\,\beta})\right)}{e^{j\,d\,\pi\,(1-\beta)}}+$$
$$\frac{j\,\beta\,\cos(\frac{\pi\,(1+\beta)}{2\,\beta})\,\left(2\,d\,\beta\,\cos(\frac{\pi\,(-1+\beta)}{2\,\beta})+j\,\sin(\frac{\pi\,(-1+\beta)}{2\,\beta})\right)}{e^{j\,d\,\pi\,(1+\beta)}}-$$
$$\frac{\beta\,\sin(\frac{\pi\,(1-\beta)}{2\,\beta})\,\left(-\cos(\frac{\pi\,(-1+\beta)}{2\,\beta})-2\,j\,d\,\beta\,\sin(\frac{\pi\,(-1+\beta)}{2\,\beta})\right)}{e^{j\,d\,\pi\,(1-\beta)}}+$$
$$\frac{\beta\,\sin(\frac{\pi\,(-1-\beta)}{2\,\beta})\,\left(\cos(\frac{\pi\,(-1+\beta)}{2\,\beta})-2\,j\,d\,\beta\,\sin(\frac{\pi\,(-1+\beta)}{2\,\beta})\right)}{e^{j\,d\,\pi\,(-1-\beta)}}-$$
$$\frac{\beta\,\sin(\frac{\pi\,(-1+\beta)}{2\,\beta})\,\left(\cos(\frac{\pi\,(-1+\beta)}{2\,\beta})-2\,j\,d\,\beta\,\sin(\frac{\pi\,(-1+\beta)}{2\,\beta})\right)}{e^{j\,d\,\pi\,(-1+\beta)}}+$$
$$\left.\frac{\beta\,\left(-\cos(\frac{\pi\,(-1+\beta)}{2\,\beta})-2\,j\,d\,\beta\,\sin(\frac{\pi\,(-1+\beta)}{2\,\beta})\right)\,\sin(\frac{\pi\,(1+\beta)}{2\,\beta})}{e^{j\,d\,\pi\,(1+\beta)}}\right)\Big/\,(2\,\pi\,\,(-1+2\,d\,\beta)\,\,(1+2\,d\,\beta))+$$
$$\left(\frac{-j\,\beta\,\cos(\frac{\pi\,(-1-\beta)}{\beta})\,\left(d\,\beta\,\cos(\frac{\pi\,(-1+\beta)}{\beta})-j\,\sin(\frac{\pi\,(-1+\beta)}{\beta})\right)}{e^{j\,d\,\pi\,(-1-\beta)}}+\right.$$
$$\frac{j\,\beta\,\cos(\frac{\pi\,(-1+\beta)}{\beta})\,\left(d\,\beta\,\cos(\frac{\pi\,(-1+\beta)}{\beta})-j\,\sin(\frac{\pi\,(-1+\beta)}{\beta})\right)}{e^{j\,d\,\pi\,(-1+\beta)}}-$$
$$\frac{j\,\beta\,\cos(\frac{\pi\,(1-\beta)}{\beta})\,\left(d\,\beta\,\cos(\frac{\pi\,(-1+\beta)}{\beta})+j\,\sin(\frac{\pi\,(-1+\beta)}{\beta})\right)}{e^{j\,d\,\pi\,(1-\beta)}}+$$
$$\frac{j\,\beta\,\cos(\frac{\pi\,(1+\beta)}{\beta})\,\left(d\,\beta\,\cos(\frac{\pi\,(-1+\beta)}{\beta})+j\,\sin(\frac{\pi\,(-1+\beta)}{\beta})\right)}{e^{j\,d\,\pi\,(1+\beta)}}-$$
$$\frac{\beta\,\sin(\frac{\pi\,(1-\beta)}{\beta})\,\left(-\cos(\frac{\pi\,(-1+\beta)}{\beta})-j\,d\,\beta\,\sin(\frac{\pi\,(-1+\beta)}{\beta})\right)}{e^{j\,d\,\pi\,(1-\beta)}}+$$
$$\frac{\beta\,\sin(\frac{\pi\,(-1-\beta)}{\beta})\,\left(\cos(\frac{\pi\,(-1+\beta)}{\beta})-j\,d\,\beta\,\sin(\frac{\pi\,(-1+\beta)}{\beta})\right)}{e^{j\,d\,\pi\,(-1-\beta)}}-$$
$$\frac{\beta\,\sin(\frac{\pi\,(-1+\beta)}{\beta})\,\left(\cos(\frac{\pi\,(-1+\beta)}{\beta})-j\,d\,\beta\,\sin(\frac{\pi\,(-1+\beta)}{\beta})\right)}{e^{j\,d\,\pi\,(-1+\beta)}}+$$
$$\left.\frac{\beta\,\left(-\cos(\frac{\pi\,(-1+\beta)}{\beta})-j\,d\,\beta\,\sin(\frac{\pi\,(-1+\beta)}{\beta})\right)\,\sin(\frac{\pi\,(1+\beta)}{\beta})}{e^{j\,d\,\pi\,(1+\beta)}}\right)\Big/\,(16\,\pi\,\,(-1+d\,\beta)\,\,(1+d\,\beta))$$

After algebraic simplification

$$z_1 = \frac{j\,\left(3 - 3\,e^{2\,j\,(1+\beta)\,d\,\pi} + \left(-5 + 8\,\beta^2\,d^2\right)\,\left(e^{2\,j\,d\,\pi} - e^{2\,j\,\beta\,d\,\pi}\right)\right)}{16\,\pi\,d\,\left(1 - 5\,\beta^2\,d^2 + 4\,\beta^4\,d^4\right)\,e^{j\,(1+\beta)\,d\,\pi}}. \tag{111}$$

With regards to z_2,

$$\begin{aligned}
&\frac{-j}{8\,d\,e^{j\,d\,\pi\,(1-\beta)}\,\pi} + \frac{j}{8\,d\,e^{j\,d\,\pi\,(1+\beta)}\,\pi} + \\
&\left(\frac{-j\,\beta\,\cos(\frac{\pi\,(1-\beta)}{\beta})\,\left(d\,\beta\,\cos(\frac{\pi}{\beta}) - j\,\sin(\frac{\pi}{\beta})\right)}{e^{j\,d\,\pi\,(1-\beta)}} + \right. \\
&\frac{j\,\beta\,\cos(\frac{\pi\,(1+\beta)}{\beta})\,\left(d\,\beta\,\cos(\frac{\pi}{\beta}) - j\,\sin(\frac{\pi}{\beta})\right)}{e^{j\,d\,\pi\,(1+\beta)}} + \frac{\beta\,\left(\cos(\frac{\pi}{\beta}) - j\,d\,\beta\,\sin(\frac{\pi}{\beta})\right)\,\sin(\frac{\pi\,(1-\beta)}{\beta})}{e^{j\,d\,\pi\,(1-\beta)}} \\
&\left. - \frac{\beta\,\left(\cos(\frac{\pi}{\beta}) - j\,d\,\beta\,\sin(\frac{\pi}{\beta})\right)\,\sin(\frac{\pi\,(1+\beta)}{\beta})}{e^{j\,d\,\pi\,(1+\beta)}}\right) \Big/ \,(16\,\pi\,\,(-1 + d\,\beta)\,\,(1 + d\,\beta)),
\end{aligned} \tag{112}$$

which simplifies to

$$z_2 = \frac{j\,\left(-1 + e^{2\,j\,\beta\,d\,\pi}\right)}{8\,\pi\,d\,\left(-1 + \beta\,d\right)\,\left(1 + \beta\,d\right)\,e^{j\,(1+\beta)\,d\,\pi}}. \tag{113}$$

It can be easily seen that by substituting f by $-f$ in (96), we have that z_2 is the conjugate of z_3. Simplifying,

$$z_2 = z_3^* = \frac{-2\,\cos(d\,\pi)\,\sin(d\pi\beta) + 2\,j\,\sin(d\,\pi)\,\sin(d\pi\beta)}{16\,\pi\,d\,((\beta\,d)^2 - 1)}. \tag{114}$$

Therefore,

$$\begin{aligned}
\mathrm{Sg}(\tau_1, \tau_2) = z_2 e^{-j2\pi\tau_2/T_c} + z_3 e^{j2\pi\tau_2/T_c} + z_1 = &\frac{j\,e^{-j\,(1+\beta)\,d\,\pi - 2\,j\,\pi\,\tau_2/T_c}\,\left(-1 + e^{2\,j\,\beta\,d\,\pi}\right)}{16\pi d\,\left(-1 + \beta\,d\right)\,\left(1 + \beta\,d\right)} \\
&+ \frac{j\,e^{-j\,(-1+\beta)\,d\,\pi + 2\,j\,\pi\,\tau_2/T_c}\,\left(-1 + e^{2\,j\,\beta\,d\,\pi}\right)}{16\pi d\,\left(-1 + \beta\,d\right)\,\left(1 + \beta\,d\right)} \\
&+ \frac{\frac{j}{16}\,\left(3 + \left(-5 + 8\,\beta^2\,d^2\right)\,e^{2\,j\,d\,\pi} + \left(5 - 8\,\beta^2\,d^2\right)\,e^{2\,j\,\beta\,d\,\pi} - 3\,e^{2\,j\,(1+\beta)\,d\,\pi}\right)}{d\,\left(1 - 5\,\beta^2\,d^2 + 4\,\beta^4\,d^4\right)\,e^{j\,(1+\beta)\,d\,\pi}\,\pi}
\end{aligned} \tag{115}$$

The first two terms simplify as follows:

$$\begin{aligned}
\frac{1}{16\pi} \cdot \frac{-4\cos(d\pi)\sin(d\pi\beta)\cos(2\pi\tau_2/T_c) + 4\sin(d\pi)\sin(d\pi\beta)\sin(2\pi\tau_2/T_c)}{-d(1-\beta^2d^2)} \\
= \frac{\sin(d\pi\beta)(\cos(d\pi)\cos(2\pi\tau_2/T_c) - 4\sin(d\pi)\sin(2\pi\tau_2/T_c))}{4\pi d(1-\beta^2d^2)} \\
= \frac{\sin\beta d\pi}{4\pi d(1-\beta^2d^2)}\cos(\pi(t_1+t_2)/T_c)
\end{aligned} \tag{116}$$

And the third term to

$$\begin{aligned}
&\frac{j(-6j\sin(1+\beta)d\pi) + (8\beta^2d^2-5)(e^{j(d\pi-\beta d\pi)} - e^{-j(d\pi-\beta d\pi)})}{16d(1-4\beta^2d^2)(1-\beta^2d^2)\pi} \\
&= \frac{3\sin((1+\beta)d\pi) + 3\sin(d\pi-\beta d\pi) + (2-8\beta^2d^2)\sin(d\pi-\beta d\pi)}{8d(1-4\beta^2d^2)(1-\beta^2d^2)\pi} \\
&= \frac{3\sin((1-\beta)d\pi) + 3\sin((1+\beta)d\pi)}{8d\pi(1-4\beta^2d^2)(1-\beta^2d^2)} + \frac{2\sin(d\pi(1-\beta))}{4d\pi(1-\beta^2d^2)}. \qquad (117)
\end{aligned}$$

Using partial fractions for the first term in the sum (117)

$$\begin{aligned}
&\frac{3\sin((1-\beta)d\pi) + 3\sin((1+\beta)d\pi)}{8d\pi(1-4\beta^2d^2)(1-\beta^2d^2)} = \\
&\frac{-\sin((1-\beta)d\pi) - \sin((1+\beta)d\pi)}{8d\pi(1-\beta^2d^2)} + \frac{4\sin((1-\beta)d\pi) + 4\sin((1+\beta)d\pi)}{8d\pi(1-4\beta^2d^2)}, \qquad (118)
\end{aligned}$$

but $\sin((1+\beta)d\pi) + \sin((1-\beta)d\pi) = 2\sin(d\pi)\cos(\beta d\pi)$, the second term in (118) is simply $g_2(d)$. Putting together the remaining terms of $\mathrm{Sg}(\tau_1, \tau_2)$:

$$\begin{aligned}
\mathrm{Sg}(\tau_1,\tau_2) &= \frac{1}{4\pi}\cdot\frac{\sin\beta d\pi}{d(1-\beta^2d^2)}\cos(\pi(t_1+t_2)/T_c) \\
&\quad -\frac{2\sin(d\pi)\cos(\beta d\pi)}{8d\pi(1-\beta^2d^2)} + g_2(d) + \frac{2\sin(d\pi(1-\beta))}{4d\pi(1-\beta^2d^2)} \\
&= g_2(d) + \frac{\sin(\beta d\pi)\cos(\pi(\tau_1+\tau_2)/T_c) - \sin(\beta d\pi)\cos(d\pi)}{4\pi d(1-\beta^2d^2)} \qquad (119)
\end{aligned}$$

Redefining $d = (\tau_1 - \tau_2)$,

$$\mathrm{Sg}(\tau_1,\tau_2) = g_2(d) - \frac{\sin(\beta(d/T_c)\pi)}{2\pi(d/T_c)(1-\beta^2(d/T_c)^2)}\sin(\frac{\pi\tau_1}{T_c})\sin(\frac{\pi\tau_2}{T_c}). \qquad (120)$$

3.2 General Nyquist Pulses

In the study of the forward and reverse link of bandlimited CDMA systems with pulse $p(t)$, chip period T_c, and roll-off factor β, often appears a sum of the form $\sum_{n=-\infty}^{\infty} p(\tau_1 - nT_c)p(\tau_2 - nT_c)$, where τ_1 and τ_2 are time differences related to the delay profile and finger allocation in the RAKE receiver. In the previous section, a close form is presented for a raised cosine (RC) pulse with arbitrary β. Recently, novel pulses have been presented that have certain properties better than those of the RC pulse. A "Better than" Nyquist (BTN) pulse [9] has an eye diagram that is better than that for the RC pulse with the same β. In [14], a pulse was presented that is optimum in terms of multi-access interference. Also, in

[59], a family of Nyquist filters is presented that has an asymptotic decay faster than that of the raised cosine; this property is important when considering that in practise, the filters have to be truncated. We present an elegant approach that can be applied to any Nyquist pulse with arbitrary β and use the approach to obtain the close forms for the first two pulses for any τ_1 and τ_2, and close forms for the family of Nyquist filters for $\tau_1 = \tau_2 = \tau$.

3.2.1 Closed-Form Representation and Applications

Let $P(f)$ be the FT of a Nyquist pulse $\mathrm{p}(t)$. We have that because $\sum_{n=-\infty}^{\infty} P(f - n/T_c) = T_c$, for a pulse that is bandlimited with arbitrary $0 \leq \beta \leq 1$,

$$P(f) = \begin{cases} T_c & : \quad 0 \leq |f| \leq \frac{1-\beta}{2T_c} \\ \phi(|f|) \leq T_c & : \quad \frac{1-\beta}{2T_c} \leq |f| \leq \frac{1}{2T_c} \\ T_c - \phi(1-|f|) & : \quad \frac{1}{2T_c} \leq |f| \leq \frac{1+\beta}{2T_c} \\ 0 & : \quad |f| > \frac{1+\beta}{2T_c} \end{cases} \tag{121}$$

and using the properties of FTs, $p(t)$ is real and even as $P(f)$. Let also, $\hat{p}(t) = p(t \cdot T_c)$ be the normalized Nyquist pulse and $\hat{P}(f) = P(f/|T_c|)/|T_c|$ be the respective FT.

It was shown in the previous section that if the FT of a pulse is bandlimited such that it is zero for $|f'| > \frac{1+\beta}{2T_c}$, then

$$\begin{aligned} \mathrm{S_{NY}}(\tau_1, \tau_2, \beta) \equiv \sum_{n=-\infty}^{\infty} \mathrm{p}(nT_c - \tau_1)\mathrm{p}(nT_c - \tau_2) = \frac{1}{T_c} \Bigg(& \int_{-\infty}^{\infty} P^2(f') e^{-j2\pi f'(\tau_1 - \tau_2)} \mathrm{d}f' + \\ & \int_{-\infty}^{\infty} P(f') P(\frac{1}{T_c} - f') e^{-j2\pi f'(\tau_1 - \tau_2)} e^{-j\frac{2\pi\tau_2}{T_c}} \mathrm{d}f' \\ & + \int_{-\infty}^{\infty} P(f') P(-\frac{1}{T_c} - f') e^{-j2\pi f'(\tau_1 - \tau_2)} e^{j\frac{2\pi\tau_2}{T_c}} \mathrm{d}f' \Bigg), \end{aligned} \tag{122}$$

which is in the form $z_1 + z_2 e^{-j2\pi\tau_2/T_c} + z_3 e^{j2\pi\tau_2/T_c}$. Notice that the first integral, z_1, is the FT of $P^2(f)$ divided by T_c, and after using the duality and convolution properties of FTs and the fact that $p(d)$ is an even function, z_1 simplifies to $\frac{p(d) * p(d)}{T_c}$. Making the substitutions $f' = f/T_c$ and and using the equality $\hat{P}(-1-f) = \hat{P}(f+1)$, the sum $\mathrm{S_{NY}}(\tau_1, \tau_2, \beta)$ becomes

$$\begin{aligned} \int_{-\infty}^{\infty} \hat{P}^2(f) e^{-\frac{j2\pi fd}{T_c}} \mathrm{d}f + & \int_{-\infty}^{\infty} \hat{P}(f)\hat{P}(f-1) e^{-\frac{j2\pi fd}{T_c}} e^{-\frac{j2\pi\tau_2}{T_c}} \mathrm{d}f \\ & + \int_{-\infty}^{\infty} \hat{P}(f)\hat{P}(f+1) e^{-\frac{j2\pi fd}{T_c}} e^{\frac{j2\pi\tau_2}{T_c}} \mathrm{d}f. \end{aligned} \tag{123}$$

Using the equality $\hat{P}(f) = 1 - (1 - \hat{P}(f))$ and taking into account that $1 - \hat{P}(f) = 0$ for

$|f| < \frac{1-\beta}{2}$,

$$z_1 = \int_{-\infty}^{\infty} \hat{P}(f) e^{-\frac{j2\pi fd}{T_c}} \mathrm{d}f + \int_{(1-\beta)/2}^{(1+\beta)/2} \hat{P}(f)(1-\hat{P}(f)) e^{-\frac{j2\pi fd}{T_c}} \mathrm{d}f + \int_{-(1+\beta)/2}^{-(1-\beta)/2} \hat{P}(f)(1-\hat{P}(f)) e^{-\frac{j2\pi fd}{T_c}} \mathrm{d}f. \quad (124)$$

Using duality from the f to the d domain, the first integral is just $\hat{p}(-d/T_c) = p(-d)$. Noticing that $\hat{P}(f \pm 1) = 1 - \hat{P}(f)$ for $|f| > \frac{1-\beta}{2}$ and considering the domain of $\hat{P}(f)$ in (123), the second and third integrals in (124) are respectively z_2 and z_3 are respectively z_2 and z_3. As a result,

$$z_1 = p(-d) - z_2 - z_3 = p(d) - z_2 - z_3. \quad (125)$$

Using the change of variable $f = f' - 1/2$ for the second integral and $f = f' + 1/2$ for the third one,

$$z_1(d) = p(d) - \int_{-\beta/2}^{\beta/2} \hat{P}(f+\frac{1}{2})\hat{P}(f-\frac{1}{2}) e^{-\frac{j2\pi fd}{T_c}} e^{-\frac{j\pi d}{T_c}} \mathrm{d}f - \int_{-\beta/2}^{\beta/2} \hat{P}(f-\frac{1}{2})\hat{P}(-f-\frac{1}{2}) e^{-\frac{j2\pi fd}{T_c}} e^{\frac{j\pi d}{T_c}} \mathrm{d}f. \quad (126)$$

We can see that $\hat{P}(f+\frac{1}{2})\hat{P}(f-\frac{1}{2}) = \hat{P}(-f-\frac{1}{2})\hat{P}(f-\frac{1}{2})$ is an even function and $\Re\{e^{-j2\pi fd}\}$ is even and $\Im\{e^{-j2\pi fd}\}$ is odd; also, observe that $z_3 = z_2^*$:

$$\begin{aligned}
z_2 &= \int_0^{\beta/2} 2\hat{P}(f+\frac{1}{2})\hat{P}(f-\frac{1}{2}) \cos(\frac{2\pi fd}{T_c}) \mathrm{d}f e^{-\frac{j\pi d}{T_c}}, \\
z_3 &= \int_0^{\beta/2} 2\hat{P}(f+\frac{1}{2})\hat{P}(f-\frac{1}{2}) \cos(\frac{2\pi fd}{T_c}) \mathrm{d}f e^{\frac{j\pi d}{T_c}}, \\
z_{23} &= z_2 e^{-j2\pi\tau_2/T_c} + z_3 e^{j2\pi\tau_2/T_c} \\
&= 4\int_0^{\beta/2} \hat{P}(f+\frac{1}{2})\hat{P}(f-\frac{1}{2}) \cos(\frac{2\pi fd}{T_c}) \mathrm{d}f \cos(\pi(\tau_1+\tau_2)/T_c), \\
z_1 &= \frac{p(d) * p(d)}{T_c} = p(d) - 4\int_0^{\beta/2} \hat{P}(f+\frac{1}{2}) \cdot \\
&\quad \hat{P}(f-\frac{1}{2}) \cos(2\pi fd/T_c) \mathrm{d}f \cos(\pi d/T_c). \quad (127)
\end{aligned}$$

Therefore,

$$\begin{aligned}
\mathrm{S_{NY}}(\tau_1, \tau_2, \beta) &= p(d) - 8\sin(\frac{\pi\tau_1}{T_c})\sin(\frac{\pi\tau_2}{T_c}) \int_0^{\beta/2} \cdot \\
&\quad \hat{P}(f'+\frac{1}{2})\hat{P}(f'-\frac{1}{2}) \cos(\frac{2\pi f'd}{T_c}) \mathrm{d}f' \\
&= p(d) - 4\sin(\frac{\pi\tau_1}{T_c})\sin(\frac{\pi\tau_2}{T_c})\, z_2\, e^{j\pi d/T_c}, \quad (128)
\end{aligned}$$

where $f' = f - 1/2$ and $\hat{P}(f)$ is the normalized version of (121). As mentioned in [28], this infinite sum with arbitrary τ_1 and τ_2 has applications towards [10, eq. 26] , while the convolution form (127) can be used towards [33, eq. A7]. The special case $\tau_1 = \tau_2 = \tau$, $d = 0$ in (128), has applications towards the infinite sum in [62, eqs. 9-10, 19-23], [36, eq. A2.6], and in [69, eqs. 18 and 21].

Since the optimum pulse has a simple spectrum [14] ($\mathrm{P_{opt}}(f) = T_c$ for $|f| \leq \frac{1-\beta}{2T_c}$, $\mathrm{P_{opt}}(f) = \frac{T_c}{2}$ for $\frac{1-\beta}{2T_c} \leq |f| \leq \frac{1+\beta}{2T_c}$, and zero elsewhere) it is easy to demonstrate that

$$\sum_{n=-\infty}^{\infty} p(\tau_1 - nT_c)p(\tau_2 - nT_c) = p(d) - \frac{\sin(\pi\tau_1/T_c)\sin(\pi\tau_2/T_c)}{d\pi}\sin((d/T_c)\pi\beta), \tag{129}$$

$$\frac{\mathrm{p}(d) * \mathrm{p}(d)}{T_c} = p(d) - \frac{\cos(\pi d/T_c)}{2(d/T_c)\pi}\sin((d/T_c)\pi\beta),$$

where

$$p(t) = \frac{1-\beta}{2}\mathrm{sinc}((1-\beta)t/T_c) + \frac{1+\beta}{2}\mathrm{sinc}((1+\beta)t/T_c) = \mathrm{sinc}(t/T_c)\cdot\cos(\pi\beta t/T_c). \tag{130}$$

For the frequency spectrum of the BTN pulse [9] (corrected for a minus sign), using $B = \frac{1}{2T_c}$,

$$\phi(f) = 2^{-\frac{2T_c}{\beta}(f - \frac{1-\beta}{2T_c})}. \tag{131}$$

The BTN pulse, using $\alpha = \frac{2\ln 2}{\beta}$ can be rewritten in the following way:

$$\mathrm{p}(t) = \mathrm{sinc}(t/T_c)\cdot\frac{4\alpha\pi(t/T_c)\sin(\pi\alpha t/T_c) + 2\alpha^2\cos(\pi\alpha t/T_c) - \alpha^2}{4\pi^2(t/T_c)^2 + \alpha^2}$$

$$= \frac{\sin(\pi\, t/T_c)\,\left(-\ln(2)^2 + 2\,\cos(\pi\, t\,\beta/T_c)\ln(2)^2 + 2\,\pi\,(t/T_c)\,\beta\,\ln(2)\,\sin(\pi\, t\,\beta/T_c)\right)}{\pi\,(t/T_c)\,\left(\pi^2\,(t/T_c)^2\,\beta^2 + \ln(2)^2\right)}. \tag{132}$$

Therefore,

$$\sum_{n=-\infty}^{\infty} p(\tau_1 - nT_c)p(\tau_2 - nT_c) = \mathrm{p}(d) +$$

$$\frac{2\,\beta\,\ln(2)\,\sin(\pi\,\tau_1/T_c)\,\sin(\pi\,\tau_2/T_c)\,[2\,\cos(\beta\,(d/T_c)\,\pi) - 3\,(d/T_c)\,\mathrm{p}(d)\,\pi\,\csc((d/T_c)\,\pi)]}{\beta^2\,(d/T_c)^2\,\pi^2 + 4\ln(2)^2} \tag{133}$$

$$\frac{\mathrm{p}(d) * \mathrm{p}(d)}{T_c} = \mathrm{p}(d) +$$

$$\frac{\beta\,\ln(2)\,\cos((d/T_c)\,\pi)\,\,(2\,\cos((d/T_c)\,\pi\,\beta) - 3\,(d/T_c)\,\mathrm{p}(d)\,\pi\,\csc((d/T_c)\,\pi))}{(d/T_c)^2\,\pi^2\,\beta^2 + 4\ln(2)^2} \tag{134}$$

Because $d\,\pi\,\csc(d\,\pi) = 1/\mathrm{sinc}(d\,\pi)$, for d=0 (and $\tau_1 = \tau_2 = \tau$) the previous expression simplifies to

$$\sum_{n=-\infty}^{\infty} p^2(\tau - nT_c) = 1 - \frac{\beta}{2\ln(2)}\sin^2(\frac{\pi\tau}{T_c}) \tag{135}$$

Averaging over τ, the factor $1 - \frac{\beta}{4\ln(2)} = 1 - 1/(2\alpha)$ is obtained; it is equal to 2/3 for rectangular pulses, $1 - \frac{\beta}{4}$ for raised cosine [7], and $1 - \frac{\beta}{2}$ for the optimum pulse [14]; this implies that for a given roll-off factor the Multiuser Interference is smaller for BTN pulses than Raised Cosine Pulses.

In Figs. (32) and (33), the infinite sums (dotted lines) for the BTN and optimum pulses are compared with the closed forms presented (solid lines) for $\beta = 0.50$.

On the other hand, the generalized Nyquist filters are of the form

$$P(f) = T_c \cos^2\left(\frac{\pi}{4} V_n(\frac{2T_c}{\beta}(|f| - \frac{1}{2T_c}))\right) \tag{136}$$

where

$$V_n(x) = \begin{cases} -1 & : \quad (x < -1) \\ x & : \quad n = 1 \quad \text{and} \quad (-1 \le x \le 1) \\ 2^{-1}(-x^3 + 3x) & : \quad n = 2 \quad \text{and} \quad (-1 \le x \le 1) \\ 2^{-3}(3x^5 - 10x^3 + 15x) & : \quad n = 3 \quad \text{and} \quad (-1 \le x \le 1) \\ 2^{-4}(-5x^7 + 21x^5 - 35x^3 + 35x) & : \quad n = 4 \quad \text{and} \quad (-1 \le x \le 1) \\ 2^{-7}(35x^9 - 180x^7 + 378x^5 \\ \quad -420x^3 + 315x) & : \quad n = 5 \quad \text{and} \quad (-1 \le x \le 1) \\ 1 & : \quad (x > 1), \end{cases} \tag{137}$$

Notice that when $n = 1$, it results in the RC function. The expression

$$\int_0^{\beta/2} \cos^2(\frac{\pi}{4} + \frac{\pi}{4} V(\frac{-2\,f}{\beta})) \cos^2(\frac{\pi}{4} + \frac{\pi}{4} V(\frac{2\,f}{\beta}))\ \cos(\frac{2\,d\,f\,\pi}{T_c})\mathrm{d}f \tag{138}$$

can be obtained numerically, particularly for the special case $d = 0$ ($\tau_1 = \tau_2 = \tau$), the substitution $f' = f/\beta$ can be made and the result becomes β times a constant a_n. Therefore,

$$\sum_{n=-\infty}^{\infty} p(nT_c - \tau)p(nT_c - \tau) = 1 - a_n \cdot \beta \cdot \cos^2(\frac{\pi\,\tau}{T_c}) \tag{139}$$

where

$$a_n = \begin{cases} 0.5 & : \quad n = 1 \\ 0.360733 & : \quad n = 2 \\ 0.295872 & : \quad n = 3 \\ 0.256695 & : \quad n = 4 \\ 0.229808 & : \quad n = 5. \end{cases} \tag{140}$$

The average of (139) is simply $1 - \frac{a_n}{2}$.

In conclusion, in this section the study started in this chapter was extended to include bandlimited CDMA systems using arbitrary Nyquist pulses and roll-off factors. Close form expressions were presented for the "Better than" Nyquist pulse, the optimum pulse, and a family of Nyquist filters based on generalized-cosine spectra. The work is going to facilitate the study of both the forward and reverse link of CDMA systems with novel pulses.

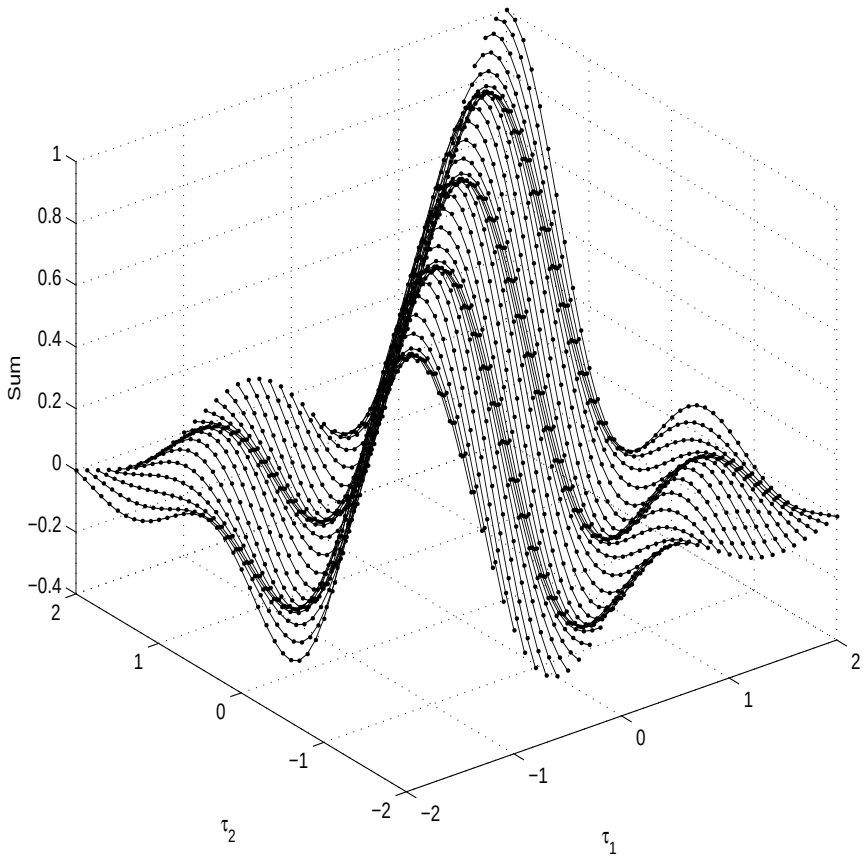

Figure 32: Comparison of Infinite Sum (dotted lines) and Derived Formula (dotted lines) for the "Better than" Nyquist pulse for $\beta = 1.00$

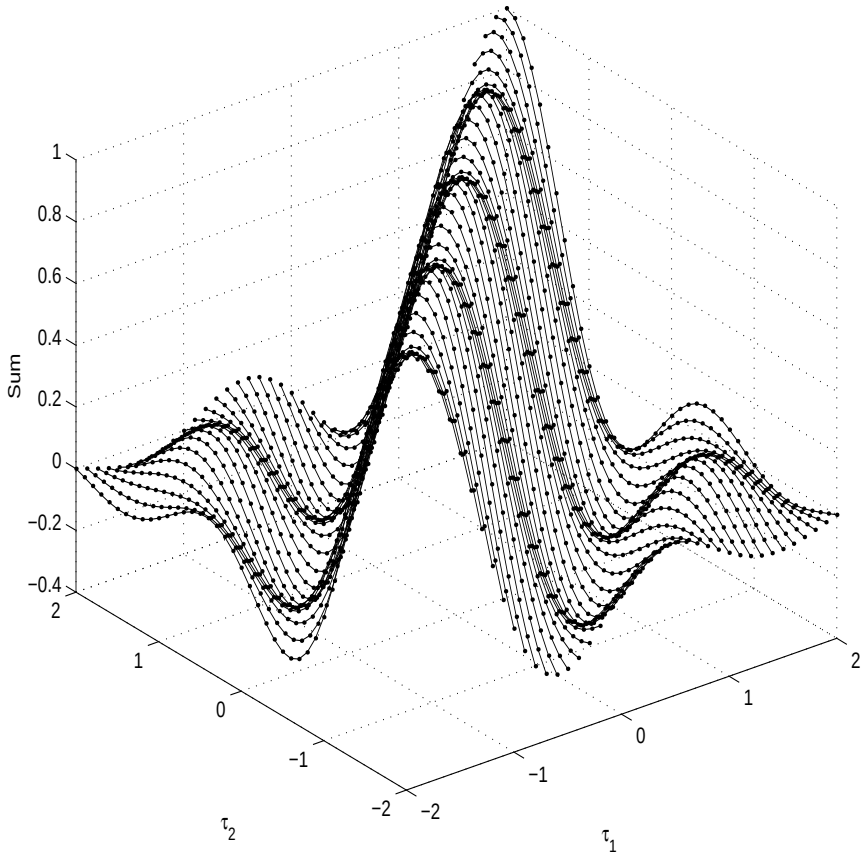

Figure 33: Comparison of Infinite Sum (dotted lines) and Derived Formula (dotted lines) for the optimum pulse for $\beta = 1.00$

3.2.2 Detailed Proof

3.2.2.1 "Better Than" Nyquist Pulse

The spectrum [9] with the correct sign in the exponential of 2 is

$$P(f) = \begin{cases} T_c & : \quad (0 \leq |f| \leq \frac{1-\beta}{2T_c} \\ T_c \cdot 2^{-\frac{2T_c}{\beta}(|f|-\frac{1-\beta}{2T_c})} & : \quad \frac{1-\beta}{2T_c} \leq |f| \leq \frac{1}{2} \\ T_c \cdot \left(1 - 2^{-\frac{2T_c}{\beta}(\frac{1+\beta}{2T_c}-|f|)}\right) & : \quad \frac{1}{2} \leq |f| \leq \frac{1+\beta}{2T_c} \\ 0 & : \quad |f| > \frac{1+\beta}{2T_c} \end{cases} \tag{141}$$

We are going to obtain $\mathrm{S}_{NY}(\tau_1, \tau_2, \beta)$ by expanding z_1, z_2, and z_3 from 122 and then compare the result with that from (128).

We have that for a real number c, $\int e^{-j\,2\,\pi\,f\,d}\,2^{-c\,f/\beta}\mathrm{d}f = \frac{2^{-c\,f/\beta}\,e^{-2\,j\,d\,f\,\pi}}{(-j\,2\,d\,\pi - c\,\ln(2)/\beta)}$.

$$z_1 = \int_{\frac{1-\beta}{2}}^{\frac{1}{2}} 2^{2\,(1-\beta-2\,f)/\beta}\,e^{-2\,j\,d\,f\,\pi}\mathrm{d}f + \int_{\frac{1}{2}}^{\frac{1+\beta}{2}} \left(1-2^{-\,(1+\beta-2\,f)/\beta}\right)^2 e^{-2\,j\,d\,f\,\pi}\mathrm{d}f + \int_{-\frac{1}{2}}^{\frac{-1+\beta}{2}} 2^{2\,(1-\beta+2\,f)/\beta}\,e^{-2\,j\,d\,f\,\pi}\mathrm{d}f + \int_{-\frac{1+\beta}{2}}^{-\frac{1}{2}} \left(1-2^{-(1+\beta+2\,f)/\beta}\right)^2 e^{-2\,j\,d\,f\,\pi}\mathrm{d}f + \int_{\frac{-1+\beta}{2}}^{\frac{1-\beta}{2}} e^{-2\,j\,d\,f\,\pi}\mathrm{d}f \tag{142}$$

$$\begin{aligned} z_2 &= \int_{\frac{1-\beta}{2}}^{\frac{1}{2}} 2^{(1-\beta-2\,f)/\beta}\left(1-2^{(1-\beta-2\,f)/\beta}\right)e^{-2\,j\,d\,f\,\pi}\mathrm{d}f + \\ &\quad \int_{\frac{1}{2}}^{\frac{1+\beta}{2}} 2^{-(1+\beta-2\,f)/\beta}\left(1-2^{-(1+\beta-2\,f)/\beta}\right)e^{-2\,j\,d\,f\,\pi}\mathrm{d}f \end{aligned} \tag{143}$$

$$\begin{aligned} z_3 &= \int_{-\frac{1}{2}}^{-\frac{1-\beta}{2}} 2^{(1-\beta+2\,f)/\beta}\left(1-2^{(1-\beta+2\,f)/\beta}\right)e^{-2\,j\,d\,f\,\pi}\mathrm{d}f + \\ &\quad \int_{-\frac{1+\beta}{2}}^{-\frac{1}{2}} 2^{-(1+\beta+2\,f)/\beta}\left(1-2^{-(1+2\,f+\beta)/\beta}\right)e^{-2\,j\,d\,f\,\pi}\mathrm{d}f \end{aligned} \tag{144}$$

The first integral in z_1 becomes $\frac{e^{-j\,d\,\pi-j\,d\,\pi\,(1-\beta)}\left(-4\,e^{j\,d\,\pi}+e^{j\,d\,\pi\,(1-\beta)}\right)\beta}{8\,(-j\,d\,\pi\,\beta-2\,\ln(2))}$.

The second integral in z_1 becomes

$$e^{-j\,(1+\beta)\,d\,\pi}\left(\frac{j}{2\,d\,\pi}+\frac{\beta}{j\,\beta\,d\,\pi-\ln(2)}+\frac{\frac{j}{2}\,\beta}{\beta\,d\,\pi+2\,j\,\ln(2)}\right) - e^{-j\,d\,\pi}\left(\frac{j}{2\,d\,\pi}+\frac{2^{\frac{1}{\beta}-\frac{1+\beta}{\beta}}\,\beta}{j\,\beta\,d\,\pi-\ln(2)}+\frac{j\,2^{-1+\frac{2}{\beta}-\frac{2\,(1+\beta)}{\beta}}\,\beta}{\beta\,d\,\pi+2\,j\,\ln(2)}\right). \tag{145}$$

The third integral in z_1 becomes

$$\frac{j\,e^{-j\,d\,\pi\,(-1+\beta)}\,\beta}{2\,(d\,\pi\,\beta+2\,j\,\ln(2))} - \frac{j\,2^{-\frac{2}{\beta}-\frac{2\,(-1+\beta)}{\beta}}\,e^{j\,d\,\pi}\,\beta}{2\,(d\,\pi\,\beta+2\,j\,\ln(2))}. \tag{146}$$

The fourth integral without the limits becomes

$$\frac{\left(1-2^{\frac{(-1-2\,f-\beta)}{\beta}}\right)^2\left(\frac{j\,2^{1+\frac{2}{\beta}-\frac{2\,(1+\beta)}{\beta}}}{d\,\pi}+\frac{2^{-1-\frac{4\,f}{\beta}-\frac{2\,(1+\beta)}{\beta}}\,\beta}{-j\,d\,\pi\,\beta-2\,\ln(2)}-\frac{j\,2^{1+\frac{1}{\beta}-\frac{2\,f}{\beta}-\frac{2\,(1+\beta)}{\beta}}\,\beta}{d\,\pi\,\beta-j\,\ln(2)}\right)}{2^{2\left(-1-\frac{1}{\beta}-\frac{2\,f}{\beta}\right)}\left(-1+2^{1+\frac{1}{\beta}+\frac{2\,f}{\beta}}\right)^2 e^{2\,j\,d\,f\,\pi}}. \tag{147}$$

The fifth integral becomes $\frac{j\,e^{-j\,d\,\pi\,(1-\beta)}}{2\,d\,\pi} - \frac{j\,e^{-j\,d\,\pi\,(-1+\beta)}}{2\,d\,\pi}$.

Putting it all together, z_1 can be rewritten as

$$\begin{aligned}
&\frac{\beta\,\cos(d\,\pi)}{8\,(-j\,\beta\,d\,\pi-2\,\ln(2))}-\frac{\beta\,\cos((1-\beta)\,d\,\pi)}{2\,(-j\,\beta\,d\,\pi-2\,\ln(2))}+\frac{\beta\,\cos(d\,\pi)}{8\,(j\,\beta\,d\,\pi-2\,\ln(2))}\\
&-\frac{(\beta\,\cos(d\,\pi\,(1-\beta)))}{2\,(j\,d\,\pi\,\beta-2\,\ln(2))}+\frac{d^2\,\pi^2\,\beta^3\,(\cos(d\,\pi)-j\,\sin(d\,\pi))}{8\,(j\,d\,\pi\,\beta-2\,\ln(2))\,(d\,\pi\,\beta+j\,\ln(2))\,(d\,\pi\,\beta+2\,j\,\ln(2))}\\
&+\frac{7\,d\,\pi\,\beta^2\,\ln(2)\,(j\,\cos(d\,\pi)\sin(d\,\pi))}{8\,(j\,d\,\pi\,\beta-2\,\ln(2))\,(d\,\pi\,\beta+j\,\ln(2))\,(d\,\pi\,\beta+2\,j\,\ln(2))}\\
&-\frac{9\,\beta\,\ln(2)^2\,(\cos(d\,\pi)-j\,\sin(d\,\pi))}{4\,(j\,d\,\pi\,\beta-2\,\ln(2))\,(d\,\pi\,\beta+j\,\ln(2))\,(d\,\pi\,\beta+2\,j\,\ln(2))}\\
&-\frac{2\,j\,\ln(2)^3\,(\cos(d\,\pi)-j\,\sin(d\,\pi))}{d\,\pi\,(j\,d\,\pi\,\beta-2\,\ln(2))\,(d\,\pi\,\beta+j\,\ln(2))\,(d\,\pi\,\beta+2\,j\,\ln(2))}\\
&+\frac{d\,\pi\,\beta^2\,(\cos(d\,\pi)+j\,\sin(d\,\pi))}{8\,(-j\,d\,\pi\,\beta-\ln(2))\,(d\,\pi\,\beta-2\,j\,\ln(2))}\\
&-\frac{5\,\beta\,\ln(2)\,(j\,\cos(d\,\pi)-1\,\sin(d\,\pi))}{8\,(-j\,d\,\pi\,\beta-\ln(2))\,(d\,\pi\,\beta-2\,j\,\ln(2))}-\frac{\ln(2)^2\,(\cos(d\,\pi)+j\,\sin(d\,\pi))}{d\,\pi\,(-j\,d\,\pi\,\beta-\ln(2))\,(d\,\pi\,\beta-2\,j\,\ln(2))}\\
&-\frac{j\,\beta\,\sin(d\,\pi)}{8\,(-j\,d\,\pi\,\beta-2\,\ln(2))}+\frac{j\,\beta\,\sin(d\,\pi)}{8\,(j\,d\,\pi\,\beta-2\,\ln(2))}\\
&+\frac{\ln(2)^2\,(\cos(d\,\pi\,(-1-\beta))-j\,\sin(d\,\pi\,(-1-\beta)))}{d\,\pi\,(-j\,d\,\pi\,\beta-\ln(2))\,(d\,\pi\,\beta-2\,j\,\ln(2))}\\
&+\frac{\beta\,\ln(2)^2\,(\cos(d\,\pi\,(-1-\beta))+j\,\sin(d\,\pi\,(-1-\beta)))}{(j\,d\,\pi\,\beta-2\,\ln(2))\,(d\,\pi\,\beta+j\,\ln(2))\,(d\,\pi\,\beta+2\,j\,\ln(2))}\\
&+\frac{2\,j\,\ln(2)^3\,(\cos(d\,\pi\,(-1-\beta))+j\,\sin(d\,\pi\,(-1-\beta)))}{d\,\pi\,(j\,d\,\pi\,\beta-2\,\ln(2))\,(d\,\pi\,\beta+j\,\ln(2))\,(d\,\pi\,\beta+2\,j\,\ln(2))}\\
&+\frac{\frac{j}{2}\,\beta\,\sin(d\,\pi\,(1-\beta))}{2\,(-j\,d\,\pi\,\beta-2\,\ln(2))}-\frac{j\,\beta\,\sin(d\,\pi\,(1-\beta))}{2\,(j\,d\,\pi\,\beta-2\,\ln(2))}-\frac{\sin(d\,\pi\,(-1+\beta))}{d\,\pi}
\end{aligned}\tag{148}$$

Expanding the sine and cosine functions such as $\sin((1-\beta)\,d\,\pi)$ and $\cos((1-\beta)\,d\,\pi)$ and putting all the terms under one denominator, the numerator of z_1 can be written as

$$\begin{aligned}
&2\,d^3\,\pi^3\,\beta^3\,\cos(d\,\pi)\,\cos(d\,\pi\,\beta)\,\ln(2)\\
&+3\,d\,\pi\,\beta\,\cos(d\,\pi)\ln(2)^3-4\,d\,\pi\,\beta\,\cos(d\,\pi)\,\cos(d\,\pi\,\beta)\ln(2)^3\\
&-d^2\,\pi^2\,\beta^2\ln(2)^2\,\sin(d\,\pi)+2\,d^2\,\pi^2\,\beta^2\,\cos(d\,\pi\,\beta)\ln(2)^2\,\sin(d\,\pi)\\
&-4\ln(2)^4\,\sin(d\,\pi)+8\,\cos(d\,\pi\,\beta)\ln(2)^4\,\sin(d\,\pi)\\
&-6\,d^2\,\pi^2\,\beta^2\,\cos(d\,\pi)\ln(2)^2\,\sin(d\,\pi\,\beta)\\
&+2\,d^3\,\pi^3\,\beta^3\,\ln(2)\,\sin(d\,\pi)\,\sin(d\,\pi\,\beta)+8\,d\,\pi\,\beta\ln(2)^3\,\sin(d\,\pi)\,\sin(d\,\pi\,\beta)
\end{aligned}\tag{149}$$

which simplifies to

$$\begin{aligned}
&\ln(2)\,\left(d\,\pi\,\beta\,\cos(d\,\pi)\,\left(2\,\cos(d\,\pi\,\beta)\,\left(d^2\,\pi^2\,\beta^2-2\ln(2)^2\right)+A\right)\right.\\
&\left.+\sin(d\,\pi)\,\left(\cos(d\,\pi\,\beta)\,\left(8\ln(2)^3+d^2\,\pi^2\,\beta^2\,\ln(4)\right)+B\right)\right),\\
&A=3\,\ln(2)\,\left(\ln(2)-2\,d\,\pi\,\beta\,\sin(d\,\pi\,\beta)\right),\\
&B=\left(d^2\,\pi^2\,\beta^2+4\ln(2)^2\right)\,\left(-\ln(2)+2\,d\,\pi\,\beta\,\sin(d\,\pi\,\beta)\right).
\end{aligned}\tag{150}$$

The denominator of z_1 is

$$d^5\,\pi^5\,\beta^4+5\,d^3\,\pi^3\,\beta^2\ln(2)^2+4\,d\,\pi\ln(2)^4=\left(d^2\,\pi^2\,\beta^2+\ln(2)^2\right)\,\left(d^2\,\pi^2\,\beta^2+4\ln(2)^2\right).$$

The expression z_1 can be rewritten as

$$\begin{aligned}
&\frac{2\,\beta\,\cos(d\,\pi)\,\cos(d\,\pi\,\beta)\,\ln(2)}{d^2\,\pi^2\,\beta^2+4\ln(2)^2}+\frac{3\,\beta\,\cos(d\,\pi)\ln(2)^3}{\left(d^2\,\pi^2\,\beta^2+\ln(2)^2\right)\,\left(d^2\,\pi^2\,\beta^2+4\ln(2)^2\right)}\\
&-\frac{6\,\beta\,\cos(d\,\pi)\,\cos(d\,\pi\,\beta)\ln(2)^3}{\left(d^2\,\pi^2\,\beta^2+\ln(2)^2\right)\,\left(d^2\,\pi^2\,\beta^2+4\ln(2)^2\right)}\\
&-\frac{\ln(2)^2\,\sin(d\,\pi)}{d\,\pi\,\left(d^2\,\pi^2\,\beta^2+\ln(2)^2\right)}\\
&+\frac{2\,\cos(d\,\pi\,\beta)\ln(2)^2\,\sin(d\,\pi)}{d\,\pi\,\left(d^2\,\pi^2\,\beta^2+\ln(2)^2\right)}-\frac{6\,d\,\pi\,\beta^2\,\cos(d\,\pi)\ln(2)^2\,\sin(d\,\pi\,\beta)}{\left(d^2\,\pi^2\,\beta^2+\ln(2)^2\right)\,\left(d^2\,\pi^2\,\beta^2+4\ln(2)^2\right)}\\
&+\frac{2\,\beta\,\ln(2)\,\sin(d\,\pi)\,\sin(d\,\pi\,\beta)}{d^2\,\pi^2\,\beta^2+\ln(2)^2},
\end{aligned}\tag{151}$$

which can in turn be rewritten as

$$\begin{aligned}
&\frac{\sin(d\,\pi)\,\left(-\ln(2)^2+2\,\cos(d\,\pi\,\beta)\ln(2)^2+2\,d\,\pi\,\beta\,\ln(2)\,\sin(d\,\pi\,\beta)\right)}{d\,\pi\,\left(d^2\,\pi^2\,\beta^2+\ln(2)^2\right)}\\
&+\frac{2\,\beta\,\cos(d\,\pi)\,\cos(d\,\pi\,\beta)\,\ln(2)}{d^2\,\pi^2\,\beta^2+4\ln(2)^2}+\frac{3\,\beta\,\cos(d\,\pi)\ln(2)^3}{\left(d^2\,\pi^2\,\beta^2+\ln(2)^2\right)\,\left(d^2\,\pi^2\,\beta^2+4\ln(2)^2\right)}\\
&-\frac{6\,\beta\,\cos(d\,\pi)\,\cos(d\,\pi\,\beta)\ln(2)^3}{\left(d^2\,\pi^2\,\beta^2+\ln(2)^2\right)\,\left(d^2\,\pi^2\,\beta^2+4\ln(2)^2\right)}\\
&-\frac{6\,d\,\pi\,\beta^2\,\cos(d\,\pi)\ln(2)^2\,\sin(d\,\pi\,\beta)}{\left(d^2\,\pi^2\,\beta^2+\ln(2)^2\right)\,\left(d^2\,\pi^2\,\beta^2+4\ln(2)^2\right)}
\end{aligned}\tag{152}$$

The last four terms can be written as

$$\frac{\beta\,\cos(d\,\pi)\,\ln(2)\,\left(2\,\cos(d\,\pi\,\beta)-\frac{3\left(-\ln(2)^2+2\,\cos(d\,\pi\,\beta)\ln(2)^2+2\,d\,\pi\,\beta\,\ln(2)\,\sin(d\,\pi\,\beta)\right)}{d^2\,\pi^2\,\beta^2+\ln(2)^2}\right)}{d^2\,\pi^2\,\beta^2+4\ln(2)^2}\tag{153}$$

Therefore,

$$z_1 = \mathrm{p}(d) + \frac{\beta \ln(2)\ \cos(d\,\pi)\ (2\ \cos(d\,\pi\,\beta) - 3\,d\,\mathrm{p}(d)\,\pi\ \csc(d\,\pi))}{d^2\,\pi^2\,\beta^2 + 4\ln(2)^2} \tag{154}$$

The first integral in z_2 is

$$\begin{aligned}
& e^{-j\,d\,\pi}\ \left(\frac{2^{-1-\frac{1}{\beta}-\frac{-1+\beta}{\beta}}\,\beta}{-j\,d\,\pi\,\beta - \ln(2)} - \frac{j\,2^{-1-\frac{2}{\beta}-\frac{2\,(-1+\beta)}{\beta}}\,\beta}{d\,\pi\,\beta - 2\,j\ \ln(2)}\right) \\
-e^{-j\,d\,\pi\,(1-\beta)}\ & \left(\frac{2^{-1-\frac{1-\beta}{\beta}-\frac{-1+\beta}{\beta}}\,\beta}{-j\,d\,\pi\,\beta - \ln(2)} - \frac{j\,2^{-1-\frac{2\,(1-\beta)}{\beta}-\frac{2\,(-1+\beta)}{\beta}}\,\beta}{d\,\pi\,\beta - 2\,j\ \ln(2)}\right) \\
= e^{-j\,d\,\pi}\ & \left(\frac{\beta}{4\ (-j\,\beta\,d\,\pi - \ln(2))} - \frac{j\,\beta}{8(\beta\,d\,\pi - 2\,j\ \ln(2))}\right) \\
-e^{-j\,(1-\beta)\,d\,\pi}\ & \left(\frac{\beta}{2\ (-j\,\beta\,d\,\pi - \ln(2))} - \frac{\frac{j}{2}\,\beta}{\beta\,d\,\pi - 2\,j\ \ln(2)}\right)
\end{aligned} \tag{155}$$

Putting the expression under one denominator and expanding the exponential function, an expression is obtained; its numerator is

$$\begin{aligned}
& \beta\ (\beta\,d\,\pi\ \cos((1-\beta)\ d\,\pi) + 4\,j\ \cos(d\,\pi)\ \ln(2) - 3\,j\ \cos((1-\beta)\ d\,\pi)\ \ln(2) \\
& -4\ \ln(2)\ \sin(d\,\pi) + j\,\beta\,d\,\pi\ \sin((1-\beta)\ d\,\pi) + 3\ \ln(2)\ \sin((1-\beta)\ d\,\pi))\cdot \\
& \qquad (\cos(d\,\pi + (1-\beta)\ d\,\pi) - j\ \sin(d\,\pi + (1-\beta)\ d\,\pi))
\end{aligned}$$

and denominator $8\ (-j\,\beta\,d\,\pi - 2\ \ln(2))\ (\beta\,d\,\pi - j\ \ln(2))$.

With regards to the second integral in z_2

$$\begin{aligned}
& \frac{e^{-j\,d\,\pi\,(1+\beta)}\,2^{\frac{-1-2\,\beta}{\beta}}\ \left(-2^{2+\frac{1}{\beta}} + 2^{\frac{1+\beta}{\beta}}\right)\ \beta\ \ln(2)}{(d\,\pi\,\beta + j\ \ln(2))\ (d\,\pi\,\beta + 2\,j\ \ln(2))} - \\
& \frac{e^{-j\,d\,\pi}\,2^{\frac{-1-3\,\beta}{\beta}}\,\beta\ \left(j\ \left(2^{1+\frac{1}{\beta}} - 2^{\frac{1}{\beta}}\right)\ d\,\pi\,\beta + \left(-2^{2+\frac{1}{\beta}} + 2^{\frac{1}{\beta}}\right)\ \ln(2)\right)}{(d\,\pi\,\beta + j\ \ln(2))\ (d\,\pi\,\beta + 2\,j\ \ln(2))}
\end{aligned} \tag{156}$$

Multiplying out and converting the exponentials with imaginary argument to trigonometric form

$$\begin{aligned}
= & \frac{d\,\pi\,\beta^2\ (\cos(d\,\pi) - j\ \sin(d\,\pi)) + 3\,j\,\beta\ \ln(2)\ (\cos(d\,\pi) - j\ \sin(d\,\pi))}{8\ (j\,d\,\pi\,\beta - 2\ \ln(2))\ (d\,\pi\,\beta + j\ \ln(2))} \\
& - \frac{j\,\beta\ \ln(2)\ (\cos(d\,\pi\ (1+\beta)) - j\ \sin(d\,\pi\ (1+\beta)))}{2\ (j\,d\,\pi\,\beta - 2\ \ln(2))\ (d\,\pi\,\beta + j\ \ln(2))}
\end{aligned} \tag{157}$$

Adding the two parts of the integral, putting the expression under one denominator and expanding the trigonometric expressions,

$$\frac{-\left(\beta\,\ln(2)\,\left(\cos(d\,\pi)-j\,\sin(d\,\pi)\right)\,\left(2\,\cos(d\,\pi\,\beta)\,\left(d^2\,\pi^2\,\beta^2-2\,\ln(2)^2\right)+B_{12}\right)\right)}{2\,\left(d^4\,\pi^4\,\beta^4+5\,d^2\,\pi^2\,\beta^2\,\ln(2)^2+4\,\ln(2)^4\right)},$$

$$B_{12}=3\,\ln(2)\,\left(\ln(2)-2\,d\,\pi\,\beta\,\sin(d\,\pi\,\beta)\right) \tag{158}$$

The numerator of the quantity $z_2\,e^{-j\,2\,\pi\,t}+z_3\,e^{j\,2\,\pi\,t}$ is (for $t=\tau_2/T_c$)

$$\begin{aligned}
&-4\,d^2\,\pi^2\,\beta^3\,\cos(d\,\pi)\,\cos(2\,\pi\,t)\,\cos(d\,\pi\,\beta)\,\ln(2)-6\,\beta\,\cos(d\,\pi)\,\cos(2\,\pi\,t)\,\ln(2)^3\\
&+8\,\beta\,\cos(d\,\pi)\,\cos(2\,\pi\,t)\,\cos(d\,\pi\,\beta)\,\ln(2)^3\\
&+4\,d^2\,\pi^2\,\beta^3\,\cos(d\,\pi\,\beta)\,\ln(2)\,\sin(d\,\pi)\,\sin(2\,\pi\,t)\\
&+6\,\beta\,\ln(2)^3\,\sin(d\,\pi)\,\sin(2\,\pi\,t)-8\,\beta\,\cos(d\,\pi\,\beta)\,\ln(2)^3\,\sin(d\,\pi)\,\sin(2\,\pi\,t)\\
&+12\,d\,\pi\,\beta^2\,\cos(d\,\pi)\,\cos(2\,\pi\,t)\,\ln(2)^2\,\sin(d\,\pi\,\beta)\\
&-12\,d\,\pi\,\beta^2\,\ln(2)^2\,\sin(d\,\pi)\,\sin(2\,\pi\,t)\,\sin(d\,\pi\,\beta)
\end{aligned} \tag{159}$$

Using the identity $\cos(d\,\pi)\,\cos(2\,\pi\,t)-\sin(d\,\pi)\,\sin(2\,\pi\,t)=\cos(\pi\,\,(d+2\,t))$, for $z_2e^{-j2\pi t}+z_3e^{j2\pi t}$,

$$-\frac{\beta\,\cos(\pi\,\,(d+2\,t))\,\ln(2)\,\left(2\,\cos(d\,\pi\,\beta)\,\left(d^2\,\pi^2\,\beta^2-2\,\ln(2)^2\right)+B_{12}\right)}{d^4\,\pi^4\,\beta^4+5\,d^2\,\pi^2\,\beta^2\,\ln(2)^2+4\,\ln(2)^4}, \tag{160}$$

which replacing $d+2\,t=(\tau_1+\tau_2)/T_c)$ and redefining $d=\tau_1-\tau_2$,

$$-\frac{\beta\,\cos(\pi\,\,(\tau_1+\tau_2)\,/T_c)\,\ln(2)\,\left(2\,\cos(d\,\pi\,\beta/T_c)-3\,(d/T_c)\,\mathrm{p}(d)\,\pi\,\csc(d\,\pi/T_c)\right)}{(d/T_c)^2\,\pi^2\,\beta^2+4\,\ln(2)^2} \tag{161}$$

Since $\cos(\pi\,(\tau_1-\tau_2)/T_c)-\cos(\pi\,\,(\tau_1+\tau_2)\,/T_c)=\sin(\pi\,\tau_1/T_c)\,\sin(\pi\,\tau_2/T_c)$,

$$\mathrm{S}_{NY}(\tau_1,\tau_2,\beta)=\mathrm{p}(d)+$$

$$\frac{2\,\beta\,\ln(2)\,\sin(\frac{\pi\,\tau_1}{T_c})\,\sin(\frac{\pi\,\tau_2}{T_c})\,\left[2\,\cos(\beta\,d\,\pi/T_c)-3\,(d/T_c)\,\mathrm{p}(d)\,\pi\,\csc(d\,\pi/T_c)\right]}{\beta^2\,(d/T_c)^2\,\pi^2+4\,\ln(2)^2} \tag{162}$$

When using (128), replacing the value obtain for z_2, the second term in (128) (for $d=(\tau_1-\tau_2)/T_c)$ becomes

$$\frac{4\sin(\frac{\pi\,\tau_1}{T_c})\,\sin(\frac{\pi\,\tau_2}{T_c})\,\left(\beta\,\ln(2)\,\,\left(2\,\cos(d\,\pi\,\beta)\,\left(d^2\,\pi^2\,\beta^2-2\,\ln(2)^2\right)+B_{12}\right)\right)}{2\,\left(d^4\,\pi^4\,\beta^4+5\,d^2\,\pi^2\,\beta^2\,\ln(2)^2+4\,\ln(2)^4\right)} \tag{163}$$

Using a similar simplification from (160) to (161), adding the first term in (128), for $d=\tau_1-\tau_2$, (162) is obtained.

3.2.2.2 Optimum Pulse

$$
\begin{aligned}
z_1 &= \int_{-(1-\beta)/2}^{(1-\beta)/2} e^{-j\,2\,\pi\,f\,d}\mathrm{d}f + \int_{(1-\beta)/2}^{(1+\beta)/2} e^{-j\,2\,\pi\,f\,d}\,(1/4)\mathrm{d}f + \int_{-(1+\beta)/2}^{-(1-\beta)/2} e^{-j\,2\,\pi\,f\,d}\,(1/4)\mathrm{d}f \\
&= \frac{-j\,e^{-j\,d\,\pi\,(-1-\beta)}}{8\,d\,\pi} - \frac{j\,e^{-j\,d\,\pi\,(1-\beta)}}{8\,d\,\pi} + \frac{j\,e^{-2\,j\,d\,\pi\,\left(1+\frac{-1+\beta}{2}-\beta\right)}}{2\,d\,\pi} \\
&\quad - \frac{j\,e^{-j\,d\,\pi\,(-1+\beta)}}{2\,d\,\pi} + \frac{j\,e^{-2\,j\,d\,\pi\,\left(\frac{-1-\beta}{2}+\frac{-1+\beta}{2}+\frac{1+\beta}{2}\right)}}{8\,d\,\pi} + \frac{j\,e^{-2\,j\,d\,\pi\,\left(\frac{1-\beta}{2}+\frac{-1+\beta}{2}+\frac{1+\beta}{2}\right)}}{8\,d\,\pi} \qquad (164)
\end{aligned}
$$

After converting the exponentials to trigonometric function,

$$
\begin{aligned}
z_1 &= \frac{-3\,\sin(d\,\pi\,(-1+\beta)) + \sin(d\,\pi\,(1+\beta))}{4\,d\,\pi} \\
&= \frac{4\,\cos(d\,\pi\,\beta)\sin(d\,\pi) - 2\cos(d\,\pi)\sin(d\,\pi\,\beta)}{4\,d\,\pi} \\
&= p(d) - \frac{\cos(d\,\pi)\sin(d\,\pi\,\beta)}{2\,d\,\pi} \qquad (165)
\end{aligned}
$$

$$
\begin{aligned}
z_2 &= \int_{(1-\beta)/2}^{(1+\beta)/2} (1/4)\,e^{-j\,2\,\pi\,f\,d}\,\mathrm{d}f = \frac{-j\,e^{-j\,d\,\pi\,(1-\beta)}}{8\,d\,\pi} + \frac{j\,e^{-2\,j\,d\,\pi\,\left(\frac{1-\beta}{2}+\frac{-1+\beta}{2}+\frac{1+\beta}{2}\right)}}{8\,d\,\pi} \\
&= \frac{(\cos(d\,\pi) - j\,\sin(d\,\pi))\,\sin(d\,\pi\,\beta)}{4\,d\,\pi} \qquad (166)
\end{aligned}
$$

$$
z_3 = z_2^* = \frac{(\cos(d\,\pi) + j\,\sin(d\,\pi))\,\sin(d\,\pi\,\beta)}{4\,d\,\pi} \qquad (167)
$$

$$
z_{23} = \frac{\cos(\pi\,(\tau_1+\tau_2))\,\sin(d\,\pi\,\beta)}{2\,d\,\pi} \qquad (168)
$$

$$
\begin{aligned}
\sum_{n=-\infty}^{\infty} \mathrm{p_{opt}}(nT_c-\tau_1)\mathrm{p_{opt}}(nT_c-\tau_2) &= p(d) - \frac{\cos(d\,\pi)\sin(d\,\pi\,\beta)}{2\,d\,\pi} \\
&\quad + \frac{\cos(\pi\,(\tau_1+\tau_2))\,\sin(d\,\pi\,\beta)}{2\,d\,\pi} \\
&= p(d) - \frac{\sin(\pi\,\tau_1)\,\sin(\pi\,\tau_2)\,\sin(d\,\pi\,\beta)}{d\,\pi}. \qquad (169)
\end{aligned}
$$

CHAPTER IV

REVERSE LINK ESTIMATION THROUGH SIMPLIFIED IMPROVED GAUSSIAN APPROXIMATION

It was mentioned in Section 1.2.3 that the assumption that the MAI is Gaussian in distribution is inaccurate at low BER values (below 10^{-3}). Nevertheless, it has been observed [43, 44] that the distribution of the MAI is Gaussian over the codes given that the other parameters remain constant (set of phases and path delays for all the interfering users). As a result, a more accurate method would be to calculate

$$P_e = \mathrm{E}\left[Q\left(1/\sqrt{\Psi}\right)\right], \tag{170}$$

where Ψ is the variance of the interference over codes normalized by the power of the desired signal (in other words, the inverse of the SNR) and the expectation is over the the set of phases and path delays. In the Simplified Improved Gaussian Approximation (SIGA) method, the probability of error (BER) is approximated as

$$P_e = \frac{2}{3}Q\left(1/\sqrt{\mathrm{E}[\Psi]}\right) + \frac{1}{6}Q\left(1/\sqrt{\mathrm{E}[\Psi] + \sqrt{3\mathrm{Var}[\Psi]}}\right) + \frac{1}{6}Q\left(1/\sqrt{\mathrm{E}[\Psi] - \sqrt{3\mathrm{Var}[\Psi]}}\right). \tag{171}$$

Closed-form expressions for the values of $\mathrm{E}[\Psi]$ and $\mathrm{Var}[\Psi]$ will be presented for BPSK and OQPSK modulation, Adjacent Channel Interference, and RAKE receiver for multipath channel.

4.1 BPSK

Oftentimes the reverse link (also called uplink) in CDMA mobile communications is modelled as one path coming from each user; due to the random location of the subscribers, each of these paths has different phase and delay. The power received from each user can also be modelled as constant if perfect power control is assumed. Instead of OQPSK, for simplicity, the modulation is modelled as BPSK. The analysis for the reverse link can be

obtained by making some simplifications to the analysis and models used in the forward link (Chapter 2).

Referring to Figure 1, in BPSK, the data $d^{(i)}$ is only spread by the random PN chip sequence $c_{I,n}^{(i)}$ (the quadrature branch is eliminated); also, instead of $\sqrt{P^{(i)}}$, it is $\sqrt{2P^{(i)}}$ to maintain the same total power in the signal. Modifying (1) and (2), the received signal can be expressed as follows:

$$r(t) = \sum_{i=1}^{K} \bar{\alpha}_i \sqrt{2P^{(i)}}\, \tilde{s}_I^{(i)}(t - \tau_i) + \mathcal{I}(t). \tag{172}$$

At the RAKE receiver, correlation is performed only with $S_{N,I}^{(k)}(t - \tau_k)$; therefore, the output of the RAKE receiver due to in-cell interference becomes

$$Z = \frac{1}{2} \sum_{i=1}^{K} \alpha_k \alpha_i \sqrt{2P^{(i)}} \sum_{n=0}^{N-1} \sum_{a=-\infty}^{\infty} \left(c_{I,n}^{(k)} d_{\lfloor \frac{a}{N} \rfloor}^{(i)} c_{I,a}^{(i)} g_2((n-a)T_c - \tau_{ik}) \cos(\theta_i - \theta_k) \right) \tag{173}$$

The delay τ_i and the phase θ_i for the received signal of each user are modelled as uniformly distributed in $[0, T_c]$ and $[0, 2\pi]$, respectively. Without any loss in generality, τ_k and θ_k for the desired user are set both to zero.

It is straightforward to show that the desired signal is

$$Z_{\text{Des}} = N\, d^{(k)} \sqrt{P^{(k)}}. \tag{174}$$

Following the analysis to equations (56) and (57), it can be seen that without averaging over the phase

$$\text{Var}[Z] = P^{(i)} N \sum_{n-\infty}^{\infty} p^2(nT_c - \tau_i) \cos^2 \theta_i, \tag{175}$$

where $p(t)$ is the pulse used (convolution of the receiver and transmitter pulses). It was already shown that

$$\sum_{n=-\infty}^{\infty} p^2(nT_c - \tau_i) = 1 - A \sin^2(\pi\, \tau_i). \tag{176}$$

It was already shown in Chapter 3 that $A = \beta$ for OPT pulses, $A = \beta/2$ for RRC pulses, and $A = \beta/(2\ln(2))$ for BTN pulses.

Therefore, for a given τ_i and θ_i, the interference due to user i at the output of the RAKE receiver normalized by the square of the desired signal Z_{Des} becomes

$$\Psi_i = \frac{P^{(i)}}{NP^{(k)}} \cdot (1 - A\sin^2(\pi\, t)) \cdot \cos^2\theta_i. \tag{177}$$

Taking expectations with respect to τ_i and θ_i,

$$\mu_i \equiv \mathrm{E}[\Psi_i] = \frac{P^{(i)}}{NP^{(k)}}\left(1 - \frac{A}{2}\right) \cdot \frac{1}{2}, \tag{178}$$

$$\mathrm{E}^2[\Psi_i] = \left(\frac{P^{(i)}}{NP^{(k)}}\right)^2 \cdot \left(1 - A + \frac{3A^2}{8}\right) \cdot \frac{3}{8}, \tag{179}$$

$$\sigma_i^2 \equiv \mathrm{Var}[\Psi_i] = \mathrm{E}[\Psi_i^2] - \mathrm{E}^2[\Psi_i] = \left(\frac{P^{(i)}}{NP^{(k)}}\right)^2 \cdot \left(\frac{1}{8} - \frac{A}{8} + \frac{5A^2}{64}\right). \tag{180}$$

For Raised Cosine:

$$\mu_i = \frac{P^{(i)}}{NP^{(k)}} \cdot \left(1 - \frac{\beta}{4}\right) \cdot \frac{1}{2}, \tag{181}$$

$$\sigma_i^2 = \left(\frac{P^{(i)}}{NP^{(k)}}\right)^2 \cdot \left(\frac{1}{8} - \frac{\beta}{16} + \frac{5\beta^2}{256}\right). \tag{182}$$

For BTN:

$$\mu_i = \frac{P^{(i)}}{NP^{(k)}} \cdot \left(1 - \frac{\beta}{(4\ln(2))}\right) \cdot \frac{1}{2}, \tag{183}$$

$$\sigma_i^2 = \left(\frac{P^{(i)}}{NP^{(k)}}\right)^2 \cdot \left(\frac{1}{8} - \frac{\beta}{(16\ln(2))} + \frac{5\beta^2}{(256(\ln(2))^2)}\right). \tag{184}$$

For OPT:

$$\mu_i = \frac{P^{(i)}}{NP^{(k)}} \cdot \left(1 - \frac{\beta}{2}\right) \cdot \frac{1}{2}, \tag{185}$$

$$\sigma_i^2 = \left(\frac{P^{(i)}}{NP^{(k)}}\right)^2 \cdot \left(\frac{1}{8} - \frac{\beta}{8} + \frac{5\beta^2}{64}\right). \tag{186}$$

Noticing that $\Psi = \sum_{i=1}^{K} \Psi_i$, and that $\mathrm{E}[\Psi_{i_1}\Psi_{i_2}] = \mathrm{E}[\Psi_{i_1}]\mathrm{E}[\Psi_{i_2}]$ for $i_1 \neq i_2$, the above results and

$$\mu \equiv \mathrm{E}[\Psi] = \sum_{i=1}^{K} \mu_i, \tag{187}$$

$$\sigma \equiv \mathrm{Var}[\Psi] = \sum_{i=1}^{K} \sigma_i, \tag{188}$$

are used to obtain the probability of error.

On the other hand, the method of Characteristic Function (CF), first presented in [19], is another way to obtain the BER. Recently, Yoon in [68, 69], based on the method in [18], expanded the work from square pulses to arbitrary bandlimited pulses:

$$P_e = \frac{1}{2} - \frac{1}{\pi}\int_0^\infty \phi_{\mathrm{MAI}}(w)\phi_{\mathrm{I}}(w)\frac{\sin(w)}{w}\mathrm{d}w, \tag{189}$$

where ϕ_{MAI} and $\phi_{\mathrm{I}}(w)$ are the characteristic functions of the MAI and the noise, respectively.

From [69],

$$\phi_{\mathrm{MAI}} = \prod_{i=1}^{K'} \phi_{\mathrm{MAI}_i},$$

$$\phi_{\mathrm{MAI}_i} = \frac{1}{T_c}\int_0^{T_c} \exp(-\frac{w^2}{2}\sigma^2_{\mathrm{MAI}_i|\tau_k})\mathrm{I}_0(\frac{w^2}{2}\sigma^2_{\mathrm{MAI}_i|\tau_k})\mathrm{d}\tau_k \tag{190}$$

where $K' = K - 1$, the interfering users, I_o is the modified Bessel Function of the first kind and order zero and

$$\sigma^2_{\mathrm{MAI}_i|\tau} = \frac{1}{2N}\frac{P^{(i)}}{P^{(k)}}\sum_{m=-M}^{M} p^2(mT_c - \tau_k), \tag{191}$$

where that author used a time-limited waveform defined in $(-MT_c, MT_c)$. Setting $\phi_I(w)$ to unity since the interest is in the effect of MAI, and setting all the powers $P^{(i)} = P^{(k)}$, the probability of error is now obtained. Notice that $\sum_{m=-M}^{M} p^2(mT_c - \tau_k)$ can be replaced by $1 - A\sin^2(\pi\tau_k/T_c)$ as $M \to \infty$.

The BER was obtained through Monte Carlo simulations (Sim), the SIGA, CF, and Standard Gaussian Approximation (SGA) methods in Figs. 34 and 35 for the OPT and BTN pulses (the BER for RRC has already been in [22]). For the Monte Carlo simulations, a Root-OPT pulse and a Root-BTN pulse were first derived for the transmitter and the receiver (the composite effect is an OPT and a BTN pulse respectively).

It can be observed in Figs. 34 and 35 that the SIGA method matches well the simulations and the CF method.

4.2 Offset-QPSK

The actual modulation used by IS-95 is OQPSK, which is similar to two BPSK transmitters (one for the in-phase carrier, and the other for the quadrature carrier), but with the

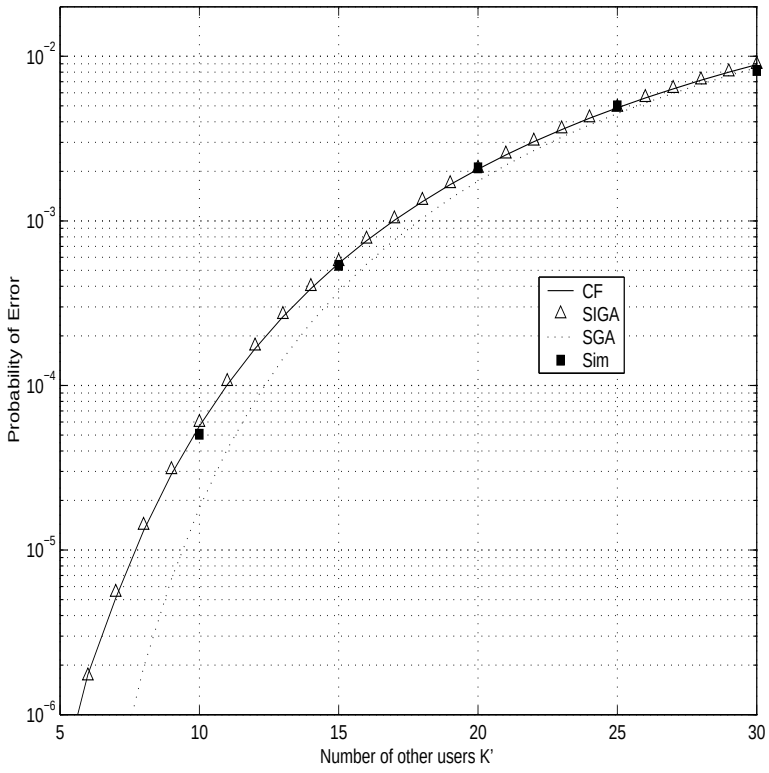

Figure 34: Output Bit Error Rate vs K' for Optimum Pulse Shape ($\beta = 0.5$).

quadrature carrier *offset* by $T_c/2$; as a result, the received signal becomes

$$r(t) = \sum_{i=1}^{K} \bar{\alpha}_i \sqrt{2P^{(i)}} \left(d_I^{(i)} s_I^{(i)}(t - \tau_i) - j\, d_Q^{(i)} s_Q^{(i)}(t - T_c/2 - \tau_i) \right) + \mathcal{I}(t) \tag{192}$$

The tilde has been removed from $\tilde{s}$ to emphasize that each the spreading waveforms for the in-phase and quadrature carriers are multiplied by different bits as opposed to balance QPSK, where they are multiplied by the same; the chip sequences used are PN random codes. The analysis is very similar to that of QPSK and complex-spreading QPSK. The desired signal is the same as the one for BPSK. At the receiver, correlation with $S_{N,I}^{(k)}(t - \tau_k)$ is performed to obtain the in-phase data $d_I^{(i)}$ and correlation with $S_{N,I}^{(k)}(t - \tau_k)$ is performed to obtain the quadrature data $d_Q^{(i)}$. Since the performance of the system is symmetric over $d_I^{(i)}$ and $d_Q^{(i)}$, the analysis can be concentrated only on the in-phase data. could just be on the in-phase data.

Following again equations (56) and (57), the variance of the output of the RAKE receiver

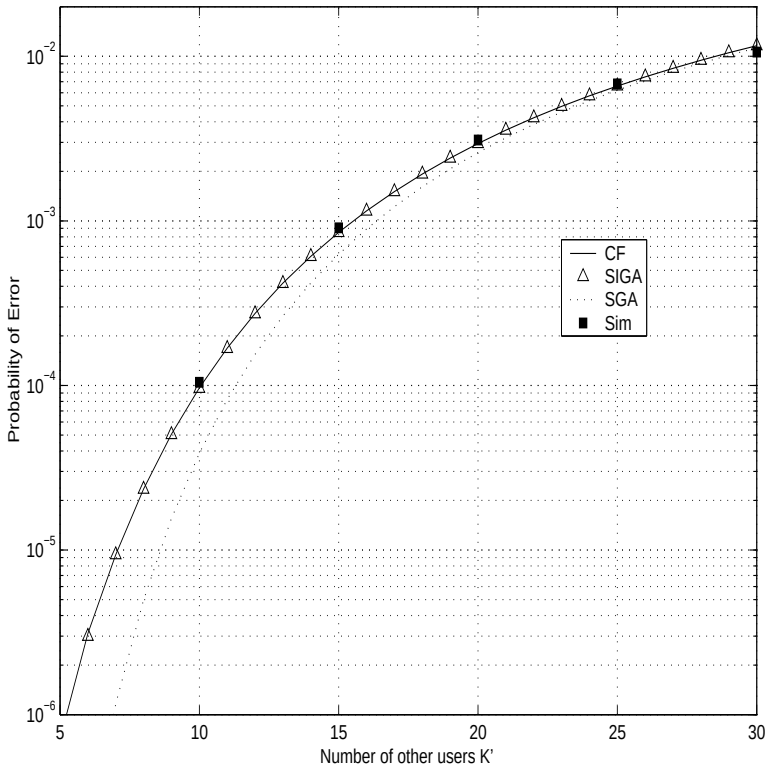

Figure 35: Output Bit Error Rate vs K' for BTN Pulse Shape ($\beta = 0.5$).

becomes

$$\mathrm{Var}_c[Z] = \frac{1}{2}\sum_{\substack{i=1\\ i\neq k}}^{K} \alpha_k^2\alpha_i^2 P^{(i)}\Big\{\mathrm{E}_c\Big[\Big(\int_{-\infty}^{\infty} s_I^{(k)}(t)\tilde{s}_I^{(i)}(t-\tau_{lf})\mathrm{d}t\Big)^2\Big]\cdot\cos^2\theta_i$$
$$+\mathrm{E}_c\Big[\Big(\int_{-\infty}^{\infty} s_I^{(k)}(t)\tilde{s}_Q^{(i)}(t-T_c/2-\tau_{lf})\mathrm{d}t\Big)^2\Big]\sin^2\theta_i\Big\}, \tag{193}$$

where again the delays and phase of the other users are set to be respect to the delay and phase of the reference user k, that is, τ_k and θ_k were set to zero. Following the code cases that lead to (57) when taking the expectations only over the codes,

$$\mathrm{Var}[Z] = \sum_{\substack{i=1\\ i\neq k}}^{K} \alpha_k^2\alpha_i^2 P^{(i)} N\left(\left\{1 - A\sin^2(\frac{\pi\tau_i}{T_c})\right\}\cos^2\theta_i\right.$$
$$\left. + \sum_{n-\infty}^{\infty} p^2(nT_c - T_c/2 - \tau_i)\sin^2\theta_i\right), \tag{194}$$

but

$$\sum_{n-\infty}^{\infty} p^2(nT_c - \tau_i - T_c/2) = 1 - A\sin^2(\frac{\pi\,(\tau_i + T_c/2)}{T_c}) = 1 - A\cos^2(\frac{\pi\,\tau_i}{T_c}). \tag{195}$$

Therefore, $\mathrm{Var}[Z^{(i)}]$ (variance of interference due to user i at the output of the RAKE receiver) normalized by the Z_{Des}^2 (same as in the BPSK case) becomes

$$\Psi_i = \frac{P^{(i)}}{NP^{(k)}} \cdot (1 - A\sin^2(\pi\,\tau_i/T_c)) \cdot \cos^2(\theta_i) + \frac{P^{(i)}}{NP^{(k)}} \cdot (1 - A\cos^2(\pi\,\tau_i/T_c)) \cdot \sin^2\theta_i, \tag{196}$$

and

$$\mu_i = \frac{P^{(i)}}{NP^{(k)}} \cdot \left(1 - \frac{A}{2}\right), \tag{197}$$

$$\mathrm{E}[(\Psi_i)^2] = \left(\frac{P^{(i)}}{NP^{(k)}}\right)^2 \cdot \left(1 - A + \frac{5A^2}{16}\right), \tag{198}$$

$$\sigma_i^2 = \left(\frac{P^{(i)}}{NP^{(k)}}\right)^2 \cdot \left(\frac{A^2}{16}\right). \tag{199}$$

The SGA and the SIGA method were used to obtain the BER for an OQPSK system with $\beta = 0.0, 0.5, 1.0$ and RRC, BTN, and OPT pulses (see Figs. 36-38). It can be seen that the results obtained using the SGA method are very close to those obtained using SIGA, except at very low BER levels. Moreover, except for $\beta = 0.0$, where all the pulses become sinc pulses, it can be seen that the performance is best for the OPT pulses, then the BTN pulses, and then the RRC pulses; that is because the OPT pulse is the optimum for same-carrier MAI. The impact of adjacent carrier interference is going to be explored in the next section.

4.3 Adjacent Channel Interference

The effect of adjacent channel interference (ACI) is rarely presented in the literature. The previous mathematical analysis results is still applicable to systems with ACI if it is noticed that instead of using a pulse $g_1(t) * g_1(t)$, the pulse

$$g_h = g_1(t) * \left(g_1(t) \cdot e^{j2\,\pi\,\Delta f\,t}\right) \tag{200}$$

is used for the band to the right. It is assumed that the carriers are separated by $\Delta f = 1/T_c$.

From simulations and curve-fitting, it was observed that

$$\sum_{n=-\infty}^{\infty} g_h^2(t-\tau) = \frac{A}{8} + \frac{A}{8}\cos\frac{2\,\pi\,\tau}{T_c}. \tag{201}$$

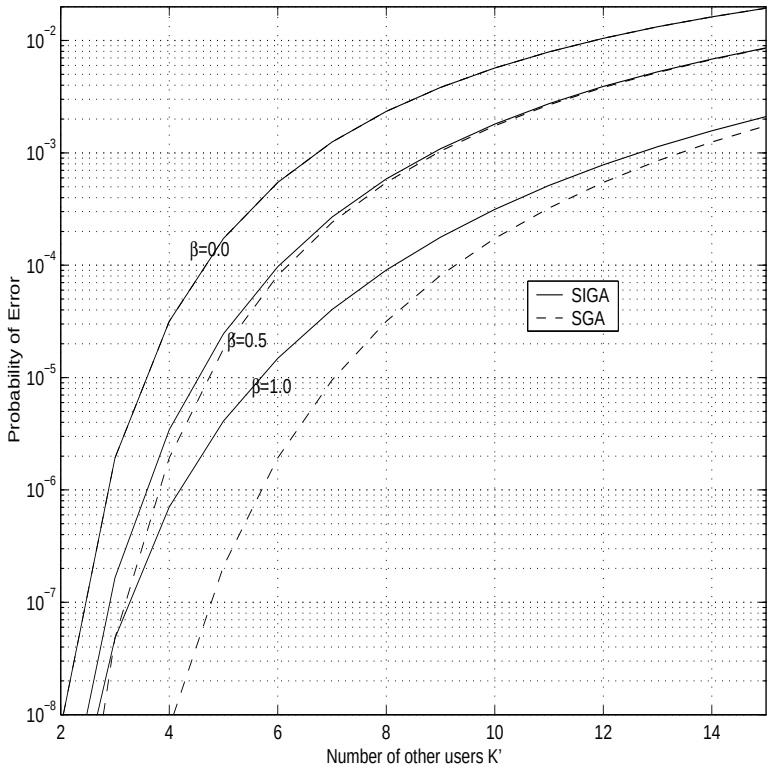

Figure 36: Output Bit Error Rate vs K' for OPT Pulse Shape in OQPSK.

It was observed that the effect of delay and the phase of the interfering carrier can be lumped together into the variable τ.

The result is the same for the band to the left. Therefore, assuming the same number of interfering users $K' = K - 1$ in the middle band, the left band, and the right band, and all users having the same power, it can be shown that the at the output of the RAKE receiver for user k in the middle band, the variance of the interference normalized by the power of the desired signal is given as

$$\Psi_i = \sum_{i=1}^{K'} \frac{1}{N} \cdot \left(1 - A \sin^2(\frac{2\,\pi\,\tau_i}{T_c})\right) \cdot \cos^2\theta_i + \sum_{i=1}^{K'} \frac{1}{N} \cdot \left(\frac{A}{8} + \frac{A}{8}\cos\frac{2\,\pi\,\tau_{i2}}{T_c}\right) + \sum_{i=1}^{K'} \frac{1}{N} \cdot \left(\frac{A}{8} + \frac{A}{8}\cos\frac{2\,\pi\,\tau_{i3}}{T_c}\right). \quad (202)$$

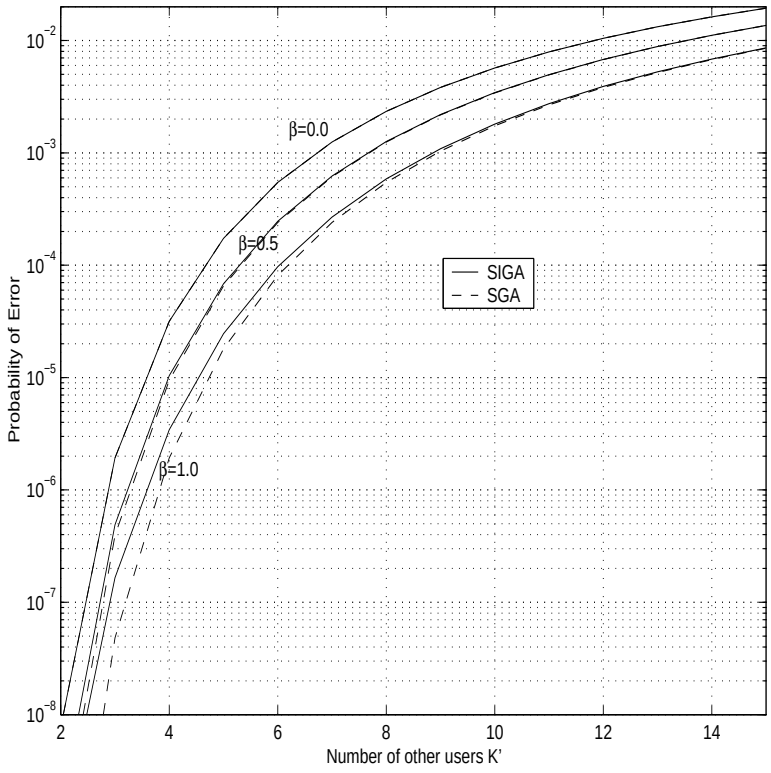

Figure 37: Output Bit Error Rate vs K' for RRC Pulse Shape in OQPSK.

Then,

$$\begin{aligned} \mathrm{E}[\Psi_i] &= \frac{1}{2N}, \\ \mathrm{E}[\Psi_i^2] &= \frac{1}{N} \cdot \left(\frac{3}{8} - \frac{1}{8} + \frac{3A^2}{32} \right), \\ \mathrm{Var}[\Psi_i] &= \frac{1}{N} \cdot \left(\frac{1}{8} - \frac{A}{8} + \frac{3A^2}{32} \right). \end{aligned} \tag{203}$$

An important conclusion is that the mean of the interference power does not depend on the shape of the Nyquist pulse under these conditions. It was also observed that, at low values of β, the value for $\mathrm{Var}[\Psi_i]$ was slightly smaller for the OPT pulse than for the BTN pulse, and for the BTN pulse it was slightly smaller than for the RRC pulse; essentially, the performance for the OPT pulse is slightly better (not in a significative way) than the other two at low BER values. This conclusion suggests that pulses should be optimized in terms of eye diagram and effect under truncation rather than in terms of MAI minimization (since all pulses under the presence of the same number of interferers in the left, same, or

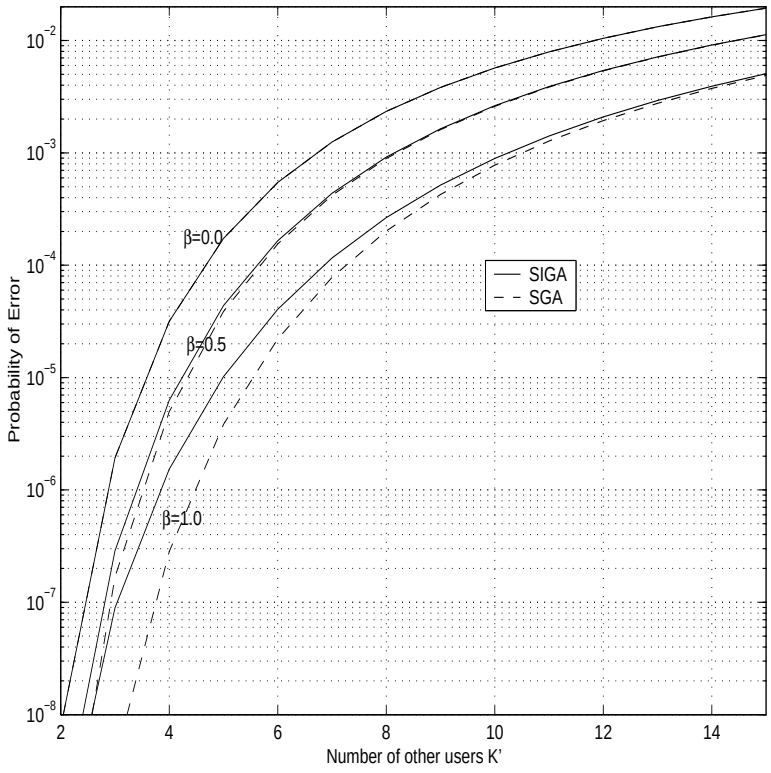

Figure 38: Output Bit Error Rate vs K' for BTN Pulse Shape in OQPSK.

right bands would have essentially the same performance).

4.4 Simplified Improved Gaussian Approximation for RAKE and Multipath

Up until now, the signal from each user was assumed to come through one path. In this section, the SIGA analysis is extended to channels with two paths and systems with a RAKE receiver with two fingers; the power of each path for each user is normalized such that $\sum_{l=1}^{L} \alpha_l^2 = 1$, and thus the power received from each user is $P^{(i)}$. The modulation used is BPSK. The channel model for the reference user k are two paths arriving at 0 and T_c, while for the other users the time of arrival of their two paths are uniformly distributed over $[0, T_c]$ and $[T_c, 2T_c]$. The pulse shape to be studied is the RRC pulse.

4.4.1 Multiple-Access Interference

Following the same analysis as for QPSK with MRC, at the output of the RAKE receiver, the variance of the interference due to user i normalized by the power of the desired signal, $P^{(k)}N^2$, is given as

$$\Psi_i = \frac{P^{(i)}}{NP^{(k)}} \sum_{l_1=1}^{L} \sum_{l_2=1}^{L} \sum_{f_1=1}^{F} \sum_{f_2=1}^{F} \alpha_{l_1}\alpha_{l_2}\alpha_{f_1}\alpha_{f_2}\,\mathrm{Sg}(\tau_{l_1 f_1}, \tau_{l_2 f_2}) \cos(\theta_{l_1} - \theta_{f_1}) \cos(\theta_{l_2} - \theta_{f_2}). \quad (204)$$

Notice that the f subindexes are assigned to the fingers of the reference user k, and the l weights are assigned to the paths for the user i. Without any loss in generalization, time is going to be normalized such that $T_c = 1$.

It is straightforward to see that for $\alpha_f = \alpha_l = 1/\sqrt{2}$,

$$\begin{aligned} \mathrm{E}_{\tau,\theta}[\Psi_i] &= \frac{P^{(i)}}{NP^{(k)}} \mathrm{E}_{\tau,\theta} \left[\sum_{l=1}^{L} \sum_{f=1}^{F} \alpha_l^2 \alpha_f^2 \mathrm{Sg}(\tau_{lf}, \tau_{lf}) \cos^2(\theta_l - \theta_f) \right] \\ &= \frac{P^{(i)}}{NP^{(k)}} \sum_{l=1}^{L} \sum_{f=1}^{F} \alpha_l^2 \alpha_f^2 (1 - \frac{\beta}{4}) \cdot 12 = \frac{P^{(i)}}{NP^{(k)}} (1 - \frac{\beta}{4}) \cdot \frac{1}{2}. \end{aligned} \quad (205)$$

In the calculation of the second moment of Ψ_k, the following cases are encountered (cases that do not go to zero):

Case 1: $l_1 = l_2 = l_3 = l_4$ and $f_1 = f_2 = f_3 = f_4$.

Case 2: a)$f_1 = f_2 \neq f_3 = f_4$ and $l_1 = l_2 = l_3 = l_4$ or b)$f_1 = f_2 = f_3 = f_4$ and $l_1 = l_2 \neq l_3 = l_4$.

Case 3: a) $l_1 = l_3 \neq l_2 = l_4$, $f_1 = f_3 \neq f_2 = f_4$, b)$l_1 = l_4 \neq l_2 = l_2$, $f_1 = f_4 \neq f_2 = f_3$.

Case 4: $f_1 = f_2 = f_3 = f_4$ and a)$l_1 = l_3 \neq l_2 = l_4$ or b)$l_1 = l_4 \neq l_2 = l_2$.

Case 5: $f_1 = f_2 \neq f_3 = f_4$ and a)$l_1 = l_2 \neq l_3 = l_4$ or b)$l_1 = l_3 \neq l_2 = l_4$.

Case 6: $l_1 = l_2 = l_3 = l_4$ and i)$f_1 = f_3 \neq f_2 = f_4$ or ii)$f_1 = f_4 \neq f_2 = f_3$.

Case 7: $f_2 = f_4 \neq f_1 = f_3$ and a)$l_1 = l_3 \neq l_2 = l_4$ or b)$l_1 = l_4 \neq l_2 = l_3$.

Case 8: $l_1 = l_2 \neq l_3 = l_4$ a)$f_1 = f_3 \neq f_2 = f_4$ or b)$f_1 = f_4 \neq f_2 = f_3$.

Notice that except for cases 1 and 2, all the other cases would disappear for $L = F = 1$.

The following properties of the function $\mathrm{Sg}(t_1, t_2)$ will be used:

1.$\mathrm{Sg}(a, b) = \mathrm{Sg}(b, a)$,

2.$\mathrm{Sg}(a,0) = g_2(a)$,

3.$\mathrm{Sg}(a,b) = \mathrm{Sg}(a+k, b+k)$.

While taking the expectation of the cases 1 through 8, the following integrals are encountered:

$$\mathrm{C}_1(\beta) = \int_a^{a+1} \mathrm{Sg}^2(t_1,t_1)\,\mathrm{d}t_1, \quad a \in \{-1,0,1\}, \tag{206}$$

$$\begin{aligned}\mathrm{C}_{2a}(\beta) &= \int_a^{a+1} \mathrm{Sg}(t_1,t_1)\,\mathrm{Sg}(t_1+1,t_1+1)\,\mathrm{d}t_1 \\ &= \int_{a+1}^{a+2} \mathrm{Sg}(t_1,t_1)\,\mathrm{Sg}(t_1-1,t_1-1)\,\mathrm{d}t_1, \quad a \in \{-1,0\},\end{aligned} \tag{207}$$

$$\mathrm{C}_{2b}(\beta) = \int_b^{b+1}\int_a^{a+1} \mathrm{Sg}(t_1,t_1)\,\mathrm{Sg}(t_2,t_2)\,\mathrm{d}t_1\,\mathrm{d}t_2, \quad a,b \in \{-1,0,1\} \quad \text{and} \quad a\cdot b \neq 1, \tag{208}$$

$$\mathrm{C}_3(\beta) = \int_0^1\int_0^1 \mathrm{Sg}^2(t_1,t_2)\,\mathrm{d}t_1\,\mathrm{d}t_2, \tag{209}$$

$$\mathrm{C}_4(\beta) = \int_{a-1}^{a-2}\int_a^{a+1} \mathrm{Sg}^2(t_1,t_2)\,\mathrm{d}t_1\,\mathrm{d}t_2, \quad a \in \{0,1\}, \tag{210}$$

$$\begin{aligned}\mathrm{C}_5(\beta) &= \int_{-1}^0\int_0^1 \mathrm{Sg}(t_1,t_2)\,\mathrm{Sg}(t_1-1,t_2-1)\,\mathrm{d}t_1\,\mathrm{d}t_2 \\ &= \int_0^1\int_1^2 \mathrm{Sg}(t_1,t_2)\,\mathrm{Sg}(t_1+1,t_2+1)\,\mathrm{d}t_1\,\mathrm{d}t_2 = \mathrm{C}_4(\beta),\end{aligned} \tag{211}$$

$$\mathrm{C}_{6a} = \int_{-1}^0 \mathrm{Sg}^2(t_1,1-t_1)\mathrm{d}t_1, \tag{212}$$

$$\mathrm{C}_{6b}(\beta) = \int_a^{a+1} \mathrm{Sg}^2(t_1,t_1+1)\,\mathrm{d}t_1 = \int_{a+1}^{a+2} \mathrm{Sg}^2(t_1,t_1-1)\,\mathrm{d}t_1, \quad a \in \{-1,0\}, \tag{213}$$

$$\mathrm{C}_7(\beta) = \int_{-1}^0\int_1^2 \mathrm{Sg}^2(t_1,t_2)\,\mathrm{d}t_1\,\mathrm{d}t_2 = \int_1^2\int_{-1}^0 \mathrm{Sg}^2(t_1,t_2)\,\mathrm{d}t_1\,\mathrm{d}t_2, \tag{214}$$

$$\begin{aligned}\mathrm{C}_8(\beta) &= \int_0^1\int_{-1}^0 \mathrm{Sg}(t_1,1+t_1)\,\mathrm{Sg}(t_2,1+t_2)\,\mathrm{d}t_1\,\mathrm{d}t_2 \\ &= \int_{-1}^0\int_0^1 \mathrm{Sg}(t_1,1+t_1)\,\mathrm{Sg}(t_2,1+t_2)\,\mathrm{d}t_1\,\mathrm{d}t_2.\end{aligned} \tag{215}$$

A change of variables and property 2 of $\mathrm{Sg}(t_1,t_2)$ was used to show that $\mathrm{C}_5(\beta) = \mathrm{C}_4(\beta)$. The values of the first two integrals are known; they can be easily shown to be section in this chapter:

$$\mathrm{C}_1(\beta) = (1 - \beta/2 + 3\beta^2/32), \tag{216}$$

$$\mathrm{C}_2(\beta) = (1 - \beta/2 + \beta^2/16). \tag{217}$$

It can also be shown that $\mathrm{C}_8(\beta) = 2\mathrm{C}_{6b}(\beta)/3$. As a matter of fact,

$$\mathrm{Sg}(t_1, 1+t_1) = \mathrm{RC}(1) - \frac{\sin(\beta\pi)\sin(\pi t_1)\sin(\pi t_1+\pi)}{2\pi(1-\beta^2)} = \frac{\sin(\beta\pi)\sin^2(\pi t_1)}{2\pi(1-\beta^2)},$$

$$\mathrm{C}_{6b}(\beta) = \int_0^1 \mathrm{Sg}^2(t_1, 1+t_1)\,\mathrm{d}t_1 = \frac{\sin^2(\beta\pi)}{4\pi^2(1-\beta^2)^2}\int_0^1 \sin^4(\pi t_1)\mathrm{d}t_1 = \frac{3\sin^2(\beta\pi)}{32\pi^2(1-\beta^2)^2}, \quad (218)$$

$$\text{and} \quad \mathrm{C}_8(\beta) = \int_0^1\int_{-1}^0 \mathrm{Sg}(t_1, 1+t_1)\,\mathrm{Sg}(t_2, 1+t_2)\,\mathrm{d}t_1\,\mathrm{d}t_2$$

$$= \frac{\sin^2(\beta\pi)}{4\pi^2(1-\beta^2)^2}\int_0^1\int_{-1}^0 \sin^2(\pi t_1)\,\sin^2(\pi t_2)\mathrm{d}t_1\mathrm{d}t_2 = \frac{\sin^2(\beta\pi)}{16\pi^2(1-\beta^2)^2}. \quad (219)$$

For the case that $\beta = 0$, integration for the remaining terms $C_3(0)$, $C_4(0)$, $C_{6a}(0)$, $C_7(0)$ can be done. First, notice the following identities:

$$\begin{aligned}\int \frac{\sin^2(\pi d)}{\pi^2 d^2}\mathrm{d}d &= \int \frac{1-\cos(2\pi d)}{2\pi^2 d^2}\mathrm{d}d \\ &= \int \frac{1}{2\pi^2 d^2} - \left(\frac{\cos(2\pi d)}{2\pi^2 d^2} + \frac{\sin(2d\pi)}{d\pi}\right) + \frac{\sin(2d\pi)}{d\pi}\mathrm{d}d \\ &= -\frac{1}{2\pi^2 d} + \frac{\cos(2\,d\,\pi)}{2\,d\pi^2} + \frac{\mathrm{Si}(2\pi d)}{\pi}, \end{aligned} \quad (220)$$

$$\int \frac{\sin^2(\pi d)}{\pi^2 d}\mathrm{d}d = \int \frac{1-\cos(2\pi d)}{2\pi^2 d}\mathrm{d}d = \frac{\ln(d)}{2\pi^2} - \frac{\mathrm{Ci}(2d\pi)}{2\pi^2}, \quad (221)$$

where the Sine Integral $\mathrm{Si}(d)$ and Cosine Integral $\mathrm{Ci}(d)$ are given as [3]

$$\mathrm{Si}(z) = \int_0^z \frac{\sin(x)}{x}\mathrm{d}x, \quad \mathrm{Ci}(z) = -\int_z^\infty \frac{\cos(x)}{x}\mathrm{d}x = \gamma + \ln(z) - \int_0^z \frac{1-\cos(x)}{x}\mathrm{d}x. \quad (222)$$

As a result

$$\int \frac{(K-d)\sin^2(\pi d)}{\pi^2 d^2}\mathrm{d}d = -\frac{K}{2\pi^2 d} + \frac{K\,\cos(2\,d\,\pi)}{2\,d\pi^2} + \frac{K\,\mathrm{Si}(2\pi d)}{\pi} - \frac{\ln(d)}{2\pi^2} + \frac{\mathrm{Ci}(2d\pi)}{2\pi^2}. \quad (223)$$

Since $\mathrm{Si}(0) = 0$, as d approaches zero, $\frac{K\,(\cos(2\,d\,\pi)-1)}{2\,d\pi^2}$ approaches zero; therefore as d approaches zero, the expression 223 simplifies to just $\frac{\gamma+\ln(2\pi)}{2\pi^2}$. Therefore,

$$\mathrm{C}_3(0) = 2\int_0^1 (1-d)\frac{\sin^2(\pi d)}{(\pi d)^2}\mathrm{d}d = \frac{2\mathrm{Si}(2\pi)}{\pi} + \frac{\mathrm{Ci}(2\pi)}{\pi^2} - \frac{\gamma+\ln(2\pi)}{\pi^2} \approx 0.65355. \quad (224)$$

$$\mathrm{C}_4(0) = \int_{-2}^{-1}(2+d)\frac{\sin^2(\pi d)}{(\pi d)^2}\mathrm{d}d + \int_{-1}^0(-d)\frac{\sin^2(\pi d)}{(\pi d)^2}\mathrm{d}d =$$

$$\frac{2}{\pi}(\mathrm{Si}(-2\pi) - \mathrm{Si}(-4\pi)) - \frac{\ln(2)}{2\pi^2} + \frac{\mathrm{Ci}(-4\pi) - 2\mathrm{Ci}(-2\pi)}{2\pi^2} + \frac{\gamma}{2\pi^2} + \frac{j}{2\pi} \approx 0.13633. \quad (225)$$

$$\mathrm{C}_{6a}(0) = \int_{-1}^{0} \frac{\sin^2(\pi(2t_1-1))}{(\pi(2t_1-1))^2}\mathrm{d}t_1 = \int_{-1.5}^{-0.5} \frac{\sin^2(2\pi t_1)}{(2\pi t_1)^2}\mathrm{d}t_1 = \frac{\mathrm{Si}(6\pi)-\mathrm{Si}(2\pi)}{2\pi}$$
$$\approx 0.0158958. \quad (226)$$

$$\mathrm{C}_7(0) = \int_{-2}^{-1}(-1-d)\frac{\sin^2(\pi d)}{(\pi d)^2}\mathrm{d}d + \int_{-3}^{-2}(3+d)\frac{\sin^2(\pi d)}{(\pi d)^2}\mathrm{d}d =$$
$$\frac{\mathrm{Ci}(-6\pi) - 2\,\mathrm{Ci}(-4\pi) + \mathrm{Ci}(-2\pi) + \ln(\frac{4}{3}) + 2\pi\,(\mathrm{Si}(2\pi) - 4\,\mathrm{Si}(4\pi) + 3\,\mathrm{Si}(6\pi))}{2\,\pi^2} =$$
$$\frac{1}{2\pi^2}\left(\mathrm{Ci}(-6\pi) - 2\,\mathrm{Ci}(-4\pi) + \mathrm{Ci}(-2\pi) + \ln\left(\frac{4}{3}\right)\right)$$
$$+\frac{1}{\pi}\,(\mathrm{Si}(2\pi) - 4\,\mathrm{Si}(4\pi) + 3\,\mathrm{Si}(6\pi)) \approx 0.015060. \quad (227)$$

For $\beta > 0$, numerical integration and curve fitting to obtain $C_3(\beta)$, $C_4(\beta)$, $C_{6a}(\beta)$, $C_7(\beta)$ can be done:

$$\mathrm{C}_3(\beta) \approx 0.655837 - 0.349163\,\beta - 0.0325283\,\beta^2 + 0.0409641\,\beta^3 + 0.0106074\,\beta^4$$
$$-0.00648542\,\beta^5, \quad (228)$$

$$\mathrm{C}_4(\beta) \approx 0.136297 + 0.0344131\,\beta - 0.0509339\,\beta^2 + 0.126899\,\beta^3 - 0.175946\,\beta^4$$
$$+0.066279\,\beta^5, \quad (229)$$

$$\mathrm{C}_{6a}(\beta) \approx 0.0162891 - 0.00847849\,\beta + 0.185908\,\beta^2 - 0.605793\,\beta^3 + 0.611257\,\beta^4$$
$$-0.198451\,\beta^5, \quad (230)$$

$$\mathrm{C}_7(\beta) \approx 0.0152837 - 0.00371089\,\beta + 0.0685334\,\beta^2 - 0.298431\,\beta^3 + 0.331247\,\beta^4$$
$$-0.112576\,\beta^5. \quad (231)$$

The previous factors show that for $L > 1$, the variance of Ψ differs from 0.

The cosine factors when averaged over the phases for the above cases results in $\frac{3}{8}$ for

case 1), $\frac{1}{4}$ for cases 2, 3, 4, 6, and 7, and $\frac{1}{8}$ for cases 5 and 8. Therefore, for $\sigma_i^2 = \mathrm{Var}_{\tau,\theta}[\Psi_i]$,

$$\left(\frac{NP^{(k)}}{P^{(i)}}\right)^2 \cdot \sigma_i^2 = \mathrm{C}_1 \sum_{l=1}^{L}\sum_{f=1}^{F} \alpha_l^4 \alpha_f^4 \cdot \frac{3}{8} +$$
$$\mathrm{C}_2 \left(\sum_{l_1=1}^{L} \sum_{\substack{l_2=1 \\ l_2 \neq l_1}}^{L} \sum_{f_1=1}^{F} \sum_{f_2=1}^{F} \alpha_{l_1}^2 \alpha_{l_2}^2 \alpha_{f_1}^2 \alpha_{f_2}^2 + \sum_{l}^{L} \sum_{f_1=1}^{F} \sum_{\substack{f_2=1 \\ f_2 \neq f_1}}^{F} \alpha_l^4 \alpha_{f_1}^2 \alpha_{f_2}^2 \right) \cdot \frac{1}{4}$$
$$+2\mathrm{C}_3 \sum_{l_1=1}^{L} \sum_{\substack{l_2=1 \\ l_2 \neq l_1}}^{L} \alpha_{l_1}^2 \alpha_{l_2}^2 \alpha_{k,l_1}^2 \alpha_{k,l_2}^2 \cdot \frac{1}{4} + 2\mathrm{C}_4 \sum_{l_1=1}^{L} \sum_{\substack{l_2=1 \\ l_1 \neq l_2}}^{L} \sum_{f=1}^{F} \alpha_{l_1}^2 \alpha_{l_2}^2 \alpha_f^4 \cdot \frac{1}{4} +$$
$$2\mathrm{C}_5 \sum_{l_1=1}^{L} \sum_{\substack{l_2=1 \\ l_1 \neq l_2}}^{L} \sum_{f_1=1}^{F} \sum_{\substack{f_1=1 \\ f_1 \neq f_2}}^{F} \alpha_{l_1}^2 \alpha_{l_2}^2 \alpha_{f_1}^2 \alpha_{f_2}^2 \cdot \frac{1}{8} + 2\mathrm{C}_{6a} \sum_{l=1}^{L} \sum_{f_1=1}^{F} \sum_{\substack{f_2=1 \\ f_1 \neq f_2}}^{F} \alpha_l^4 \alpha_{f_1}^2 \alpha_{f_2}^2 \cdot \frac{1}{4} +$$
$$2\mathrm{C}_{6b} \sum_{l=1}^{L} \sum_{f_1=1}^{F} \sum_{\substack{f_2=1 \\ f_1 \neq f_2}}^{F} \alpha_l^4 \alpha_{f_1}^2 \alpha_{f_2}^2 \cdot \frac{1}{4} + 2\mathrm{C}_7 \sum_{l_1=1}^{L} \sum_{\substack{l_2=1 \\ l_2 \neq l_1}}^{L} \alpha_{l_1}^2 \alpha_{l_2}^2 \alpha_{k,l_1}^2 \alpha_{k,l_2}^2 \cdot \frac{1}{4}$$
$$+2\mathrm{C}_8 \sum_{l_1=1}^{L} \sum_{\substack{l_2=1 \\ l_1 \neq l_2}}^{L} \sum_{f_1=1}^{F} \sum_{\substack{f_1=1 \\ f_1 \neq f_2}}^{F} \alpha_{l_1}^2 \alpha_{l_2}^2 \alpha_{f_1}^2 \alpha_{f_2}^2 \cdot \frac{1}{8} - \mathrm{C}_2 \left(\sum_{l=1}^{L}\sum_{f=1}^{F} \alpha_l^2 \alpha_f^2 \right)^2 \cdot \frac{1}{4}, \qquad (232)$$

which can be simplified to

$$\left(\frac{NP^{(k)}}{P^{(i)}}\right)^2 \cdot \sigma_i^2 = (\frac{3}{8}\mathrm{C}_1 - \frac{1}{4}\mathrm{C}_2) \sum_{l=1}^{L}\sum_{f=1}^{F} \alpha_l^4 \alpha_f^4$$
$$+2(\mathrm{C}_3 + \mathrm{C}_7) \sum_{l_1=1}^{L} \sum_{\substack{l_2=1 \\ l_2 \neq l_1}}^{L} \alpha_{l_1}^2 \alpha_{l_2}^2 \alpha_{k,l_1}^2 \alpha_{k,l_2}^2 \cdot \frac{1}{4}$$
$$+2\mathrm{C}_4 \sum_{l_1=1}^{L} \sum_{\substack{l_2=1 \\ l_1 \neq l_2}}^{L} \sum_{f=1}^{F} \alpha_{l_1}^2 \alpha_{l_2}^2 \alpha_f^4 \cdot \frac{1}{4} + 2(\mathrm{C}_5 + \mathrm{C}_8) \sum_{l_1=1}^{L} \sum_{\substack{l_2=1 \\ l_1 \neq l_2}}^{L} \sum_{f_1=1}^{F} \sum_{\substack{f_1=1 \\ f_1 \neq f_2}}^{F} \alpha_{l_1}^2 \alpha_{l_2}^2 \alpha_{f_1}^2 \alpha_{f_2}^2 \cdot \frac{1}{8}$$
$$+2(\mathrm{C}_{6a} + \mathrm{C}_{6b}) \sum_{l=1}^{L} \sum_{f_1=1}^{F} \sum_{\substack{f_2=1 \\ f_1 \neq f_2}}^{F} \alpha_l^4 \alpha_{f_1}^2 \alpha_{f_2}^2 \cdot \frac{1}{4}. \qquad (233)$$

For the case that each of the two paths has the same power and the power received from each user is equal to that of the reference user (perfect power control), $\alpha_f = \alpha_l = 1/\sqrt{2}$,

$$N^2 \cdot \sigma_i^2 = \frac{1}{16} \left(4\mathrm{C}_1 \frac{3}{8} + 12\mathrm{C}_2 \cdot \frac{1}{4} + 4\mathrm{C}_3 \cdot \frac{1}{4} + 8\mathrm{C}_4 \cdot \frac{1}{4} + 8\mathrm{C}_5 \cdot \frac{1}{8} + 4\mathrm{C}_{6a} \cdot \frac{1}{4} + 4\mathrm{C}_{6b} \cdot \frac{1}{4} \right.$$
$$\left. +4\mathrm{C}_7 \cdot \frac{1}{4} + 8\mathrm{C}_8 \cdot \frac{1}{8} - 16\mathrm{C}_2 \cdot \frac{1}{4} \right). \qquad (234)$$

Since $\mathrm{E}[\cos^2(\theta_l^{(i_1)} - \theta_f) \cdot \cos^2(\theta_l^{(i_2)} - \theta_f)] = \mathrm{E}[\cos^2(\theta_l^{(i_1)} - \theta_f)] \cdot \mathrm{E}[\cos^2(\theta_l^{(i_2)} - \theta_f)]$ for

$i_2 \neq i_2$, then $\mathrm{E}[\Psi_{i_1}\Psi_{i_2}] = \mathrm{E}[\Psi_{i_1}]\mathrm{E}[\Psi_{i_2}]$ for $i_1 \neq i_2$,

$$\sigma^2 = \left(\frac{K'}{16N^2}\right)\left(1.5963 - 0.508113\,\beta + 0.303581\,\beta^2 - 0.482564\,\beta^3 + 0.221699\,\beta^4 - 0.118675\,\beta^5 + 0.141729\,\beta^6 - 0.0554373\,\beta^7\right). \quad (235)$$

We simulated systems with different conditions:

Table 11: BER comparison for RAKE system with two fingers using an RRC pulse with $\beta = 0.5$

Conditions	Simulations	SIGA	SGA
N=32, K'=5, $\beta = 0.5$	2.57E-4	2.06E-4	6.54E-5
N=32, K'=10, $\beta = 0.5$	4.30E-3	4.08E-3	3.42E-3
N=64, K'=10, $\beta = 0.5$	1.65E-4	1.34E-4	6.55E-5

4.4.2 Third Moment of Self-interference and MAI

An important observation is that for large N, for fixed delays and phases, both the self-interference and the MAI can be approximated as Gaussian over the codes; both the self-interference and the MAI have third central moments (over the codes equal to zero), but once the self interference and the MAI are added together, their third moment is no longer zero and thus the pdf is skewed (asymmetrical). Taking into account that the mean of the self-interference and the MAI is zero for both, during the expansion of the third moment of their sum, there is the term

$$3\sum_{l_1=1}^{L}\sum_{l_2=1}^{L}\sum_{f_1=1}^{F}\sum_{f_2=1}^{F}\sum_{f_3=1}^{F}\sum_{\substack{f_4=1\\ f_3\neq f_4}}^{F}\cdot\mathrm{E}[\sum_{n_1=0}^{N-1}\sum_{n_2=0}^{N-1}\sum_{n_3=0}^{N-1}\sum_{n_4=0}^{N-1}\sum_{a_1=-\infty}^{\infty}\sum_{a_2=-\infty}^{\infty} c_{n_1}^{(k)}c_{a_1}^{(i)}c_{n_2}^{(k)}c_{a_2}^{(i)}c_{n_3}^{(k)}c_{n_4}^{(k)}\cdot g_2((n_1-a_1)T_c - \tau_{l_1f_1})\cdot g_2((n_2-a_2)T_c - \tau_{l_2f_2})\cdot g_2((n_3-n_4)T_c - \tau_{f_3f_4})\cdot \cos(\theta_{l_1}^{(i)} - \theta_{f_1})]\cdot\cos(\theta_{l_2}^{(i)} - \theta_{f_2})\cdot\cos(\theta_{f_3} - \theta_{f_4}). \quad (236)$$

We have not normalized the delay by T_c. Since $f_3 \neq f_4$ and $g_2(nT_c) = 0$ only when the integer n is zero, the equalities $n_3 = n_4 + 1$ (when $\tau_{f_3f_4} = T_c$) or $n_3 = n_4 - 1$ (when $\tau_{f_3f_4} = -T_c$) can be made. Making then $n_1 = n_3$ and $n_2 = n_4$ and $l_1 = l_2$, $f_1 = f_3$, $f_2 = f_4$, a negative third moment is obtained.

The sections on self-interference and cross-covariance have been included for the sake of completeness.

4.4.3 Self-Interference

The self-interference can be expressed in the following way

$$\sqrt{P^{(i)}}\sum_{n=1}^{N}\sum_{a=1}^{N}\sum_{f_1}^{F}\sum_{f_2}^{F}\alpha_{f_1}\alpha_{f_2}c_n c_a g_2((n-a)T_c-\tau_{f_1f_2})\cos(\theta_{f_1}-\theta_{f_2}).$$

The variance (over the codes) of the self-interference has the form

$$\mathrm{E}_c\Bigg[\sum_{n_1=1}^{N}\sum_{a_1=1}^{N}\sum_{n_2=1}^{N}\sum_{a_2=1}^{N}\sum_{f_1}^{F}\sum_{f_2}^{F}\sum_{f_3}^{F}\sum_{f_4}^{F}\alpha_{f_1}\alpha_{f_2}\alpha_{f_3}\alpha_{f_4}c_{n_1}c_{a_1}c_{n_2}c_{a_2}\cdot$$

$$g_2((n_1-a_1)T_c-\tau_{f_1f_2})\cos(\theta_{f_1}-\theta_{f_2})\cdot g_2((n_1-a_1)T_c-\tau_{f_1f_2})\cos(\theta_{f_1}-\theta_{f_2})\Bigg]. \quad (237)$$

For cases I) $n_1=a_1$ and $n_2=a_2$, II) $n_1=n_2$ and $a_1=a_2$, III) $n_1=a_2$ and $n_2=a_1$ and IV) $n_1=n_2=a_1=a_2$, the above expression does not go to zero, but cases I) and IV) belong the desired signal, therefore normalizing the variance of the interference by the power of the desired signal

$$\Psi_i=\frac{1}{N}\sum_{f_1=1}^{F}\sum_{f_2=1}^{F}\sum_{f_3=1}^{F}\sum_{f_4=1}^{F}(\mathrm{Sg}(\tau_{f_1f_2},\tau_{f_3f_4})-g_2(\tau_{f_1f_2})g_2(\tau_{f_3f_4})+$$

$$\mathrm{Sg}(\tau_{f_1f_2},\tau_{-f_3f_4})-g_2(\tau_{f_1f_2})g_2(\tau_{-f_3f_4}))\cos(\theta_{f_1}-\theta_{f_2})\cos(\theta_{f_3}-\theta_{f_4}). \quad (238)$$

Using the particular values for the delays of the fingers in this section,

$$\Psi_i=\frac{2}{N}\sum_{f_1=1}^{F}\sum_{\substack{f_2=1\\f_1\neq f_2}}^{F}\alpha_{f_1}^2\alpha_{f_2}^2\cos(\theta_{f_1}-\theta_{f_2})^2, \quad (239)$$

$$\mathrm{E}[\Psi_i]=N\sum_{f_1=1}^{F}\sum_{\substack{f_2=1\\f_1\neq f_2}}^{F}\alpha_{f_1}^2\alpha_{f_2}^2, \quad (240)$$

$$\mathrm{E}[\Psi_i^2]=\frac{4}{N^2}\mathrm{E}\left[\sum_{f_1=1}^{F}\sum_{\substack{f_2=1\\f_1\neq f_2}}^{F}\sum_{f_3=1}^{F}\sum_{\substack{f_4=1\\f_3\neq f_4}}^{F}\alpha_{f_1}^2\alpha_{f_2}^2\alpha_{f_3}^2\alpha_{f_4}^2\cos(\theta_{f_1}-\theta_{f_2})^2\cos(\theta_{f_3}-\theta_{f_4})^2\right]. \quad (241)$$

Using the cases 1) $f_1=f_3$ and $f_2=f_4$ and 2) $f_1=f_4$ and $f_2=f_3$,

$$\mathrm{Var}[\Psi_i]=\frac{3}{N^2}\sum_{f_1=1}^{F}\sum_{\substack{f_2=1\\f_1\neq f_2}}^{F}\alpha_{f_1}^4\alpha_{f_2}^4-\left(\frac{1}{N}\sum_{f_1=1}^{F}\sum_{\substack{f_2=1\\f_1\neq f_2}}^{F}\alpha_{f_1}^2\alpha_{f_2}^2\right)^2. \quad (242)$$

4.4.4 Cross-Covariance between MAI and Self-interference

The Cross-Covariance between Ψ_i and Ψ_k can be obtained as

$$\mathrm{E}[\Psi_i\Psi_k] - \mathrm{E}[\Psi_i]\mathrm{E}[\Psi_k] = 2N \sum_{f_1=1}^{F}\sum_{f_2=1}^{F} \alpha_{f_1}^2\alpha_{f_1}^2 \cos\left(\theta_{f_1} - \theta_{f_2}\right)^2 \cdot$$

$$\sum_{l_1=1}^{L}\sum_{l_2=1}^{L}\sum_{f_3=1}^{F}\sum_{f_4=1}^{F} \alpha_{l_1}^2\alpha_{l_2}^2\alpha_{f_3}^2\alpha_{f_4}^2 \mathrm{Sg}(\tau_{l_1 f_3}, \tau_{l_2 f_4}) \cos\left(\theta_{l_1} - \theta_{f_3}\right) \cos\left(\theta_{l_2} - \theta_{f_4}\right) -$$

$$N \sum_{f_1=1}^{F}\sum_{f_2=1}^{F} \alpha_{f_1}^2\alpha_{f_1}^2 \cdot N \sum_{l=1}^{F}\sum_{f_3=1}^{F} \alpha_l^2\alpha_{f_3}^2 (1 - \frac{\beta}{2})\frac{1}{2}.$$

4.5 Conclusion

In summary, closed-form expressions were presented for the SIGA method for both BPSK and OQPSK systems for different Nyquist pulses and arbitrary roll-off factors.

It was also shown that when CDMA bands are spaced by $\Delta f = 1/T_c$, the pulse shape and roll-off factor have little impact on the performance.

The SIGA method was also extended to a simple RAKE receiver with two fingers, where the desired signal propagates through two paths that are spaced by a chip. The MAI propagated through two paths randomly spaced from the two paths of the desired signal. It was shown that if the system can eliminate self-interference, then the SIGA method is much more accurate than the SGA method.

It was also shown that when the self-interference and the MAI are combined, the sum has a third moments and thus, neither the SGA nor SIGA methods would be appropriate to estimate the probability of error.

CHAPTER V

CONCLUDING REMARKS

5.1 Summary of Results

5.1.1 Forward Link Performance

Expressions were obtained to for the performance of the forward link under arbitrary channel models, two models of RAKE receiver, different processing gains, data rates, chip rates, RRC pulse with arbitrary roll-off factors. These expressions can be used with random codes, orthogonal codes, quasi-orthogonal codes, noise, multicode scheme or variable-spreading factor scheme. These expressions were several order of magnitudes faster to obtain than Monte-Carlo simulations, which were accurately matched.

The expressions were used to analyze the impact of roll-off and chip rate.

The SNR for both random and orthogonal codes improves with β.

The SMRC model can be used when the paths are well separated.

A system with a higher bandwidth does not necessarily improve the spectral efficiency for the users close to the BS.

For a given channel model, with increasing bandwith, the spectral efficiency does improve in the presence of only Gaussian noise, but up to a certain point before reaching a limit, but it does not necessarily improve with β.

The number of users increases with β for both random and orthogonal codes.

The E_b/I_o (or SNR) required to obtain a BER of 1E-3 depends on the location of the MS in the cell.

The orthogonality factor was studied from the expressions derived, and it was observed that it decreases with increasing β.

5.1.2 Closed Form for Infinite Sum of Nyquist Pulses

Expressions were first obtained for the RRC pulse and then for general Nyquist pulses with arbitrary roll-off factor. These expressions can be used in the forward and reverse link.

5.1.3 Reverse Link Estimation through Simplified Improved Gaussian Approximation

The SIGA method was applied and closed form expressions were obtained for the reverse link for both BPSK and OQPSK when using a Nyquist pulse with arbitrary β. Results where shown for specific pulses. It was observed that for the OQPSK, the results obtain with the Gaussian approximation and with the SIGA method were essentially very similar.

In the presence of equal interference power from the same carrier and from adjacent carriers, essentially no Nyquist pulse has an advantage over another. This fact suggest that Nyquist pulses should be optimized for eye diagram and performance under filter truncation, rather than MAI minimization.

Finally, the SIGA method was extended to a system with two paths and a RAKE receiver with two fingers while using BPSK modulation.

5.2 Suggestion for Further Research

5.2.1 Accurate Analysis of the Impact of Adjacent Channel Interference on the Performance of the Forward Link

The analysis presented here for the forward link is limited to the MAI, self-interference, and thermal noise, but could be easily adjusted to include the interference coming from the two adjacent bands.

5.2.2 Impact of the SMRC and AMRC Models to System-Level Analysis

System-level simulations of cellular networks usually ignore link-level details, such as modulation, channel coding, and pulse-shape. It would be of importance to obtain the system-level performance using the expressions derived here.

5.2.3 Accurate Performance Analysis for Reverse Link in More General Situations

It would be of importance to obtain accurate and simple expressions for the performance under multipath, arbitrarily-spaced RAKE fingers, and using the AMRC assignment for the finger weights.

APPENDIX A

DERIVATION OF SUM OF SQUARES OF SAMPLES OF THE RAISED COSINE FUNCTION FOR ARBITRARY ROLL-OFF FACTOR

Let $G_2(f)$ and $H(f)$ be the FTs of $g_2(t)$ and $h(t) = g_2^2(t)$, respectively.

$$G_2(f) = \begin{cases} T_c & : \quad (0 \leq |f| \leq \frac{1-\beta}{2T_c} \\ \frac{T_c}{2}\left\{1 + \cos\left[\frac{\pi T}{\beta}\left(|f| - \frac{1-\beta}{2T_c}\right)\right]\right\} & : \quad (\frac{1-\beta}{2T_c} \leq |f| \leq \frac{1+\beta}{2T_c} \\ 0 & : \quad (|f| > \frac{1+\beta}{2T_c}) \end{cases} \tag{243}$$

Time-shifting and impulse-sampling $h(t)$,

$$FT\Big\{\sum_{n=-\infty}^{\infty} h(nT_c - \tau)\delta(t - nT_c)\Big\} = \frac{1}{T_c}\sum_{n=-\infty}^{\infty} H(f - \frac{n}{T_c})\exp\left(-2\pi j\tau(f - \frac{n}{T_c})\right) \tag{244}$$

We have that $\int_{-\infty}^{\infty} f(t)\mathrm{d}t = F(0)$ for $F(w) = FT\{f(t)\}$; also, there is an overlap between the shifted replicas of $H(f)$ since the spectrum of $H(f)$ goes between $-\frac{1+\beta}{T_c}$ and $\frac{1+\beta}{T_c}$.

$$\sum_{n=-\infty}^{\infty} h(nT_c - \tau) = \int_{-\infty}^{\infty}\sum_{n=-\infty}^{\infty} h(nT_c - \tau)\delta(t - nT_c)\,\mathrm{d}t$$
$$= \frac{1}{T_c}[H(0) + H\left(-\frac{1}{T_c}\right)\exp(-2\pi j\frac{\tau}{T_c}) + H\left(\frac{1}{T_c}\right)\exp(2\pi j\frac{\tau}{T_c}) \tag{245}$$

Alternatively, this result can be attained with proper implementation of the Poisson Summation Formula [49]. Since $H(\frac{1}{T_c}) = H(-\frac{1}{T_c})$ due to symmetry of $H(f)$,

$$\sum_{n=-\infty}^{\infty} h(nT_c - \tau) = \frac{1}{T_c}[H(0) + 2H(\frac{1}{T_c})\cos(2\pi\frac{\tau}{T_c})] \tag{246}$$

$$H(0) = 4\int_{(1-\beta)/(2)}^{(1+\beta)/(2)} \frac{1}{4}\cos^4(\frac{\pi(2f - 1 + \beta)}{4\beta})\mathrm{d}f +$$
$$4\int_{(-1+\beta)/(2)}^{(1-\beta)/(2)} \frac{1}{4}\cos^4(\frac{\pi(-2f - 1 + \beta)}{4\beta})\mathrm{d}f + \int_{(-1+\beta)/(2)}^{(1-\beta)/(2)} 1\,\mathrm{d}f = \frac{3}{8}\beta + \frac{3}{8}\beta + 1 - \beta \tag{247}$$

$$\frac{1}{4}\int_{(1-\beta)/2}^{(1+\beta)/2} e^{-j2\pi fd}(1 + \cos[\frac{\pi}{\beta}(f - \frac{1-\beta}{2})])(1 + \cos[\frac{\pi}{\beta}(-f + 1 - \frac{1-\beta}{2})])\mathrm{d}f = \frac{\beta}{8} \tag{248}$$

Therefore,

$$\sum_{n=-\infty}^{\infty} h(nT_c - \tau) = 1 - \frac{\beta}{4} + \frac{\beta}{4}\cos(2\pi\frac{\tau}{T_c}) = 1 - \frac{\beta}{4}\left(1 - \cos(\frac{2\pi\tau}{T_c})\right) = 1 - \frac{\beta}{2}\sin^2(\frac{\pi\tau}{T_c}). \tag{249}$$

Making the substitution $\tau = aT_c$, whenever a is an integer between $-N$ and N, it can be easily seen that

$$\sum_{n=-(N-1)}^{N-1} (1 - \frac{|n|}{N}) g_2^2(nT_c + aT_c) = (1 - \frac{|a|}{N}) = (1 - \frac{|\tau|}{T_c}) \tag{250}$$

Whenever a is not an integer, $\lim_{N\to\infty}(1 - \frac{|n-1|}{N}) = \lim_{N\to\infty}(1 - \frac{|n|}{N}) = \lim_{N\to\infty}(1 - \frac{|n+1|}{N})$ and since the maximum values of $g_2^2(nT_c + aT_c)$ for integer n is at $n = \lfloor a \rfloor$ and $\lceil a \rceil$.

$$\lim_{N\to\infty} \sum_{n=-(N-1)}^{N-1} (1 - \frac{|n|}{N}) g_2^2(nT_c + aT_c) \approx (1 - \frac{\beta}{2}\sin^2(\frac{\pi\tau}{T_c}))(1 - \frac{|a|}{N}) \tag{251}$$

APPENDIX B

EXPRESSION USED FOR CORRELATION OF FINGERS

Defining the function $g_{2n}(t)$, such that $g_2(t) = g_{2n}(t/T_c)$, where $g_2(t)$ is the raised cosine function with roll-off factor β, $g_{2n}(t) = \frac{\sin(\pi t)}{\pi t} \cdot \frac{\cos(\pi\beta t)}{(1-2\beta t)(1+2\beta t)} = \sin(\pi t)\cos(\pi\beta t)\{\frac{1}{\pi t} + \frac{(\beta/\pi)}{1-2\beta t} - \frac{(\beta/\pi)}{1+2\beta t}\}$ can be written. Define the function $F(t,\tau) = g_{2n}(t-\tau)g_{2n}(t+\tau)$ and using trigonometric identities and partial fraction decomposition,

$$F(t,\tau) = -\sin^2(\pi\tau)[\frac{1}{2}\cos(2\pi\beta\tau)\frac{1}{2}\cos(2\pi\beta\tau) + \frac{1}{2}\cos(2\pi\beta t)] \cdot \{\frac{1}{\pi(t-\tau)} + \frac{(\beta/\pi)}{1-2\beta(t-\tau)} - \frac{(\beta/\pi)}{1+2\beta(t-\tau)}\} \cdot \{\frac{1}{\pi(t+\tau)} + \frac{(\beta/\pi)}{1-2\beta(t+\tau)} - \frac{(\beta/\pi)}{1+2\beta(t+\tau)}\} \quad (252)$$

$$\sum_{n=-\infty}^{\infty} F(n,\tau) = \sum_{n=-\infty}^{\infty} -\sin^2(\pi\tau)[\frac{1}{2}\cos(2\pi\beta n)H_1(n) + \frac{1}{2}\cos(2\pi\beta n)H_2(n)] \quad (253)$$

where

$$H_1(t) = \frac{A_1}{\pi(t-\tau)} + \frac{A_3}{1-2\beta\tau-2\beta t} + \frac{A_4}{1+2\beta\tau+2\beta t} - \frac{A_1}{\pi(t+\tau)} + \frac{A_4}{1+2\beta\tau-2\beta t} - \frac{A_3}{1-2\beta\tau+2\beta t}$$

$$H_2(t) = \frac{2A_1\tau}{\pi(t^2-\tau^2)} + \frac{2A_3(1-2\beta\tau)}{(1-2\beta\tau)^2-(2\beta t)^2} + \frac{2A_4(1+2\beta\tau)}{(1+2\beta\tau)^2-(2\beta t)^2} \quad (254)$$

$$A_1 = \frac{1}{2\pi\tau - 32\beta^2\pi\tau^3},\ A_3 = \frac{\beta}{4\pi^2\tau(1-2\beta\tau)(1-4\beta\tau)},\ A_4 = \frac{-\beta}{4\pi^2\tau(1+2\beta\tau)(1+4\beta\tau)} \quad (255)$$

From [30], the following functional series are used:

$$\sum_{n=-\infty}^{\infty} \frac{1}{n^2-a^2} = \frac{\pi}{a}\cdot\frac{\sin(2\pi a)}{\cos(2\pi a)-1} \quad (256)$$

$$\sum_{n=-\infty}^{\infty} \frac{\cos(n\theta)}{n-a} = \frac{\pi\cos(a(\pi-\theta))}{\sin(a\pi)}, \text{where } 0 \le \theta \le 2\pi \quad (257)$$

Therefore, for $\beta \neq 0$,

$$\sum_{n=-\infty}^{\infty} \frac{1}{2}\cos(2\pi\beta n)H_1(n) = -A_1\frac{\cos(\tau(2\pi\beta-\pi))}{\sin(\tau\pi)} + (\frac{A_3}{2})(\frac{\pi}{\beta})\frac{\cos((\frac{1-2\beta\tau}{2\beta})(\pi-2\pi\beta))}{\sin((\frac{1-2\beta\tau}{2\beta})\pi)} + (\frac{A_4}{2})(\frac{\pi}{\beta})\frac{\cos((\frac{1+2\beta\tau}{2\beta})(\pi-2\pi\beta))}{\sin((\frac{1+2\beta\tau}{2\beta})\pi)} \quad (258)$$

$$\sum_{n=-\infty}^{\infty} H_2(n) = 2A_1 \cdot \frac{\sin(2\pi\tau)}{\cos(2\pi\tau)-1} - D_3 \cdot \frac{\pi}{D_4} \cdot \frac{\sin(2\pi D_4)}{\cos(2\pi D_4)-1} - D_1 \cdot \frac{\pi}{D_2} \cdot \frac{\sin(2\pi D_2)}{\cos(2\pi D_2)-1} \tag{259}$$

where the coefficients D_1, D_2, D_3, and D_4 are given as

$$D_1 = \frac{2A_4(1+2\beta\tau)}{(2\beta)^2},\ D_2 = \frac{1+2\beta\tau}{2\beta},\ D_3 = \frac{2A_3(1-2\beta\tau)}{(2\beta)^2},\ D_4 = \frac{1-2\beta\tau}{2\beta}$$

Replacing all the coefficients and simplifying,

$$\begin{aligned}\frac{-\sin^2(\tau\pi)}{(1-20\beta^2\tau^2+64\beta^4\tau^4)8\tau\pi}\Bigg(&\cos(2\beta\tau\pi)\Big[(1+6\beta\tau+8\beta^2\tau^2)\cot((\frac{1}{2\beta}-\tau)\pi)\\ &+(16\beta^2\tau^2-4)\cot(\tau\pi)-(1-6\beta\tau+8\beta^2\tau^2)\cot((\frac{1}{2\beta}+\tau)\pi)\Big]\\ &-(1+6\beta\tau+8\beta^2\tau^2)\cos((\frac{1}{2\beta}-\tau+2\beta\tau)\pi)\csc((\frac{1}{2\beta}-\tau)\pi)\\ &+(16\beta^2\tau^2-4)\cos((1-2\beta)\tau\pi)\csc(\tau\pi)\\ &+(1-6\beta\tau+8\beta^2\tau^2)\cos((\frac{1}{2\beta}+\tau-2\beta\tau)\pi)\csc(\frac{\pi}{2\beta}+\tau\pi)\Bigg)\end{aligned} \tag{260}$$

There are three terms of the form $\cos(A+B)\csc(A)$; replacing them by $\cot(A)\cos(B)-\sin(B)$, several terms cancel out,

$$\begin{aligned}&-\sin^2(\tau\pi)\frac{[\sin(2\beta\tau\pi)(16\beta^2\tau^2-1)+\cos(2\beta\tau\pi)\cot(\tau\pi)(16b^2\tau^2-4)]}{4\tau\pi(1-16\beta^2\tau^2)(1-4\beta^2\tau^2)}\\ &\quad=\frac{\sin(2\pi\tau)\cos(2\beta\tau\pi)}{2\pi\tau(1-16\beta^2\tau^2)}+\frac{\sin(\pi\tau)\cos(\pi\beta\tau)}{(\pi\tau)(1-4\beta^2\tau^2)}\cdot\frac{1}{4}\frac{\sin(\pi\tau)}{\cos(\pi\beta\tau)}\sin(2\beta\tau\pi)\\ &=\sum_{n=-\infty}^{\infty} g_2(nT_c-\tau)g_2(nT_c+\tau)=g_2(2\tau)+\frac{1}{2}g_2(\tau)\sin(\tau\pi)\sin(\beta\pi\tau).\end{aligned} \tag{261}$$

Whenever $\beta = 0$, using (256), the following is obtained

$$\begin{aligned}\sum_{n=-\infty}^{\infty} g_2(nT_c-\tau)g_2(nT_c+\tau) &= -\sum_{n=-\infty}^{\infty}\frac{\sin^2(\pi\tau)}{\pi^2(t^2-\tau^2)}=\frac{-\sin(\pi\tau)}{\pi\tau}\cdot\frac{\sin(2\pi\tau)}{\cos(2\pi\tau)-1}\\ &= \operatorname{sinc}(2\tau).\end{aligned} \tag{262}$$

The expression

$$\begin{aligned}\lim_{N\to\infty}\sum_{n=-(N-1)}^{N-1}(1-\frac{|n|}{N})g_2(nT_c+aT_c)g_2(nT_c-aT_c)\\ =g_2(2\tau)+\frac{1}{2}g_2(\tau)\sin(\tau\pi)\sin(\beta\pi\tau)\end{aligned} \tag{263}$$

can be proven as follows

$$\sum_{n=-\infty}^{\infty} |n| g_2(nT_c - \tau) g_2(nT_c + \tau) \leq \sum_{n=-\infty}^{\infty} |n g_2(nT_c - \tau) g_2(nT_c + \tau)|$$

$$\leq \sum_{n=-\infty}^{\infty} |n g_2(nT_c - \tau)| \tag{264}$$

$$\sum_{n=-\infty}^{\infty} |n| g_2(nT_c - \tau) g_2(nT_c + \tau) \geq - \sum_{n=-\infty}^{\infty} |n g_2(nT_c - \tau) g_2(nT_c + \tau)|$$

$$\geq - \sum_{n=-\infty}^{\infty} |n g_2(nT_c - \tau)|, \tag{265}$$

but since $\lim_{n\to\infty} |n g_2(nT_c - \tau)|$ is $O(1/n^2)$,

$$\lim_{N\to\infty} \sum_{n=-(N-1)}^{N-1} (\frac{|n|}{N}) g_2(nT_c + aT_c) g_2(nT_c - aT_c) = 0, \tag{266}$$

APPENDIX C

NOISE

The output of finger f due to Interference, modelled as AWGN, can be expressed as follows:

$$\mathcal{I}_f = \frac{1}{2}\mathrm{Re}\left[\int_{-\infty}^{\infty} I(t)\cdot \mathrm{conj}\left\{\sum_{f=1}^{F}\bar{G}_f\left(s_I^{(k)}(t) - js_Q^{(k)}(t)\right)\right\}\mathrm{d}t\right] \tag{267}$$

Given $I(t) = \mathcal{I}_I(t) + j\mathcal{I}_Q(t)$ and $\bar{G}_f = G_{f,I} + jG_{f,Q}$, $\mathcal{I}_f$ can be rewritten as

$$\mathcal{I}_f = \frac{1}{2}\int_{-\infty}^{\infty}\left[\mathcal{I}_I(t)G_{f,I} - \mathcal{I}_Q(t)G_{f,Q}\right]s_I^{(k)}(t) + \left(\mathcal{I}_Q(t)G_{f,I} + \mathcal{I}_I(t)G_{f,Q}\right)s_Q^{(k)}(t)\mathrm{d}t \tag{268}$$

The correlation between the output of fingers f_1 and f_2 become

$$\begin{aligned}\mathrm{E}[\mathcal{I}_{f_1}\mathcal{I}_{f_2}|\bar{\boldsymbol{\alpha}}] = \frac{1}{4}\mathrm{E}\Bigg[\int_{-\infty}^{\infty}\int_{-\infty}^{\infty}\Big\{&\mathcal{I}_I(t)\mathcal{I}_I(t')G_{f_1,I}(t)G_{f_2,I}(t') + \\ &\mathcal{I}_Q(t)\mathcal{I}_Q(t')G_{f_1,Q}(t)G_{f_2,Q}(t')\Big\}s_I^{(k)}(t)s_I^{(k)}(t') \\ + \Big\{&\mathcal{I}_Q(t)\mathcal{I}_Q(t')G_{f_1,I}(t)G_{f_2,I}(t') + \mathcal{I}_I(t)\mathcal{I}_I(t')G_{f_1,Q}(t)G_{f_2,Q}(t')\Big\}s_Q^{(k)}(t)s_Q^{(k)}(t')\mathrm{d}t\Bigg]\end{aligned} \tag{269}$$

Here I is the model in the low-pass domain; $\frac{1}{2}\mathrm{E}[I(t)I^*(t')] = I_o$ and $\mathrm{E}[I_I(t)I_I^*(t')] = \mathrm{E}[I_Q(t)I_Q^*(t')] = I_o$ [52, pg. 158]

$$\begin{aligned}\mathrm{E}[\mathcal{I}_{f_1}\mathcal{I}_{f_2}|\bar{\boldsymbol{\alpha}}] = \frac{1}{4}\int_{-\infty}^{\infty} &I_o\left\{G_{f_1,I}(t)G_{f_2,I}(t) + G_{f_1,Q}(t)G_{f_2,Q}(t)\right\}s_I^{(k)}(t)s_I^{(k)}(t) + \\ &I_o\left\{G_{f_1,I}(t)G_{f_2,I}(t) + G_{f_1,Q}(t)G_{f_2,Q}(t)\right\}s_Q^{(k)}(t)s_Q^{(k)}(t)\mathrm{d}t\end{aligned} \tag{270}$$

Since

$$\begin{aligned}\int_{-\infty}^{\infty} g_1(t - nT_c - \tau_{f_1})g_1(t - nT_c - \tau_{f_2})\mathrm{d}t &= \int_{-\infty}^{\infty} g_1(t - nT_c)g_1(t - nT_c - \tau_{f_2f_1})\mathrm{d}t \\ &= \int_{-\infty}^{\infty} g_1(t - nT_c)g_1(\tau_{f_2f_1} - (t - nT_c))\mathrm{d}t = g_2(\tau_{f_2f_1}),\end{aligned}$$

$$\begin{aligned}\mathrm{E}[\mathcal{I}_{f_1}\mathcal{I}_{f_2}|\bar{\boldsymbol{\alpha}}] &= \frac{1}{4}I_o\int_{-\infty}^{\infty}\mathrm{Re}\left[\bar{G}_{f_1}\bar{G}_{f_2}^*\right]\cdot \\ &\left\{\sum_{n_1=0}^{N-1}\sum_{n_2=0}^{N-1}(c_{I,n_1}c_{I,n2} + c_{Q,n_1}c_{Q,n_2})g_1(n_1T_c - \tau_{f_1})g_1(n_2T_c - \tau_{f_2})\right\}\mathrm{d}t \\ &= \frac{1}{2}I_o\mathrm{Re}\left[\bar{G}_{f_1}\bar{G}_{f_2}^*\right]Ng_2(\tau_{f_1f_2})\end{aligned} \tag{271}$$

For the SMRC, $\mathrm{Re}\left[\bar{G}_{f_1}\bar{G}^*_{f_2}\right] = \alpha_{f_1}\alpha_{f_2}\cos\left(\theta_{f_1}-\theta_{f_2}\right)$, which when taking the expectation with respect to phase reduces to zero unless $f_1 = f_2$; therefore

$$\mathrm{E}[\mathcal{I}_{f_1}\mathcal{I}_{f_2}|\boldsymbol{\alpha}] = \frac{1}{2}I_o\alpha_{f_1}\alpha_{f_2}N\delta_{f_1 f_2} \tag{272}$$

For AMRC, since

$$\mathrm{Re}\left[\bar{G}_{f_1}\bar{G}^*_{f_2}\right] = \mathrm{Re}\left[\sum_{l_1=1}^{L}\sum_{l_2=1}^{L}\bar{\alpha}_{l_1}g_2(\tau_{l_1 f_1})\bar{\alpha}^*_{l_2}g_2(\tau_{l_2 f_2})\right] =$$
$$\sum_{l_1=1}^{L}\sum_{l_2=1}^{L}(\alpha_{l_1,I}\alpha_{l_2,I}+\alpha_{l_1,Q}\alpha_{l_2,Q})g_2(\tau_{l_1 f_1})g_2(\tau_{l_2 f_2}), \tag{273}$$

Then

$$\mathrm{E}[\mathcal{I}_{f_1}\mathcal{I}_{f_2}|\bar{\boldsymbol{\alpha}}] = \frac{1}{2}I_o N\sum_{l_1=1}^{L}\sum_{l_2=1}^{L}(\alpha_{l_1,I}\alpha_{l_2,I}+\alpha_{l_1,Q}\alpha_{l_2,Q})g_2(\tau_{l_1 f_1})g_2(\tau_{l_2 f_2})g_2(\tau_{f_1 f_2}). \tag{274}$$

For complex spreading, it is straightforward to demonstrate that the resulting formulas are the same because instead of $s_I^{(k)}$ and $s_Q^{(k)}$, there are $s_{II}^{(k)}$ and $s_{IQ}^{(k)}$.

REFERENCES

[1] *Recommendation ITU-R M.1225. Guidelines for Evaluation of Radio Transmission Technologies for IMT-2000*, 1997.

[2] "Physical layer standard for cdma2000 spread spectrum systems." TIA/EIA/IS2000.2 (Ballot Version), July 2001.

[3] ABRAMOWITZ, M. and STEGUN, I. A., *Handbook of Mathematical Functions*. Washington, D.C.: National Bureau of Standards Applied Mathematics Series 55, 1964 (ninth printing, 1970).

[4] ADACHI, F., SAWAHASHI, M., and OKAWA, K., "Tree-structured generation of orthogonal spreading codes with different lengths for foward link of ds-cdma mobile radio," *IEE Electronic Letters*, vol. 33, pp. 490–494, Jan 1997.

[5] ADACHI, F., "Effects of orthogonal spreading and rake combining on ds-cdma," *IEICE Transactions on Communications*, vol. E-80B, pp. 1692–1696, Nov 1997.

[6] ANJARIA, R. and WYRWAS, R., "The effect of chip waveform on the performance of cdma systems in multipath, fading, noisy channels," in *IEEE Proceedings of Vehicular Technology Conference*, pp. 672–675, IEEE, 1992.

[7] ASANO, Y., DAIDO, Y., and HOLTZMAN, J., "Performance evaluation for band-limited ds-cdma communication system," in *43rd Vehicular Technology Conference*, pp. 464–468, IEEE, 1993.

[8] BALACHANDRAN, K., CHANG, K., and REGE, K., "Rake receiver finger assignment in cdma terminals with fractionally spaced multipaths," in *50th Vehicular Technology Conference*, pp. 476–481, IEEE, Fall 1999.

[9] Beaulieu, N. C., Tan, C. C., and Damen, M. O., "A "better than" nyquist pulse," *IEEE Communication Letters*, vol. 5, pp. 367–371, September 2001.

[10] Bottomley, G., Ottoson, T., and Wang, Y.-P. E., "A generalized rake receiver for interference suppression," *JSAC*, vol. 18, pp. 1536–1545, August 2000.

[11] Boujemaa, H. and Siala, M., "On the rake receiver performance," in *IEEE VTS-Fall Vehicular Technology Conference 2000*, pp. 1483–1488, IEEE, 2000.

[12] Brady, P. T., "A statistical analysis of on-off patterns in 16 conversations," *Bell Syst. Tech. J.*, vol. 47, pp. 73–91, January 1968.

[13] Cheun, K., "Performance of direct-sequence spread-spectrum rake receivers with random spreading," *IEEE Transactions on Communications*, vol. 45, pp. 1130–1143, Sept 1997.

[14] Cho, J. H. and Lehner, J. S., "Optimum chip waveforms for ds/ssma communications with random spreading sequences and a matched filter receiver," in *Wireless Communications and Networking Conference WCNC99*, pp. 574–578, September 21-24 1999.

[15] Choi, J.-W., Lee, Y.-H., and Kim, Y.-H., "Performance analysis of forward link ds-cdma systems using random and orthgonal codes," in *IEEE International Conference on Communications, 2001. ICC 2001.*, pp. 1446–1450, 2001.

[16] DaSilva, V., Sousa, E., and Jovanovic, V., "Effect of multipath propagation on the forward link of a cdma cellular system," *Wireless Personal Communications*, vol. 1, no. 1, pp. 33–41, 1994.

[17] Fong, M.-H., Bhargava, V. K., and Wang, Q., "Concatenated orthogonal/pn spreading sequences and their application to cellular ds-cdma systems with integrated traffic," *IEEE Journal in Selected Areas in Communications*, vol. 14, pp. 547–558, April 1996.

[18] Geraniotis, E. and Ghaffari, B., "Performance of binary and quaternary direct-sequence spread-spectrum multiple access systems with random signature sequences," *IEEE Transactions on Communications*, vol. 39, pp. 713–724, May 1991.

[19] Geraniotis, E. and Michael B., P., "Error probability for direct-sequence spread-spectrum multi-access communications - part ii: Approximations," *IEEE Transactions on Communications*, vol. COM-30, pp. 995–985, May 1982.

[20] Geraniotis, E. and Pursley, M. B., "Performance of coherent direct-sequence spread-spectrum communications over specular multipath fading channels," *IEEE Transactions on Communications*, vol. 33, pp. 502–508, June 1985.

[21] Gilhousen, K. S., Jacobs, I. M., Padovani, R., Viterbi, A. J., Weaver, L. A., and Weatly, C. E., "On the capacity of a cellular cdma system," *IEEE Transactions on Vehicular Technology*, vol. 40, pp. 303–311, May 1991.

[22] Guozhen, Z. and Ling, C., "Performance evaluation for band-limited ds-cdma systems based on simplified improved gaussian approximation," *IEEE Transactions on Communications*, vol. 51, pp. 1204–1213, July 2003.

[23] Holtzman, J. M., "On using perturbation analysis to do sensitivity analysis: Derivatives versus differences," *IEEE Transactions on Automatic Control*, vol. 37, pp. 461–464, February 1992.

[24] Holtzman, J. M., "A simple accurate method to calculate spread-spectrum multiple-access error probabilities," *IEEE Transactions on Communications*, vol. 40, pp. 461–464, March 1992.

[25] Hunukumbure, M., Beach, M., and Allen, B., "Downlink orthogonality factor in utra fdd systems," *Electronics Letters*, vol. 38, pp. 196–197, Feb 2002.

[26] Hunukumbure, M., Beach, M., and Allen, B., "Quantifying code orthogonality factor for utra-fdd down-links," in *Third International Conference on 3G Mobile Communication Technologies*, pp. 185–190, IEEE, 2002.

[27] HWANG, K. C. and LEE, K. B., "Performance analysis of low processing gain ds/cdma systems with random spreading sequences," *IEEE Communications Letters*, vol. 2, pp. 315–317, Dec 1998.

[28] JATUNOV, L. and MADISETTI, V. K., "Closed form for infinite sum in bandlimited cdma," *IEEE Communications Letters*, vol. 8, pp. 138–140, March 2004.

[29] JERUCHIM, M. C., BALABAN, P., and SHANMUGAN, K. S., *Simulation of Communication Systems*. New York: Plenum Press, 1992.

[30] JOLLEY, L. B. W., *Summation of Series*. New York: Dover Publications, 2nd rev. ed., 1961.

[31] KAASILA, V.-P. and MÄMMELÄ, A., "Bit error probability of a matched filter in a rayleigh fading multipath channel in the presence of interpath and intersymboy interference.," *IEEE Transactions on Communications*, vol. 47, pp. 809–812, June 1999.

[32] KCHAO, C. and STÜBER, G., "Analysis of a direct-sequence spread-spectrum cellular radio system," *IEEE Transactions on Communications*, vol. 41, pp. 1507–1516, Oct 1993.

[33] KI, J., KWON, S., HONG, E. K., and WHANG, K. C., "Effect of tap spacing on the performance of direct-sequence spread-spectrum rake receiver," *IEEE Transactions on Communications*, vol. 48, pp. 1029–1036, Jun 2000.

[34] KIM, Y., V., K. Y., KIM, J. H., CHO, H., and SUNG, D. K., "A comparison of system performance using two different chip pulses in multiple-chip-rate ds/cdma systems," *IEEE Transactions on Communications*, vol. 49, pp. 1988–1996, Nov 2001.

[35] KIM, Y. W., KIM, Y. V., KIM, J. H., CHO, H.-S., and SUNG, D. K., "A comparison of system performance using two different chip pulses in multiple-chip-rate ds/cdma systems," *IEEE Transactions on Communications*, vol. 49, pp. 1988–1996, Nov 2001.

[36] Kuo, W.-Y., "Analytic forward link performance of pilot-aided coherent ds-cdma under correltated rician fading," *IEEE Journal in Selected Areas in Communications*, vol. 7, pp. 1159–1168, July 2000.

[37] Lee, D. and Milstein, L. B., "Comparison of multicarrier ds-cdma broadcast systems in a multipath fading channel," *IEEE Transactions on Communications*, vol. 47, pp. 1897–1904, December 1999.

[38] Lee, J. S. and Miller, L. E., *CDMA Systems Engineering Handbook*. Boston: Artech House Publishers, 1st ed., 1998.

[39] Lehnert, J. S. and Pursley, M., "Error probabilities for binary direct-sequence spread spectrum communications with random signature sequences," *IEEE Transactions on Communications*, vol. COM-35, pp. 87–98, January 1987.

[40] Mehta, N., Greenstein, L., Willis, T., and Kostic, Z., "Analysis and results for the orthogonality factor in wcdma downlinks," *IEEE Transactions of Wireless Communications*, vol. 2, pp. 1138–1149, Nov 2003.

[41] Mehta, N., Greenstein, L., Willis, T., and Kostic, Z., "Analysis and results for the orthogonality factor in wcdma downlinks," in *55th IEEE Vehicular Technology Conference*, vol. 1, pp. 100–104, Spring 2002.

[42] Mori, K. and Kobayashi, T., "Downlink transmission power control for cdma/shared-tdd packet communications in cellular environments," *IEICE Trans. Fundamentals*, vol. E84-B, pp. 1622–1630, June 2001.

[43] Morrow, R. K. and Lehnert, J. S., "Bit-to-bit error dependence in slotted ds/cdma packet systems with random signature sequences," *IEEE Transactions on Communications*, vol. 37, pp. 1052–1061, October 1989.

[44] Morrow, R. K. and Lehnert, J. S., "Packet throughput in slotted aloha ds/ssma packet systems with random signature segunces," *IEEE Transactions on Communications*, vol. 40, pp. 1223–1230, July 1992.

[45] Morrow Jr., R. K., "Accurate cdma ber calculations with low computational complexity," *IEEE Transactions on Communications*, vol. 46, pp. 1413–1417, November 1998.

[46] Noneaker, D. L., "On the spectral efficiency of wideband cdma systems," *IEEE Journal in Selected Areas in Communications*, vol. 19, pp. 33–47, Jan 2001.

[47] Noneaker, D. L. and Pursley, M. B., "On the chip rate of cdma systems with double fading and rake reception," *IEEE Journal in Selected Areas in Communications*, vol. 12, pp. 853–861, June 1994.

[48] Ojanperaä, T. and Prasad, R., *Wideband CDMA for Third Generation Mobile Communications*. Boston London: Artech House Publishers, 1998.

[49] Papoulis, A., *Signal Analysis*. MCGraw-Hill, Inc., 1977.

[50] Passerini, C. and Falciasecca, G., "Correlation between delay-spread and orthogonality factor in urban environments," *Electronics Letters*, vol. 37, pp. 384–386, Mar 2001.

[51] Pizarroso, M. and Jose, J., "Common basis for evaluation of atdma and codit system of concepts.," tech. rep., MPLA/TDE/SIG5/DS/P/001/b1, Sept 1995.

[52] Proakis, J. G., *Digital Communications*. Boston: McGraw-Hill, 4th ed., 2001.

[53] Pursley, M. B., Garber, F. D., and Lehnert, J. S., "Analysis of generalized quadriphase spread-spectrum communications," in *IEEE International Conference in Communications, Conf. Rec. 1*, pp. 15.3.1–15.3.6, June 1980.

[54] Pursley, M., "Performance evaluation for phase-coded spread spectrum multiple-access communication –part i: System analysis," *IEEE Transactions on Communications*, vol. 25, pp. 795–799, Aug 1977.

[55] Qiu, X., Chang, L., Kostic, Z., Willis, T.M., I., Mehta, N.and Greenstein, L., Chawla, K., Whitehead, J., and Chuang, J., "Some performance results for

the downlink shared channel in wcdma," in *IEEE International Conference on Communications*, pp. 376–380, IEEE, 2002.

[56] Sallent, O., Perez-Romero, J., Casadevall, F., and Agusti, R., "An emulator framework for a new radio resource management for qos guaranteed services in w-cdma systems," *IEEE Journal in Selected Areas in Communications*, vol. 19, pp. 1893–1904, October 2001.

[57] Schwartz, M., Bennett, W. R., and S., S., *Communication Systems and Techniques*. New York: McGraw-Hill, 1966.

[58] Sebeni, J. . and Cyril, L., "Performance of concatenated walsh/pn spreading sequences for cdma systems," in *49th Vehicular Technology Conference*, pp. 1446–1450, IEEE, 1999.

[59] Sheikholeslami, N. and Kabal, P., "A family of nyquist filters based on generalized-cosine spectra," in *Proc. 19th Biennal Communication*, pp. 131–135, June 1998.

[60] Shin, S., Ahmad, A., and Kim, K., "Performance of packet data transmission using the other-cell-interference factor in ds-cdma downlink," *IEE Proceedings on Communications*, vol. 150, pp. 129–133, April 2003.

[61] Sibata, T., Katayama, M., and Ogawa, A., "Performance of asynchronous band-limited ds/ssma systems," *Trans. IEICE*, pp. 921–927, Aug. 1993.

[62] Song, Rongfang an Leung, S. H., "Analysis and optimization of ds-cdma systems with time-limited partial response chip waveforms," *IEEE Transactions on Broadcasting*, vol. 49, pp. 202–210, June 2003.

[63] Stüber, G. L., *Principles of Mobile Communication*. Boston/Dordrecht/London: Kluwer Academic Publishers, 2nd ed., 2001.

[64] Sun, Q. and Cox, D. C., "Performance of rake receiver with non-ideal spreading codes," in *IEEE Sixth International Symposium on Spread Spectrum Technology and Applications ISSSTA 2000*, vol. 2, pp. 399–403, IEEE, Sept. 6-8 2000.

[65] TAKE, K., SATO, S., and OGAWA, A., "Uplink and downlink communications qualities in cdma cellular systems considering effects of traffic distribution," *IEICE Trans. Fundamentals*, vol. E82-A, pp. 2677–2686, December 1999.

[66] VITERBI, A. J., *CDMA : Principles of Spread Spectrum Communication.* Reading, Mass.: Addison-Wesley Pub. Co., 1995.

[67] WIN, M. Z., CHRISIKOS, G., and SOLLENBERGER, N. R., "Performance of rake reception in dense multipath channels: Implications of spreading bandwidth and selection diversity order," *IEEE Journal in Selected Areas in Communications*, vol. 18, August 2000.

[68] YOON, Y. C., "Probability of bit error and the gaussian approximation in asynchronous ds-cdma systems with chip pulse shaping," in *Proceedings of 20th Biennal Symposium on Communications, Queen's University*, (Kingston, Canada), pp. 111–115, May 28-31 2000.

[69] YOON, Y. C., "A simple and accurate method of probability of bit error analysis of asynchronous bandlimited ds-cdma systems," *IEEE Transactions on Communications*, vol. 1, pp. 656–663, April 2002.

VITA

Loran Aleksandervich Jatunov Santamaría was born in Moscow, Russia in 1973. At the age of five, he moved to the city of Chitré in the Republic of Panamá, where he attended José Daniel Crespo High School. He received his Bachelor's Degree in Electrical Engineer (with Highest Honors) in 1994 and Master of Science in Electrical Engineering in 1996, both from Georgia Institute of Technology. During Summer jobs at Motorola, Paging Division in 1995 and Motorola, Land Mobile Products Sector (Research Group) in 1997, he became very interested in the area of Wireless Communications. He has been a Teacher Assistant for many undergraduate and graduate courses at this university. Before undertaking the topic of this dissertation, he conducted research on Hierchical Cell Structures for CDMA systems.